IMPACT ANALYSIS OF CONNECTING DOCKING SHIP LOADS ON POWER SYSTEM VOLTAGE STABILITY- CASE STUDY OF MOMBASA PORT

KARUE CATHERINE NYAGUTHII

MASTER OF SCIENCE

(Electrical Engineering)

JOMO KENYATTA UNIVERSITY OF

AGRICULTURE AND TECHNOLOGY

2018

Impact Analysis of Connecting Docking Ship Loads on Power System Voltage Stability- Case Study of Mombasa Port

Karue Catherine Nyaguthii

A thesis submitted in partial fulfilment for the degree of Master of Science in Electrical Engineering in the Jomo Kenyatta University of Agriculture and Technology

2018

DECLARATION

This thesis is my original work and has not been presented for a degree in any other University.

Signature …… Date ……..

Karue Catherine Nyaguthii

This thesis has been submitted for examination with our approval as University supervisors:

Signature …… Date ……..

Prof. D.K Murage, PhD

JKUAT, Kenya

Signature ……. Date ……..

Prof. C. M. Muriithi, PhD

MUT, Kenya

DEDICATION

This work is dedicated to my family for their support and encouragement. My gratitude is to the almighty God for His grace and mercy.

ACKNOWLEDGEMENTS

First, I thank Almighty God for the gift of life and strength that He gave me to enable me complete this work successfully. My most sincere thanks go to my supervisors Prof. D. K. Murage and Prof. C. M Muriithi for their support, commitment and relentless effort they made on my work to completion. Their guidance, materials and discussions all enabled me complete this work. My thanks to entire Department of Electrical and Electronics Engineering JKUAT and most specifically the Chairman Prof. D Kamau and the Dean Prof. Nderu for their support and encouragement. To my family members, God bless you for the support, encouragement and great love that you gave to me all through. My thanks goes to Head of Port Electrical Engineering Department at Kenya Ports Authority Eng. J Birir and Eng. G Mjambili for their support during the entire period of my study. I must thank everybody who contributed towards the completion of my work. May the Almighty God bless you all.

TABLE OF CONTENTS

LIST OF TABLES

LIST OF FIGURES

LIST OF APPENDICES

LIST OF SYMBOLS

δ	Delta
θ	Theta
λ	Lamda

LIST OF ABBREVIATIONSAND NOTATIONS

A	Ampere
AI	Artificial intelligence
ALDWYCH	Aldwych International Ltd
ATP-EMTP	Alternative Transients Program- Electromagnetic Transients Program
BV	Bureau Veritas
BWSC	Burmeister &Wain Scandinavian Contractor A/S
CB	Circuit Breaker
CO_2	Carbon Dioxide
DC	Direct Current
DFIG	Doubly Fed Induction Generator
DG	Distributed generation
DNV	Det Norske Veritas
ESI	Environmental Ship Index
EU	European Union
FACTS	Flexible Alternating Current Transmission Systems

FVSI	Fast Voltage Stability Index
GHG	Green House Gas
HV	High Voltage
HVDC	High Voltage Direct Current
IEC	International Electrotechnical Commission
IEEE	Institute of Electrical and Electronic Engineers
IMO	International Maritime Organization
IPP	Independent Power Producer
ISO	International Organization for Standardization
KENGEN	Kenya Generating Company
KPA	Kenya Ports Authority
KVA	Kilo Volt Ampere
LF	Line Flow Index
LNG	Liquefied Natural Gas
LTC	Load Tap Changers
LV	Low Voltage
MARPOL	International Convention for the Prevention of Pollution from Ships

MATLAB	Matrix Laboratory
MVAR	Mega Volt Amperes Reactive
MW	MegaWatt
NGR	Neutral Grounding Resistance
NO_x	Nitrogen Oxide
OFP	Over frequency protection
OVP	Over voltage protection
P	Power
PCC	Point of Common Coupling
PM	Particle Matter
PSAT	Power System Analysis Toolbox
PSS	Power System Simulator
Q	Reactive Power
ROPAX	Roll-On/Roll-Off Passenger
Ro-Ro	Roll on Roll off
RRagg	Aggregate rotor resistance
Rsagg	Aggregate stator resistance
sagg	Aggregate slip

SCADA	Supervisory Control and Data Acquisition
SISTI	Italian Study on Susceptibility to Temperature and Air Pollution
SO_x	Sulphur Oxide
STATCOM	Static Synchronous Compensators
SVCs	Static Var Compensators
TEU	Twenty Equivalent Unit
UFLS	Under Frequency Load Shedding
UFP	Under Frequency Protection
ULTC	Under Load Tap Changers
UVP	Under voltage protection
VOCs	Volatile Organic Compounds
VSC	Voltage Source Converter
WPCI	World Ports Climate Initiative
XMagg	Aggregate magnetizing reactance
Xsagg	Aggregate stator reactance
ZIP	Constant Impedance, Current and Power
ZLRagg	Aggregate locked-rotor impedance

ZLRi Locked-rotor impedance for individual motors

ZNLagg Aggregate no-load impedance

ABSTRACT

The Port of Mombasa handles cargo from container ships, cruise ships, conventional ships, roll on roll off and vehicle ships, military, oil and product ships. At berth the main engine is switched off and the auxiliary generators take control of all the power generation on board. Auxiliary engines on ships use heavy fuels which result in release of pollutants such as greenhouse gases in addition to being a source of noise and vibrations. Ship-to-shore power has been identified as one technology to reduce emissions by at least 90% in harbour areas. To implement shore power technology for commercial ships in Kenya, detailed analysis of the existing power system is required to ensure that the additional load can be connected to the grid without resulting in voltage collapse. This study applied induction motor load aggregation (implemented in MATLAB/SIMULINK) to develop a composite load model for berthed ships. The coast 132kV power grid was modelled, with transmission lines represented as pi networks, substation loads as static PQ loads and generating stations as PV generators. Load flow analyses was then completed on the grid and load model using MATLAB/PSAT. Continuation power flow was applied to establish loadability limits using PV curves. The results showed that it is possible to connect the additional load without losing voltage stability. The lowest voltages experienced were at the Mtito and Voi buses with a line voltage of 0.93p.u. Installation of appropriate static VAR compensation at Mtito was found to be an adequate mitigation measure. Bus voltage was observed to rise to 1p.u at Mtito and 0.97p.u at Voi on installation of VAR compensation.

CHAPTER ONE

INTRODUCTION

1.1 Background of Study

It is well known that economic progress and globalisation has resulted in the rapid growth of international trade. Maritime operations have played an increasingly significant role in providing international cargo and passenger transportation. For ships at berth, the main engine is switched off and on board auxiliary generators take over all the power supply on board. The electricity generated on board is used to provide power for a wide range of applications like lighting, cooling, ventilation, pumps, navigation systems, cargo loading and offloading activities. Consequently, seaports all over the world are suffering from the problem of fuel consumption and exhaust gases coming from ships during their stopover in harbours[1]. This continued discharge of pollutants has drawn the attention of several regulatory parties including International Maritime Organization / International Convention for the Prevention of Pollution from Ships (IMO/ MARPOL) and European Union (EU). In the EU, strict environmental legislation have been enacted forcing the shipping industry to look for ways and means to reduce this negative environmental impact. According to Italian Study on Susceptibility to Temperature and Air Pollution (SISTI), these pollutants have adverse effect on human health. In addition, at a global level, Carbon Dioxide (CO_2) is the most significant contributor to global climate change[2].

Berthed ships can either generate their own electricity using clean fuel, or connect to utility power sockets at the port. Research so far done has shown that the latter is the most sustainable solution, in every way [3], [4]. However further studies are necessary to ensure full benefits are realised.

Shore power has the following benefits:

(i) Reduced port fees – Where relevant legislation exists such as in the EU, port fees can vary depending on the environmental rating of a ship. Created by World Ports Climate Initiative (WPCI), the Environment Ship Index (ESI) measures the quantities of Nitrogen Oxide (NOx), Sulphur Oxide (SOx), Particle Matter (PM) and CO_2 emissions from a ship and assigns a grade to each ship. As shore connection is a green technology, ships equipped with the solution receive a higher grade. Greener ships can enjoy fees rebate up to 10% on Port fees.

(ii) Cutting emissions - Electricity generated on hydro power plants has a smaller eco-footprint than that produced by ship generator engines. Use of shore-side electricity cuts CO_2 emissions by an average of 50%.

(iii) Elimination of noise and vibrations - Use of auxiliary diesel engines on ships causes noise up to 120dB near the engines and associated vibrations are unpleasant for crew, passengers, and port personnel.

(iv) Reduced fuel costs: - Global demand for fuel is set to rise significantly and this especially affects low sulphur fuel process. The United States Energy Information Administration forecasts that demand for refined petroleum products will grow by 1.5% per year over the next five years. Current fuel prices make use of shore-side electricity that is partially generated from non-fossil fuel sources financially attractive.

(v) Lower maintenance costs - Motor maintenance costs (estimated at 1.6 Euro/h/motor) fall sharply when shore-side electricity is used. The annual average saving per ship is estimated at Euro 9,600.The total costs for on-board generation of electricity will depend on the design of the ship's power supply system and the fuel used. The fuel prices vary largely over time and by fuel quality. The total cost will also depend on costs for investments and maintenance.

The investment costs for on board auxiliaries have been ignored in this study, as the power supply system in most cases has to be installed even if the vessel is using shore-side electricity in all harbours. The maintenance cost will mainly vary with the type of engine (two/four stroke, engine brand, size) and environmental operating conditions, age and running hours per year. A general cost of 1.6 euro/running hours for a 900 kW auxiliary engine is used in this study. The maintenance cost can be higher for larger auxiliaries. Source: www.bunkerworld.com 2004-06-07. When using on shore power which is greener, the auxiliary engines will be switch off hence reduced maintenance cost.

(vi) New business for ports - Ports installing shore connections would selling electricity to ships, more revenue will be realized by the utilities.

The size of a shore-to-ship installation will depend on the power requirements for docking ships. The average rating of vessels ranges from0.3MVA for roll-on roll-off (Ro-Ro) ships through 3MVA for container ships to 20MVA for cruise ships as illustrated in Figure 1.1 [2] and [5]

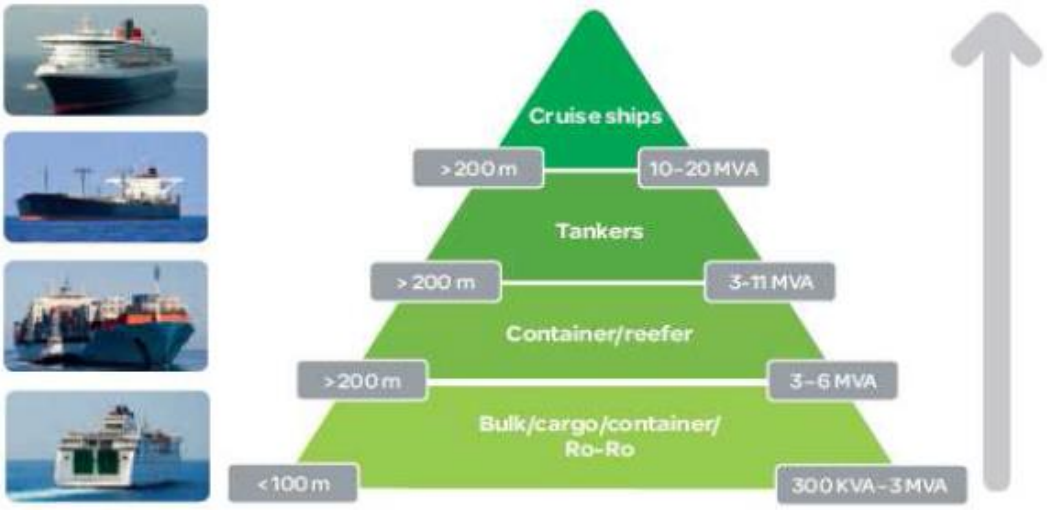

Figure 1.1: Category of vessels at berth at 415-6.6kV at 50/60Hz

Earlier shore power connections used low voltage connections but the current trend is to use medium voltage (6.6kV or 11kV) in order to cater for the largest ships and reduce the size and number of cables used in connections. According to the World Ports Climate Initiative (WPCI), currently there are 22 ports in Europe and North America that have applied shore power supply in their electrical infrastructure and they have experienced significant environmental improvement [2]. The organization also lists an additional 28 ports in Europe, North America and Asia that have ongoing plans to install on shore power connection [6].

The port of Mombasa handles cargo from container ships, cruise ships, convectional ships, Ro-Ro and vehicle ships, military and oil product ships. The port is supplied with electrical power from the national grid through a 132kV supply. The port has facilities where 21 ships with an estimated 55 MW load can berth simultaneously. An estimated 55MW load will be connected to the national grid which has an effective installed capacity of 2,261MW as at June 2017[7] with a national peak demand of 1,656MW hence a reserve of approximately 26%. In spite of data from Kenya Power showing a reserve capacity of 26%, customers still experience a lot of power outages, as can be observed from sub-station data at Kenya Ports Authority on Figure 1.3. This could be as a result of reliability issues in generation, transmission or grid control. An assumption that additional power demand, even when within the current installed generation and transmission capacity would be met consistently is therefore not correct. To meet this additional 55MW demand for berthed ships, proper planning has to be done in order to determine the maximum load that can be added into the system before exceeding the limits. This investigation will seek to identify further stresses that will be imposed on the grid by the proposed additional load. This ability to determine the maximum ship load that may be connected to a power system under certain conditions before experiencing any voltage instability allows a planner to make necessary actions to prevent such incidents as voltage collapse.

Among the major causes of recent blackouts around the world such as those reported in Germany in 2006, Russia in 2005, Greece in 2004 and in Italy, USA/Canada, Sweden and Denmark in 2003, was insufficient reactive power supply resulting in voltage collapse [8]. Mombasa, has suffered several recent blackouts (December 2015, January 2016) on the 132kV supply which resulted into huge loss of revenue to the Port. According to KPA Annual Report 2015, for 1 hour loss of power, the port loses at least 20,000 Dollars of revenue. As the load increases, the demand for power from the generation plants increases resulting into a higher possibility of operating a power system near its capacity limits posing a high risk of voltage instability which can lead to voltage collapse. Most electric utilities with Kenya not being an exception are forced to operate at such limits due to difficulty in constructing new generation, transmission and distribution lines because of economic constraints, regulations and policy, or due to reduce their operational costs and the need to maximise profits. The lack of investment raises operational risks of containing or controlling such a systems.

The mitigation factors that can be applied to prevent voltage instability on connecting docked ships loads are mainly injection of reactive power through strategically placed static capacitor banks and synchronous condensers. Other methods will be upgrading existing power stations, generation plants, and transmission and distribution networks. Integration of distributed generation and storage of energy can also be used to support the reliability of the system in emergency situations [9]. A successful determination of the mitigation factors that can be applied to avoid such system instability is based on method's accuracy and speed of indication at minimum computation time.

This study investigated the effect of installing a shore to ship connection on the voltage stability of the Kenya electricity grid. This involved data collection of electrical loads from different categories of ships. Due to the dynamic nature of ship loads which are mainly induction motors as illustrated in Figure1.2 [2], induction motors aggregation was applied for the loads on each ship. Induction motor loads require nearly constant torque at all speeds, and are the most demanding from a

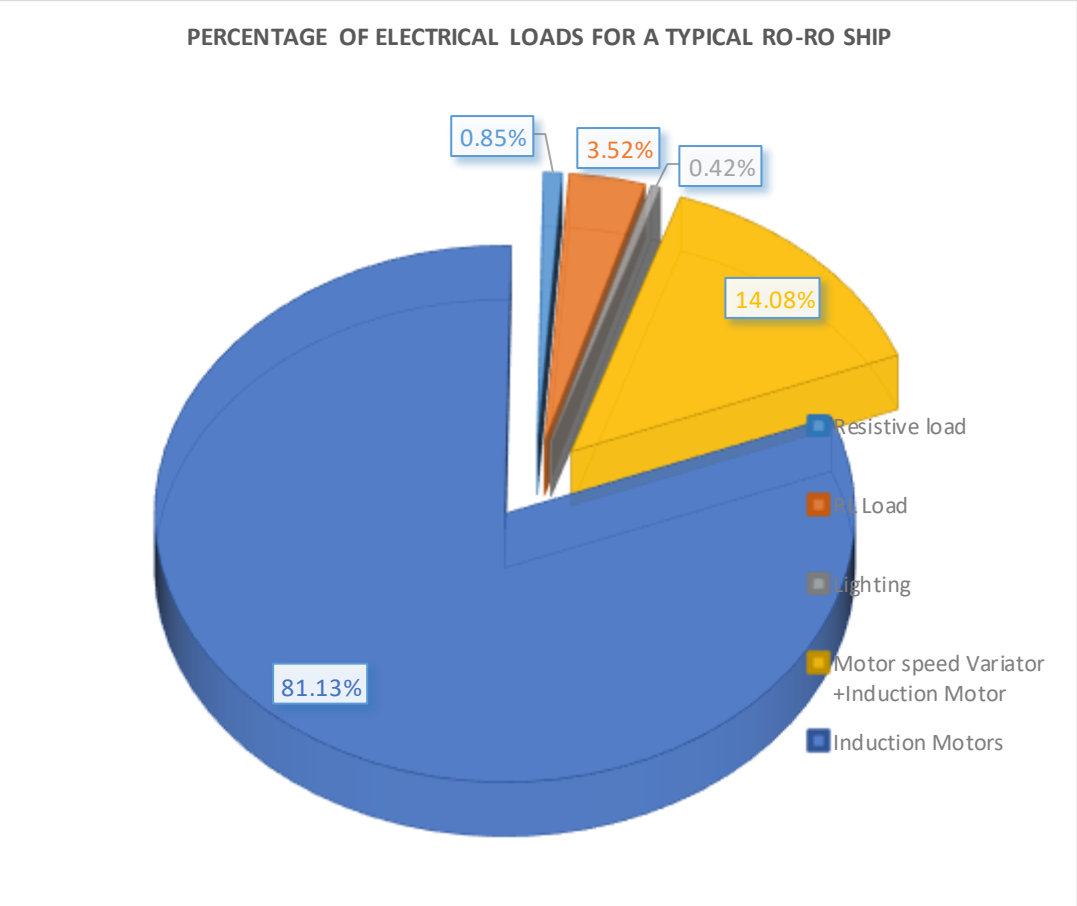

Figure 1.2: Typical ship load

stability viewpoint. These loads are mainly pumps, fans and compressors which account for more than half of the industrial motor use. Typically motors consume 60% to 70 % of the total power system energy and their dynamics are very vital for voltage stability and long-term stability studies [10]. The aggregated modelled ship load was connected to a coast power system network.

Stability of a power system can be assessed in terms of voltage stability, frequency stability or rotor angle stability. The three classifications are all inter-related and in most cases, more than one form of instability will be experienced. The classifications assist in identification of the method of analysis to apply [11]. In this study, voltage stability and rotor angle stability are the relevant forms of stability. According to [12] pure rotor angle stability applies when the system is a generator connected to an infinite bus while pure voltage stability applies when the system is an isolated load supplied from an infinite bus. The system in this study is closer to the second case than in the first case and hence voltage stability was applied as the method of analysis.

1.2 Problem Statement

A shore-to-ship power solution is attractive for port authorities and ship owners as it helps to reduce emissions in ports by connecting ships to the port electricity grid and turn off their diesel engines while at berth to improve air quality and reduce noise and vibrations in port areas. As is the case in Kenya, inland power generation in most countries depends on clean technologies such as hydro, natural gas, renewable and other carbon free technologies like fuel cells [3].

In Kenya, the bulk of the power supplied to consumers is generated by the state owned generation company, KenGen, whose power stations are located far away from the load centres, and they generate most of the reactive power required. Thus, reactive power is transmitted over long distances, resulting in low voltage profiles experienced during peak demand hours. The port of Mombasa is located near Kipevu Ken Gen plant. Currently, Kenya Ports Authority (KPA) consumption is 4 MW with

supply voltage at 132kV. Serious voltage fluctuations including blackouts have been experienced in the recent past as illustrated in Figure1.3 (KPA Data Logger).

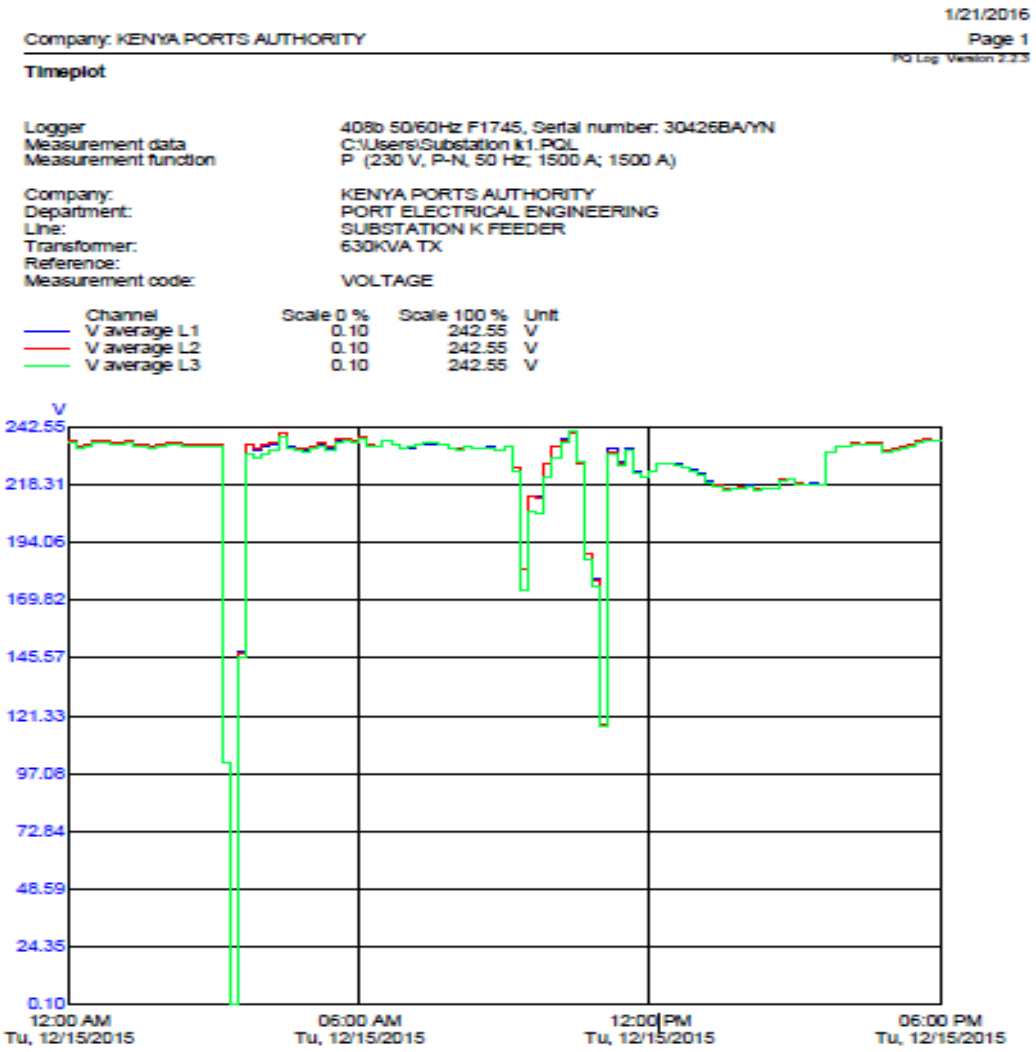

Figure 1.3: Power fluctuations at KPA substation

These voltage fluctuations have lasted a minimum of 4 hours translating into major loss in production due to high restarting time of cargo handling equipment like ship to shore cranes. With an additional 55MW required to supply berthed ships whose loads are mainly induction motors, the active and reactive power required will vary significantly and in turn affect voltage stability.

The challenges for shore power connections as cited by [1] and [2], are mainly neutral earthing system, safety of operation staff, non-standard ships and high cost of installation. The mitigation factors currently tested for these shore power challenges in developed countries address these challenges and are applicable in Kenya. However apart from these challenges, Kenya and other developing countries are likely to face another major challenge of voltage instability due to the rapid high power demand rate on a stressed system notwithstanding the power fluctuations that are currently being experienced. Implementing a shore to ship power connection arrangement with inadequate mitigation of system voltage stability can result in unstable power supply. This study modelled and carried out an analysis of shore power supply to docked ships for the case of Kenya to form the basis for formulation of mitigation factors that can work given the specific parameters in this region.

1.3 Justification

Ports produce high concentrations of Green House Gases (GHG) caused primarily by ships using heavy fuels on generators while berthed. In line with port modernisation and as an international best practice [13] it is paramount to consider shore power technology. Shore power will help to achieve a modern green port with well-coordinated framework for environmentally friendly port operations considering that there is no buffer zone between the local community and the port. Using shore power connection will reduce emissions by 90% in the harbour areas [13]. With an additional estimated sudden 55MWload proposed to be connected to the national grid, it is important to study shore power connections since this will have a strong influence on power system voltage stability. The findings can be applied in Kenya and other similar power systems in the region.

1.4 Objectives

1.4.1 General objective

The main objective of this research work was to analyse the impact of berthed ships loads and propose any mitigation factors on the static voltage stability of the Kenyan coast region power system.

1.4.2 Specific objectives

i. Aggregate and model a container ship electrical loads.
ii. Develop a model for 132 kV Coast region power system
iii. Analyse the effect of connection of the modelled ship load to the modelled local grid to determine the maximum number and size of docked ships that can be connected to the power system and propose any mitigation measures that can be applied to enhance static voltage stability.

1.5 Scope

This study analysed the impact of connecting docking ships loads at the port of Mombasa on the Kenya coast power system. The research concentrated mainly on aggregating the different ship loads in each category, modelling the coast power system and carrying out an analysis on the effect of connecting the ship loads on power system voltage stability. The models in this research were developed in (Matrix Laboratory) MATLAB/SIMULINK and Power System Analysis Toolbox (PSAT).

1.6 Thesis Organization

This thesis comprises of five chapters. Chapter one is an introduction to the research topic giving brief background information, problem statement, objectives and scope. Chapter two is the literature review on shore power, aggregation of motor loads and

voltage stability. In Chapter three, the methodology used in achieving the specific objectives is outlined from the load aggregation, developing of simulation models, analysing voltage stability. Chapter four details the research results and discussions of implementing the proposed shore power connections for docked ships. Chapter five contains the conclusion and recommendations as guided by the results obtained.

1.7 Contributions

1.7.2 Conference Proceeding

1. C N Karue, D. K. Murage, C. M. Muriithi, "Shore to Ship Power for Mombasa Port Possibilities and Challenges", Proceedings of 2016 International Annual Conference on Sustainable Research and Innovation, held at Kenya School of Monetary Studies (KSMS), Nairobi, Kenya, 4th - 6th May, 2016.
2. C N Karue, D. K. Murage, C. M. Muriithi, "Load Flow Analysis of Docked Ships at Mombasa Port", Proceedings of 2016 International Conference on Science, Technology, Innovation and Entrepreneurship, held at Dedan Kimathi University Nyeri, Kenya, 2nd-4th November 2016

1.7.3 Journal Publications

1. Catherine Nyaguthii Karue, D. K. Murage, C. M. Muriithi, Modelling and Loading Limits for Kenya Coast Power Network Using Continuation Power Flow, International Journal of Energy and Power Engineering. Vol. 5, No. 6, 2016, pp. 182-188. doi: 10.11648/j.ijepe.20160506.12

CHAPTER TWO

LITERATURE REVIEW

2.1 Recent Research in this area

2.1.1 Shore to Ship Power Connections

Previous studies on shore to ship power connection have looked both at the environmental and financial impact of shore to ship power connection and the technical details of implementing such a connection. The countries which have implemented shore power as a best practice have been presented in [14]. These ports mainly in Europe, Asia and America have realized significant benefits ranging from reduced pollution to increased revenue.

Technical details that have been investigated include the expected loads and connection time as well as the requirements for voltage and frequency. In [1] and [2], a detailed study has been done to determine a technical solution for shore power electrical infrastructure to supply vessels by ABB. The study investigates different frequency converters arrangements with the centrally placed frequency converter being recommended as the best option due its low cost and high robustness.

In both [1] and [2], it is established that berthing ships have voltage and frequency ranging from 400V 50Hz to 480V 60Hz. A frequency of 60Hz was found to be the predominant supply frequency for bigger vessels because they allow reduction in the power equipment size and weight except in small container vessels where 50Hz is the predominant frequency. Most large vessels are from North and South America where 60 Hz is the standard frequency. It is therefore recommended that shore to ship installations in countries with 50Hz grids include an on-shore 50Hz – 60Hz frequency converter and HV/LV transformers in order to supply 60Hz vessels. A typical solution by Schneider consists of a 2MVA or 3MVA unit packaged in a container with detailed safety requirement [15].

In [2] the main challenges of [14] shore power are discussed with possible solutions where the main challenge of neutral earthing is identified as a critical component of shore power connections.

Radu et al. [2] studied the ship berthing patterns at European ports. They found that the loads range from 300KVA to 20MVA while berthing times range from 3 hours to 80 hours. The high power consumption will require very large cables if the connection is based on a low voltage system. It is therefore recommended that the supply be at medium voltage (6.6kV) with an on-ship transformer to convert to rated low voltage of on board supply.

Borkowski and Tarnapowicz [14] have presented a study of a ship that was undergoing conversion to use on-shore power. Although their focus is on emissions, it is noted in their study that the conversion included an on board transformer.

Ion et al [16] have carried out steady state and transient behaviour of a current-limited system of a shore to ship connection, with focus on the operation of the frequency converter. In the study, the ship load is modelled as an induction motor and aggregation techniques are used to combine the ship into one load. None motor loads like lighting and cooking range are ignored. The study dealt with transients concerning the motor behaviours of the ship's system supplied by a shore grid with fault current limitation using ATP-EMTP software. The study concluded that direct starting of a 500 kW motor is suitable for a 3MVA shore system while for a 1000kW motor, the starting current reaches the limits imposed by the frequency converter system. This is because, the limitation period for starting a 1000 kW motor is dependent on the inertia value, hence depends on the load type. Direct starting of a 1500 kW motor was found not feasible for a restrictive system like the shore grid due to very long limitation period and it is not admissible for correct operation.

Nord [17] invetsigated voltage stabilityin an electric propulsion system for ships. In this study, the rectifiers are modelled with a capacitor, which serves as an energy storage, in parallel with a current source and enlarged in proportion to the rated

power level of the sources. The study concludes that, the main energy storage should be placed at the rectifiers using capacitors and that the sources must act quicker than the load in regards of bandwidth. Should the situation be the opposite the system will suffer a break down because of the characteristic of the constant power loads where the consumption will increase while the voltage is decreasing. This demonstrated that it is possible to study the voltage stability in the system using operational scenarios. It is also concluded that short-circuits in a DC system is much different from an ac system whereas the energy is stored in capacitors separated from the actual sources. The sources will shut themselves down before the system reaches a state of zero voltage. Therefore the fault must be cleared before this happens. The main concern of the simulations in this thesis is to address the behaviour of the voltage level as a result of the DC voltage regulators in parallel. The simulation results can be used for further studying the secondary side of the converters for the distribution net and the propulsion motors. The voltage stability of the system is reliable upon a large storage capability in the capacitors at the sources. The rotating masses inside the ac generators will not provide the system with stored energy since it is ’trapped’ behind digitally controlled rectifiers. Thus the storage must be provided on the DC side using capacitors. It has been shown that the system may be subjected to voltage collapse using oversized capacitors [17].

It is noted from the literature that the technical details have been well studied and working commercial solutions are already available. This thesis will therefore not include a study of the interconnection systems such as transformers, frequency converters and cables. It will instead focus on modelling the ship load and the shore-side grid in order to study the impact of connecting berthed ship load on a power system. As seen in [16], load modelling includes aggregation of induction motor loads RL and resistive loads for transient analyses. Unlike in [16], the model used in this thesis studies the long term voltage stability and not the transient stability.

2.1.2 Load Modelling and Aggregation of Induction Motors

The study of power system stability requires modelling of the connected load. Models used include constant power (PQ), polynomial model (ZIP), exponential recovery, induction motor and composite models [18] , [19]. Whichever model is selected, an estimation of model parameters is required. According to a worldwide survey of electric power transmission companies [19], the most common approaches to load modelling are constant power model for steady state analysis and a composite model for short term voltage stability. The survey identified measurement based methods as the most common approach for estimation of model parameters. Component based approach which is applied analytically by lumping similar loads based on the load type and then using pre-determined values for each parameter of the load [18]. In this bottom -up method, the load supplied at a bulk power delivery point is categorised into load classes and further into load components. A detailed study of the individual appliances characteristics is done and the loads aggregated to produce a composite load mode [20] and [21]. Induction motor loads are normally represented by a dynamic model with variable torque, power and slip. For a system with many induction motors, the complexity of the model can be reduced by use of aggregation models. Previous study by [22] has proposed the use of the motor equivalent circuit approach which has further been emphasized by [23] and [24]. Measurement based component approach was applied in [25], [26] and in [27], an energy conservation law approach was applied for motor loads aggregation.

On the criteria for grouping motors together for aggregation, [24]proposes that motors should be grouped together based on their impedance relationship while [16] proposed grouping together all motors connected to the same common bus. The aggregation from impedances relationship is based on steady state theory of motors with the assumption that power from the aggregate motor is equal to the total power of the individual motors. The various aggregated models are assembled in a unique aggregated motor model. The equivalent circuit approach was applied to aggregate the equivalent inductance and resistances to achieve an aggregated inductance and

resistance model [24].

This study developed a model to study long term voltage stability. It used a composite model that includes one or more induction motor models developed through motor aggregation and a static constant power load to represent non-motor loads. Existing loads and network distribution stations were modelled as static PQ loads the ship loads were modelled as a combination of static PQ loads and an aggregated motor load. The aggregation method for no load condition and locked rotor condition proposed in [24] was applied. Motors were grouped together for aggregation based on their load torque characteristics.

The equivalent PQ model of the ship load applied for power flow, was obtained by initialisation of the power flow as proposed in [28].Parameters for the model were derived from equivalent manufacturer data for specific load types.

2.2 Port Operations

World over, ports are considered as areas of high activity and profit generation that serve as a primary point for international goods import and export. They are also notorious for being major sources of air pollution and will continue to be seen as such in near future if something does not change. Previous studies show that container vessels, (Roll on Roll off) Ro-Ro and vehicle vessels, cargo, military ship, oil product tankers and cruisers are the most frequent vessels at ports with power demands, system voltage and frequency as in Table 2.1 [1], Table 2.2 [1], and Table 2.3 [1], [2].

Table 2.1: Average and Peak demand for various ships

Type of vessel	Average power demand	Peak power demand	Peak power demand for 95% of the vessels
Container vessels (<140m)	170KW	1000KW	800KW
Container vessels (>140m)	1200KW	8000KW	5000KW
Container vessels	800KW	8000KW	4000KW
Ro/Ro and vehicles	1500KW	2000KW	1800KW
Oil and product tankers	1400KW	2700KW	2500KW
Cruise ships (<200m)	4100KW	7300KW	6700KW
Cruise ships (>200m)	7500KW	11000KW	9500KW
Cruise ships	5800KW	11000KW	7300KW

Table 2.2: Voltage level for various ships

Type of vessel	**380V**	**400V**	**440V**	**450V**	**460V**	**6.6KV**	**10KV**	**11KV**
Container vessels (<140m)	**42%**	**16%**	**42%**	-	-	-	-	-
Container vessels (>140m)	**6%**	**79%**	-	**3%**	-	**12%**	-	-
Container vessels (total)	**19%**	**6%**	**64%**	**2%**	-	**9%**	-	-
Ro/Ro and vehicles	-	**30%**	**20%**	**43%**	-	-	-	-
Oil and product tankers	**13%**	-	**40%**	**47%**	-	-	-	-
Cruise ships (<200m)	**14%**	**18%**	**59%**	**9%**	-	-	-	-
Cruise ships (>200m)	-	-	**12%**	-	-	**48%**	**4%**	**36%**
Cruise ships (total)	**6%**	**9%**	**34%**	**4%**	-	**26%**	**2%**	**19%**

Table 2.3: Frequency level for various ships

Type of ship	50Hz	60Hz
Container vessels (<140m)	63%	37%
Container vessels (>140m)	6%	97%
Container vessels (total)	26%	74%
Ro/Ro and vehicles	30%	70%
Oil and product tankers	20%	80%
Cruise ships (<200m)	36%	64%
Cruise ships (>200m)	0	100%
Cruise ships (total)	17%	83%

Ships/vessels are classified as follows;

i. Container vessels are used for transportation of containers. Load capacity is measured in Twenty Foot Equivalent Units (TEU). TEU is the number of standard 20-foot container a vessel can carry. Most vessels carry 40 feet containers and this is converted to give a TEU rating. Some containers ships do not carry their loading gear so loading and unloading is done using the port's cranes. The average peak power is approximately 8MW with a mean average of 2MW for most container ships. Their voltage levels vary from 380V to 6.6kV with a greater percentage being 400volts. Vessels more than 140 meters operate at 60 Hz and vessels less than 140 meters at 50Hz.

ii. Ro-Ro and vehicle vessels are Roll-on and Roll-off ships designed to carry wheeled cargo such as auto mobiles, trucks, semitrailers trucks, trailers and rail road cars. Ro-Ro vessels have an average power demand of 2MW. Their voltage levels vary from 400Volts to 450Volts with a higher percentage operating at 60Hz.

iii. Oil and product ships also known as petroleum tankers are designed for bulk transport of oil. There are either crude tanker or product tanker. They have an average power demand of 3MW. Their voltage levels vary from 380Volts to 450Volts with a higher percentage operating at 60Hz.

iv. Cruise ships or cruise liner is a passenger ship used for pleasure voyages. Cruise ships that use diesel - electric power system have the highest power consumption of any vessel type. The average peak power is approximately 11MW with a mean average of 7MW. Their voltage levels vary from 380V to 11kV with vessels more than 200 meters operating at 60Hz and those less than 200 meters working at 50Hz.

2.2.1 Different shore power design configurations

Typical shore -side power supply configuration as per the EU recommendations 2006/339/EC are illustrated in Figure and Table 2.4 [1] , [2]. This is a representation of a decentralized topology with a standard frequency converter placed beside the berth. The dimensioning of the frequency converter adopted is that of the vessel with the highest power demand. This system lacks the galvanic protection between the port and the vessels electric system. Another method is the centrally placed frequency converter which has a small footprint at every berth. The frequency converter is only used for converting 50Hz to 60Hz hence a lower burdened converter, though this arrangement is more venerable since if a fault occurs in the frequency converter all connected berths will not be able to serve the 60Hz vessels and it is more expensive due to the double bus bar switchgears instead of standard switchgears. In this research the centrally placed frequency converter was used because of the small foot print needed at berth.

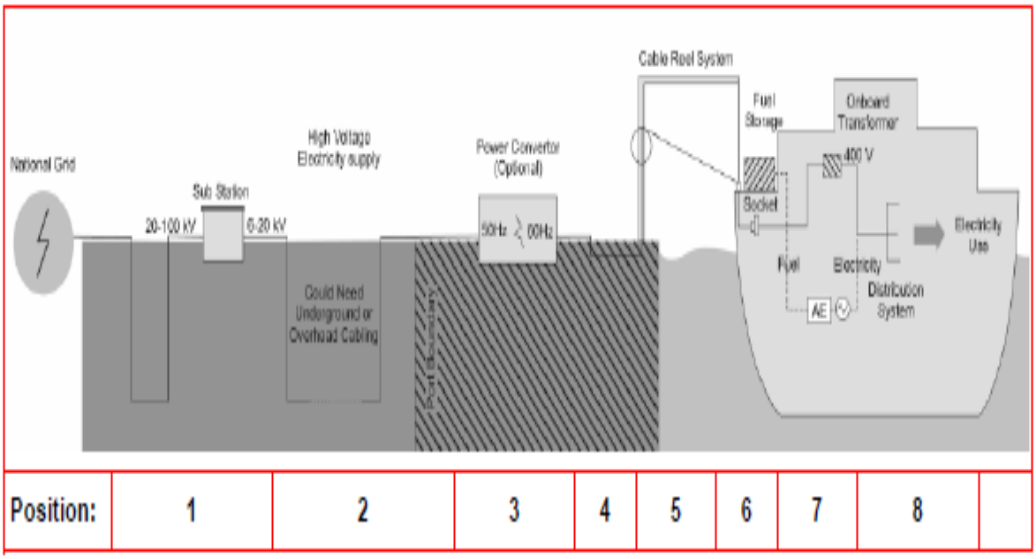

Figure 2.1: Shore - power electricity connections as per EU recommendations

Table 2.4: Shore - side power connection as per EU recommendation 2006-339-EC

Position	Description
1	Connection to national grid at 20-100KV electricity from local substation, where it is transformed to 6-20KV
2	Cables to carry 6-20KV to Port terminal
3	Power conversion where necessary. A ship designed for 60Hz electricity might be able to run on 50Hz electricity for some equipment such as lighting and heating but not on motor driven equipment such as pumps, winches and cranes. Hence the need for a 50Hz/60Hz conversion.
4	Cables to distribute to the terminal either underground within existing or new conduits
5	A cable reel system (electromagnetically powered and controlled) to avoid handling high voltage cables. This might be built on the berth supporting a cable reel, davit and frame. Davit & frame used to raise or lower the cable to vessel.
6	A socket on board the vessel for connecting cable
7	A transformer on board the vessel to transform high voltage to 400V
8	Power is distributed around the ship and the auxiliary engine switched off

2.2.2 Challenges of shore power connections

According to the World Ports Climate Initiative (WPCI), currently there are 22 ports worldwide in Europe and North America that have applied shore power supply in their electrical infrastructure as listed in Table 2.5 [29] with a standard for low voltage connections (IEC 80005-3) under preparation [30]. These ports have experienced significant environmental improvement [29] with an additional 28 ports in Europe, North America and Asia that have ongoing plans to install on shore power connection.

Table 2.5: Existing Shore Power supplies for commercial vessels in the world

Year of Introduction	Port Name	Country	Capacity (MW)	Frequency (HZ)	Voltage (kV)	Ship types with OPS
2000-2010	Gothenburg	Sweden	1.25-2.5	50 & 60	6.6 & 11	RoRo, ROPAX
2000	Zeebrugge	Belgium	1.25	50	6.6	RoRo
2001	Juneau	USA	7-9	60	6.6 & 11	Cruise
2004	Los Angeles	USA	7.5-60	60	6.6	Container , Cruise
2004	Pitea	Sweden	1.0	50	6	RoRo
2005-2006	Seattle	USA	12.8	60	6.6 & 11	Cruise
2006	Kemi	Finland	10.2	50	6.6	ROPAX
2006	Kotka	Finland	11.9	50	6.6	ROPAX
2006	Oulu	Finland	16.9	50	6.6	ROPAX
2008	Antwerp	Belgium	0.8	50 & 60	6.6	Container
2008	Lubeck	Germany	2.2	50	6	ROPAX
2009	Vancouver	Canada	16	60	6.6 & 11	Cruise
2010	San Diego	USA	16	60	6.6 & 11	Cruise
2010	San Francisco	USA	16	60	6.6 & 11	Cruise
2010	Karlskrona	Sweden	2.5	50	6.6 & 11	ROPAX
2011	Long Beach	USA	16	60	6.6	Container
2011	Oslo	Norway	4.5	50	11	Cruise
2011	Prince Rupert	Canada	7.5	60	6.6	
2012	Rotterdam	Netherlands	2.8	60	11	ROPAX
2012	Ystad	Sweden	6.25	50 & 60	11	ROPAX
2013	Trelleborg	Sweden	3.5-4.6	50	11	ROPAX
2015	Hamburg	Germany	12	50 & 60	6.6 & 11	Cruise

According to [1], [2] and [31], the main challenges of on-shore power are neutral earthing system, safety requirements for operating staff, non-standard ships and the high cost of installation.

I. Neutral earthing system

Selecting the right earthing arrangement is a determining factor in terms of continuity of service, trouble-free operation, and protection against overloads and faults. During an insulation fault or a phase-to-earth fault, fault currents, touch voltages, and over voltages depend to a large degree on the type of earthing. A direct earthed neutral helps limit over voltages but has high fault currents, while an isolated system limit fault currents but favors high voltages. For both LV and MV installations the type of earthing depends on the type of installation, type of network, type of loads, the need for continuity of service and limits to disturbances for sensitive equipment. Earthing methods and their implementation on ships follows recommendations from standards organizations such as IEC.

A ship could use different earthing methods on board for different areas with the options available being solid earthing, low resistance earthing, high resistance earthing and unearthed systems. The most common system is the high resistance earthing where the transformer neutral is connected to the earth via a high-resistance; the maximum single-phase-to-earth fault current is limited to a value in the range of approximately 5A to 25A primary current, depending on the value of capacitive leakage current of the network and the current through resistor. This is because of the low earth fault current, low damage and limited transient over voltages if the current limited by the resistance is higher than 2 times the charging current. This method is very widely used on bulk carrier ships, chemical ships, cargo ships, container ships, Ro-Ro ships, reefer ships, tankers, cruise liners, offshore supply ships, recreational vessels, coast guard ships, frigates, destroyers, supply ships and aircraft carriers.

According to the IEC/ISO/IEEE 80005-1 requirements, for Ro-Ro cargo ships, nominal voltage is 11kV - 6.6kV with low resistance earthing of 325/200 ohms NGR

with high resistance earthing on ship side. For Cruise ships, nominal voltage of 11kV - 6.6kV with low resistance earthing of 540 ohms NGR with high resistance earthing on ship side. For container ships, nominal voltage of 6.6kV with low resistance earthing of 200 ohms NGR with high resistance earthing on ship side and for LNG carriers and tankers nominal voltage of 6.6kV with unearthed system or high resistance on ship side. During the shore start sequence, there is risk that shore substation will close its main output breaker once the ship has already energized the connection cable. To prevent the shore from being connected to a ship without synchronization, dead bus verification (ANSI 84) is set up on the main output breaker. This protection enables the closing of the main output breaker only if no voltage is detected downstream.

II. Safety of operation staff

The possible risks are failure to disconnect from the shore substation, failure to disconnect from ship power system and failure to discharge the MV cable. Protecting personnel from direct and indirect electrical shocks and internal arcing requires appropriate standardized measures such as envelopes, barriers, equipotential bonding, interlocks, and safety instructions. In addition, high-voltage equipment must be internal-arc type [15].

III. Nonstandard ships

Ship design is not standard hence space, accessibility, interfacing with power management system and the diesel engines all need to be surveyed and assessed prior to installation. These equipment are also designed for extreme weather conditions (at berth).

IV. High initial cost

The cost of marine bunkers fuels is cheap compared to initial cost of shore power. Cheaper, modular, reliable, competitive and upgradable shore connection needs to be developed in order to effectively compete with on board power.

2.3 Power system modelling

A power system is an interconnection of generators, transmission facilities and loads. In order to perform a study and predict behaviour of a power system, a representative model has to be developed and implemented in an analysis tool. Most analysis tools such as Matlab/Simulink, PSAT and PSS contain standard models for generation, transmission and distribution resources and loads. The loads encountered in different distribution systems is however unique and requires to be modelled in each case. A load consists of various components with various characteristics which are represented in an equivalent single model. Load modelling is a major challenge as it heavily depends on changing system dynamics. The power system load is comprised of many different devices such as motors, ovens, heaters, lamps, refrigerators, furnaces, and air conditioners among other loads. These loads change with time, weather, and economy among other factors. In most of power system simulations the load is considered an equivalent load that represents an aggregate effect of many individual devices. For most power system studies, the aggregation is at a substation or distribution point [26].

2.3.1 Categories of load modelling

Traditionally load models are divided into two categories: static and dynamic. A composite load model includes both static and dynamic elements to represent the aggregate characteristics of various loads [32].Static load model provides the active and reactive power needed at any time based on simultaneously applied voltage and frequency. It is capable of representing static load components such as resistive and reactive elements and can also be used as a low frequency approximation of dynamic loads such as induction motors. There are two types of static load models: voltage dependent and frequency dependent. The active and reactive power component of the static load model are always treated separately [33].

Voltage dependent load is represented as an exponential model:

$$P = P_0 \left(\frac{V}{V_o}\right) a \qquad (2.1)$$

$$Q = Q_0 \left(\frac{V}{V_o}\right) b \qquad (2.2)$$

Where

V_0 Initial Load Bus Voltage

V Voltage applied on the load

P_0 and Q_0- Load active and reactive components when the applied voltage is V_0

P and *Q* - Load active and reactive components when the applied voltage is *V*

A and *b* - Exponential parameters

When a and b are equal to 0, 1, and 2, the model represents the constant power, constant current, and constant impedance load respectively. For a common composite system a falls in the range of 0.5 to 1.8 and b is in the range of 1.5 to 6. The ZIP load model is a polynomial that is composed of constant impedance, constant current, and constant power elements. The ZIP load is expressed as

$$P = P_0 \left(p_1 \left(\frac{V}{V_0}\right)^2 + p_2 \left(\frac{V}{V_0}\right) + p_3\right) \qquad (2.3)$$

$$Q = Q_0(q_1\left(\frac{V}{V_0}\right)^2 + q_2\left(\frac{V}{V_0}\right) + q_3) \tag{2.4}$$

whereV_0, V, P_0, Q_0, P, and Q represent the same parameters as shown in the voltage dependent model. Other parameters are as follows:

p1, *p2*, and *p3* - Coefficients for defining the proportion of conductance, active current, and active power components

q1, *q2*, and *q3* - Coefficients for defining the proportion of susceptance, reactive current, and reactive power components

The Frequency dependent load model is represented by multiplying a frequency dependent factor with the voltage dependent model as shown equations below

$$P = \left[P_0\left(\frac{V}{V_0}\right)^a\right]\left[1 + K_{pf}(f - f_0)\right] \tag{2.5}$$

$$Q = \left[Q_0\left(\frac{V}{V_0}\right)^b\right]\left[1 + K_{qf}(f - f_0)\right] \tag{2.6}$$

$$P = \left[P_0\left(p_1\left(\frac{V}{V_0}\right)^2 + p_2\left(\frac{V}{V_0}\right) + p_3\right)\right]\left[1 + K_{pf}(f - f_0)\right] \tag{2.7}$$

$$Q = \left[Q_0(q_1\left(\frac{V}{V_0}\right)^2 + q_2\left(\frac{V}{V_0}\right) + q_3)\right]\left[1 + K_{qf}(f - f_0)\right] \quad (2.8)$$

Where, V_0, V, P_0, Q_0, P, and Q represent the same parameters as shown in the voltage dependent model. Other parameters are as follows:

f0 - Initial bus frequency

f - Applied bus frequency

Kpf- Parameters ranging from 0 to 3.0

Kqf- Parameters ranging from -2.0 to 0

Dynamic load model represent a differential equation that gives the active and reactive power at any time based on instantaneous and past applied voltage and frequency while composite load model represent aggregate characteristics of various load components that take into account both static and dynamic behaviour [26], [18].

2.3.2 Load modelling approaches

There are two commonly used methods to acquire the parameters of a load model, namely measurement based and component based [34]:

Measurement based modelling: This method is considered a top-down approach where measurements of complex power, voltage, current, and frequency at the load bus can be used to extrapolate parameters of the composite load model. These measurements may be performed from staged tests, actual system transients, or continuous system operation [32].

Component based: This approach is considered a bottom-up method where parameters are estimated by investigating and aggregating the detailed characteristics of various types of system loads such as industrial, commercial, residential, and

agricultural which are generally well known. The mix of devices can be determined from load surveys, customer satisfactions, and typical compositions of different types of loads. The load mix is determined from customer satisfaction because it varies from bus to bus depending on what the customer wants to switch on at that time hence dependent on weather and time. The component load model could not represent accurately the steady-state reactive power versus voltage responses as well as the transient response of active and reactive power because of the complex non-linear characteristics of load components. The component based load modelling needs reliable data, which is very difficult to acquire in this method the components parameters are given by the manufacturers and can also be used where the industrial load has known motors [35].

The IEEE [10], [18] has proposed a standard composite load model for power system studies. For voltage stability studies, it recommends a composite load model consisting of constant power loads (static loads) and dynamic loads which are voltage and frequency dependent. The basic structure is as shown in Figure which includes static loads and induction motors.

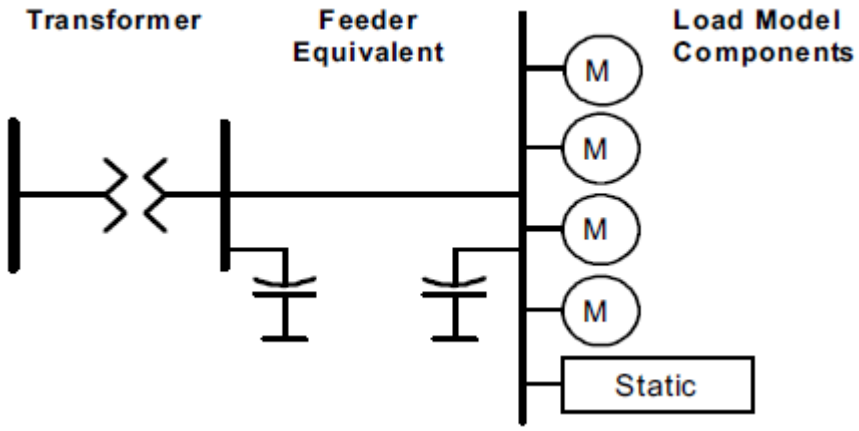

Figure 2.2: Basic Composite Load Model

The Western Electricity Coordination Council (WECC) has since produced further updates to the model [36], [37] and [38], in order to tune it to results observed on

their network. The modified models propose that air conditioning motors and electronically controlled loads should be modelled separately. It also proposes inclusion of under voltage tap changers and under frequency load shedding devices. The resulting model is shown in Figure 2.3.

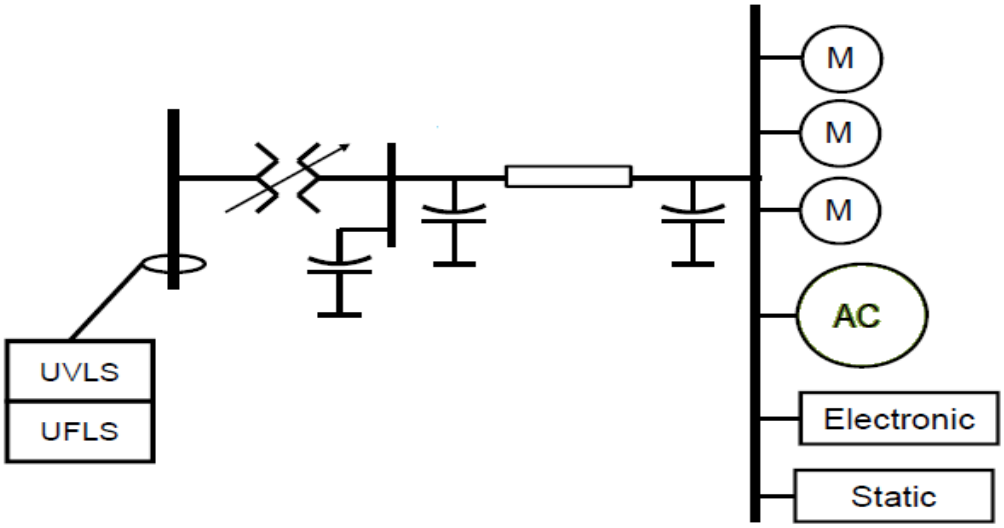

Figure 2.3: Modified Composite Load Model

In this study, the largest component of the load is induction motors followed by constant power loads such as equipment in the cooking range. The basic model of the composite load was therefore applied. This involved aggregation of induction motors which is reviewed in the next section.

2.3.3 Aggregation of induction motor load

In order to reduce complexity and to simplify the dynamic analysis of a ship power system, the number of induction motors is reduced to one equivalent load by aggregation method. The aggregation of a group of induction motors is paramount for dynamic analysis since they contribute the biggest percentage of power system loads. The accuracy of the aggregation method depends on the precise formulation of simplifying assumptions. Homogeneous motors can also be grouped using grouping criterion [39].The grouping criterion is expressed as:

$$G = a \times b \times J \tag{2.9}$$

$$a = \frac{X_m}{R_2} \tag{2.10}$$

$$b = \frac{(X_1 + X_2)}{(R_1 + R_2)} \tag{2.11}$$

Where J is the inertia of the system, G_{MAX} is the maximum grouping criteria and

G_{MIN} is the minimum grouping criteria. The group is homogeneous if the following range is met:

$$1 \leq \frac{G_{MAX}}{G_{MIN}} \leq 2.5 \tag{2.12}$$

The possible maximum limit for the grouping criteria (G) is 2.5, a value beyond this Figure will result into motors being non homogeneous. The minimum is 1.0

2.3.4 Aggregation using equivalent circuit of an induction motor

The simplified equivalent circuit of the three- phase induction motor is shown in Figure 2.4 [24].

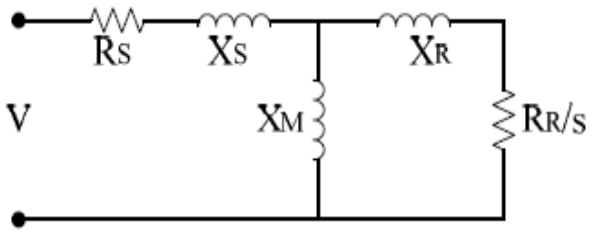

Figure 2.4: Equivalent IEEE circuit model for an induction motor

Where;

R_S Stator Resistance

X_S Stator Reactance

R_R Rotor Resistance

X_R Rotor Reactance

X_M Magnetizing Reactance

s Slip of the induction motor

The slip is calculated from:

$$s = \frac{\omega_{syn} - \omega_m}{\omega_{syn}} \tag{2.13}$$

Where:

ω_{syn} is the synchronous angular speed of the magnetic field

ω_m- The angular speed of the motor

The motor synchronous speed is calculated as

$$\omega_{syn} = \frac{2\pi f}{p} \tag{2.14}$$

Where:

p is the number of poles in the motor and

f is the supply frequency.

For N Induction motors, the representation is as in Figure [24],

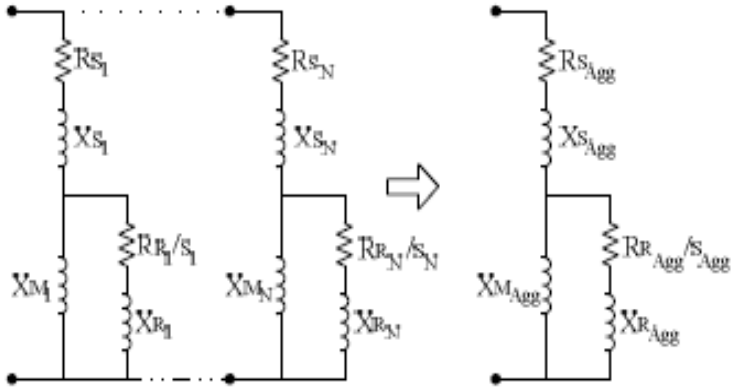

Figure 2.5: Equivalent circuit parameters for the aggregate model

The assumptions made are; Motors are connected in parallel on the same bus operating at a common voltage and frequency, the power and torque of the aggregate motor are equal to the sum of the power and the sum of the torque of the motors under consideration and the motors have the same number of poles [40]. Using this data and applying the assumptions, the equivalent circuit parameters are determined by applying two operating conditions: no-load test (slip = very small to near 0) and locked-rotor test (slip = 1).

In the no-load operating condition, it is assumed that the slips of all the induction motors are near zero, i.e., $s_1 = \ldots = s_N = s_{Agg} = 0$. Therefore, the no-load impedance of each individual motor is given by

$$Z_{NLi} = (R_{Si} + j(X_{Si} + X_{Mi}), \qquad i = 1, 2, \ldots N \tag{2.15}$$

Where:

N is the number of the induction motors.

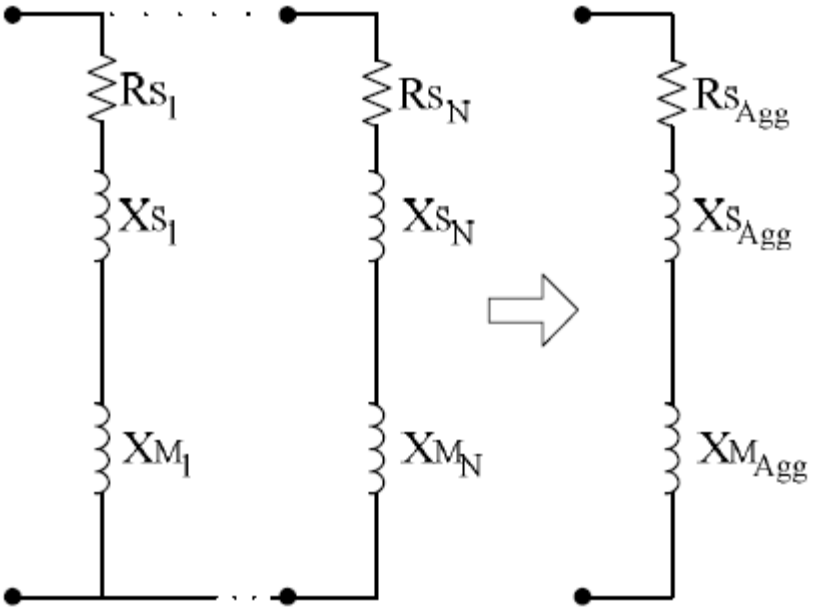

Figure 2.6: No - Load operating condition representation

Since all N motors are in parallel and on the same bus, as in Figure , the total no-load impedance is given by

$$Z_{NLeq} = {1}\Big/{\sum_{i=1}^{N} \frac{1}{Z_{NLi}}} \tag{2.16}$$

The no-load impedance of the aggregation model is given

$$Z_{NLAgg} = R_{SAgg} + j\left(X_{SAgg} + X_{MAgg}\right) \tag{2.17}$$

by comparison of (2.16) and (2.17) we get that

$$R_{SAgg} = \mathcal{R}eal\{Z_{NLeq}\}$$

$$\left(X_{SAgg} + X_{MAgg}\right) = Imag\{Z_{NLeq}\} \tag{2.18}$$

For the locked- rotor operating condition, it is assumed that the slips of all induction motors are equal to unity i.e,$s_1 = \ldots = s_N = s_{Agg} = 1$. The locked-rotor impedance of each individual motor is given by

$$Z_{LRi} = R_{Si} + R_{Ri} + j(X_{Si} + X_{Ri}), \qquad i = 1, 2, \ldots N \tag{2.19}$$

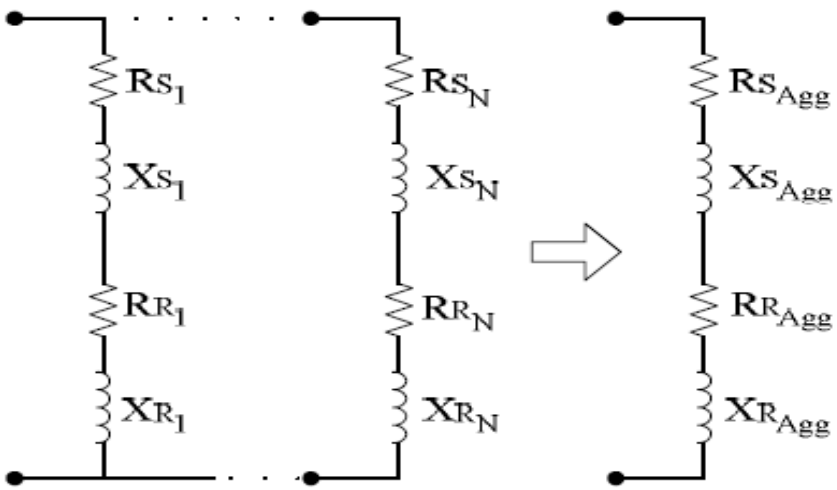

Figure 2.7: Locked - rotor operating condition representation

For all N motors connected in parallel and on a common bus as in Figure , the total locked impedance is given by

$$Z_{LReq} = 1 \Big/ \sum_{i=1}^{N} \frac{1}{Z_{LRi}} \tag{2.20}$$

The locked -rotor motor impedance of the aggregate model is given by

$$Z_{LRAgg} = R_{SAgg} + R_{RAgg} + j\left(X_{SAgg} + X_{RAgg}\right) \tag{2.11}$$

Comparing (2.20) and (2.21)we get

$$R_{SAgg} + R_{RAgg} = \mathcal{R}eal\{Z_{LReq}\}$$

$$\left(X_{SAgg} + X_{RAgg}\right) = Imag\{Z_{LReq}\} \tag{2.22}$$

R_{RAgg}can be obtained from (2.18) and 2.22) . This is given by

$$R_{RAgg} = \mathcal{R}eal\{Z_{LReq}\} - \mathcal{R}eal\{Z_{NLeq}\} \tag{2.23}$$

The reactance parameters (X_{SAgg} and X_{RAgg}) of the aggregation model can be determined based on the IEEE Standard 112-2004 , which defines the ratio (n) of leakage inductances of induction motors based on the motor class [41]. This is given by

$$n = {X_{SAgg}}\Big/{X_{RAgg}} \tag{2.24}$$

$$X_{SAgg} = \frac{n}{n+1} Imag\{Z_{LReq}\}$$

$$X_{RAgg} = \frac{1}{n+1} Imag\{Z_{LReq}\} \tag{2.25}$$

Hence, the magnetizing reactance $X_{\text{Magg can}}$ be found from (2.18) and (2.25). This is given by

$$X_{MAgg} = Imag\{Z_{NLeq}\} - \frac{n}{n+1} Imag\{Z_{LReq}\} \tag{2.26}$$

To obtain the slip, it is assumed that each individual induction motor has a steady-state slip value of s1, s2, …, and sN, respectively., and the aggregate motor has a slip of sAgg. Therefore, the impedance of each individual motor is given by

$$Z_i = Z_{Si} + \frac{Z_{Mi} . Z_{Ri}}{Z_{Mi} + Z_{Ri}} \ , \qquad i = 1, 2, \ldots, N \tag{2.27}$$

Where,

$Z_{Si} = R_{Si} + \mathrm{j}X_{Si}$

$Z_{Mi} = \mathrm{j}X_{Mi}$

$$Z_{Ri} = R_{Ri}/s_i + jX_{Ri}$$

Since all N motors are connected in parallel at the same bus, the total equivalent impedance can also be obtained by

$$Z_{eq} = 1 \Big/ \sum_{i=1}^{N} \frac{1}{Z_i} \tag{2.28}$$

Considering the impedance of the aggregate motor $Z_{Agg} = Z_{eq}$, the aggregate motor slip, s_{Agg}, can be formulated as follows:

$$\alpha s_{Agg}^2 + \beta s_{Agg} + \gamma = 0 \tag{2.29}$$

Where,

$$\alpha = \left(X_{MAgg} + X_{RAgg}\right)^2 \left(\mathcal{R}eal\{Z_{ieq}\} - R_{SAgg}\right)$$

$$\beta = R_{RAgg}.{X_{MAgg}}^2$$

$$\gamma = \left(\mathcal{R}eal\{Z_{ieq}\} - R_{SAgg}\right).{R_{RAgg}}^2$$

We then have:

$$s_{Agg} = \frac{-\beta \pm \sqrt{\beta^2 - 4\alpha\gamma}}{2\alpha} \tag{2.30}$$

As commonly assumed, the mechanical output power from the aggregate motor is equal to the total mechanical output power from all individual induction motors. This is given by

$$P_{Agg} = \sum_{i=1}^{N} P_i, \quad i = 1, 2, \ldots, N \tag{2.31}$$

N_{Agg} is obtained by N_{Agg}= Ns*(1-S_{Agg}) in radians RPM and consequently

ω_{rAgg}.is obtained by N_{Agg}*2*pi/60 in radians per second

The moment of inertia is obtained from the following relation

$$J_{Agg} = \sum_{i=1}^{N} J_i \cdot (\frac{\omega_{ri}}{\omega_{rAgg}})\text{^}2 \tag{2.32}$$

Whereω_{ri} and $\omega_{rAgg}$are the rotor angular speeds of the i^{th} individual motor and the aggregate motor, respectively.

The equivalent circuit method illustrated above is the method used in this research. This is because it is simplified and the fast availability of the required induction motor manufacturers data.

2.3.5 Aggregation using energy conservation method

In [27] a simple and efficient method of aggregating induction motor where the parameters for the motor are derived using energy conservation law is presented. In this method, the steady-state model of induction motor is represented by the equivalent circuit as shown in Figure 2.8.

Where,

R_s and R_r are stator and rotor resistance

Xls and *Xlr* are stator and rotor leakage reactance

Xm is mutual reactance.

$$Tm - Te = 0 \tag{2.33}$$

where,

$$T_m = T_0(A(1-s)^2 + B(1-s) + C) \tag{2.34}$$

$$T_e = \left((X_m V_s)^2 / \left((R_{th} + \frac{R_r}{s})^2 + (X_{th} + X_{lr})^2\right)(R_s^2 + (X_m + X_{ls})^2)\right)\frac{R_r}{s}$$

$$R_{th} = \frac{R_s X_m^2}{R_s^2 + (X_m + X_{ls})^2}$$

$$X_{th} = \frac{R_s^2 X_m + X_m X_{ls}(X_m + X_{ls})}{R_s^2 + (X_m + X_{ls})^2}$$

(2.35)

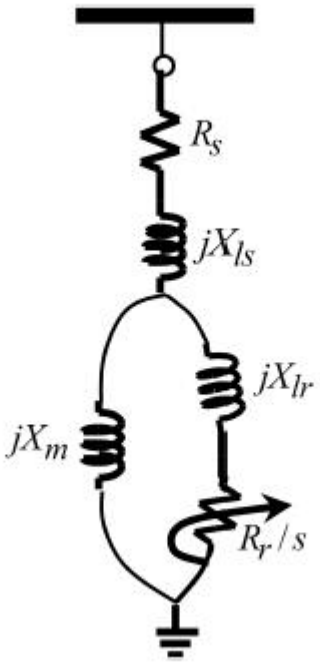

Figure 2.8: Equivalent circuit model of induction motor

By considering the group of induction motors connected at the same buses, the layout is as shown in Figure 2.9. In this grouping procedure, it is initially assumed that all parameters of each motor are known and that the parameters are required to be adjusted to the same common MVA base. If the operating slip of each individual motor is not available, it is calculated using equation 2.35 with terminal voltage of 1.0pu (Vs). In this method, as in the single equivalent circuit, with all parameters of resistance, reactance, slip and mutual reactance known, the input current, active and reactive power are computed.

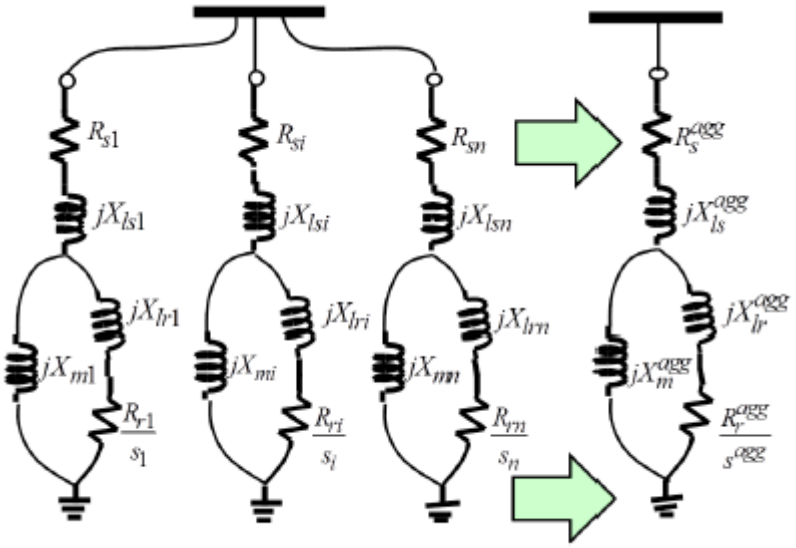

Figure 2.9: Aggregate equivalent circuit model

By applying the energy conservation law, the apparent power absorbed by the aggregate motor is equal to the total power absorbed by all motors. The phase or quantities for the stator current and rotor current are obtained. Based on the energy conservation law, the other circuit parameters are derived as follows

$$\widetilde{I}_s^{agg} = \sum_{i=1}^{n} \widetilde{I}_{si}$$

$$\widetilde{I}_r^{agg} = \sum_{i=1}^{n} \widetilde{I}_{ri} \tag{2.36}$$

$$R_s^{agg} = \frac{\sum_{i=1}^{n} |\widetilde{I}_{si}|^2 R_{si}}{|\widetilde{I}_s^{agg}|^2} \tag{2.37}$$

$$R_r^{agg} = \frac{\sum_{i=1}^{n} |\widetilde{I}_{ri}|^2 R_{ri}}{|\widetilde{I}_r^{agg}|^2} \tag{2.38}$$

$$X_{ls}^{agg} = \frac{\sum_{i=1}^{n} |\widetilde{I}_{si}|^2 X_{lsi}}{|\widetilde{I}_s^{agg}|^2} \tag{2.39}$$

$$X_{lr}^{agg} = \frac{\sum_{i=1}^{n} |\widetilde{I}_{ri}|^2 X_{lri}}{|\widetilde{I}_r^{agg}|^2} \tag{2.40}$$

$$X_{m}^{agg} = \frac{\sum_{i=1}^{n} |\widetilde{I}_{si} - \widetilde{I}_{ri}|^2 X_{mi}}{|\widetilde{I}_s^{agg} - \widetilde{I}_r^{agg}|^2} \tag{2.41}$$

The air -gap power of the aggregate motor can be expressed as

$$P_{ag}^{agg} = \sum_{i=1}^{n} \{Re(\widetilde{V}_{si}\widetilde{I}_{si}^{*}) - |\widetilde{I}_{si}|^2 R_{si}\} \tag{2.42}$$

while slip will be

$$s^{agg} = \frac{|\widetilde{I}_r^{agg}|^2 R_r^{agg}}{P_{ag}^{agg}} \tag{2.43}$$

Using the kinetic energy conservation law,

$$H^{agg} = \frac{\sum_{i=1}^{n} H_i S_i}{S^{agg}} \tag{2.44}$$

where,

$$H_i S_i = \frac{1}{2} J_i \omega_{si}^2 \tag{2.45}$$

$$S^{agg} = \sum_{i=1}^{n} S_i \tag{2.46}$$

The moment of inertia Jagg is obtained by

$$J^{agg} = \frac{2H^{agg} S^{agg}}{(\omega_m^{agg})^2} \tag{2.47}$$

where,

$$\omega_m^{agg} = \omega_s (1 - s^{agg})(\frac{2}{P^{agg}}) \tag{2.48}$$

The pseudo number of pole P_{agg} can be determined from equation 2.44 and with the assumption that the total amount of mechanical power equals to the mechanical power delivered by all motors in the group the mechanical torque is obtained by,

$$T_m^{agg}(1-s^{agg}) = \sum_{i=1}^{n} T_{mi}(1-s_i) \tag{2.49}$$

where ,

$$\begin{aligned} T_m^{agg} =& T_0^{agg}(A^{agg}(1-s^{agg})^2 \\ &+ B^{agg}(1-s^{agg}) + C^{agg}) \end{aligned}$$

$$T_{mi} = T_{0i}(A_i(1-s^{agg})^2 + B_i(1-s^{agg}) + C_i)$$

$$A^{agg} + B^{agg} + C^{agg} = 1 \tag{2.50}$$

By setting the slip to zero in equation 2.50, the parameter T*agg* is obtained as

$$T_0^{agg} = \sum_{i=1}^{n} T_{0i}(A_i + B_i + C_i) \tag{2.51}$$

The torque coefficients can then be computed as

$$A^{agg} = \frac{\sum_{i=1}^{n} T_{0i} A_i (1 - s_i)^3}{T_0^{agg} (1 - s^{agg})^3}$$

$$B^{agg} = \frac{\sum_{i=1}^{n} T_{0i} B_i (1 - s_i)^2}{T_0^{agg} (1 - s^{agg})^2}$$

$$C^{agg} = \frac{\sum_{i=1}^{n} T_{0i} C_i (1 - s_i)}{T_0^{agg} (1 - s^{agg})} \quad (2.52)$$

2.4 Motor initialization for power flow study

The original IEEE composite model [10],[18] proposed that the motor be treated as a PV load for long term voltage stability studies, with the reactive power calculated after convergence of a power flow. This approach will result in inaccuracies because motor power is not constant but is dependent on voltage. The dynamic parameters of an induction motor can be included in a load flow study if a run of the motor is simulated and initial operating conditions identified before the power flow is carried out [42]. After initialisation, only one parameter such as slip or torque will be considered as variable. The use of initialisation method is limited by the tool used for analysis. This study will therefore apply the method used in PSAT (as presented in [28]), which considers electromagnetic torque as the variable parameter after initialisation.

2.5 Power system stability

Power system stability is the ability of an electric power system, for a given initial operating condition, to regain a state of operating equilibrium after being subjected to a physical disturbance, with most system variables bounded, so that practically the entire system remains intact [11]. Stability analysis deals with the determination of the effects of disturbances on power systems. The disturbance may vary from being the usual fluctuation of the load to severe fault causing the loss of an important transmission line [43]. The power system is an extremely non-linear and dynamic system, with operating parameters continuously varying. Stability is hence, a function of the initial operating condition and the nature of the disturbance. The power system is generally designed to be stable under those disturbances which have a high degree of occurrence. The high complexity of stability problems has led to a meaningful classification of the power system stability into various categories. These are (rotor) angle stability, frequency stability and voltage stability. These classification takes into account the main variables in which instability can be observed, the size of the disturbance and the time span to be considered for assessing stability as illustrated by Figure 2.10 [32].The classification of power system stability assists in selection of the method of analysis to apply [11]. According to [12] pure rotor angle stability applies when the system is a generator connected to an infinite bus while pure voltage stability applies when the system is an isolated load supplied from an infinite bus. The system in this study is closer to the second case than in the first case and voltage stability will be applied as the method of analysis. A detailed look into voltage stability is presented in the next section.

2.5.1 Voltage stability

Voltage stability is the capability of the power system to sustain steady state voltages at all buses in the system after being subjected to a disturbance for an operating initial condition [33]. Instability results in a progressive fall or rise of voltages at

some buses, which could lead to loss of load in an area or tripping of transmission lines, leading to cascading outages. This may eventually lead to loss of synchronism of some generators. A rundown situation causing voltage instability occurs when load dynamics attempt to restore power consumption beyond the capability of the transmission network. Voltage stability is also threatened when a disturbance increases the reactive power demand beyond the sustainable capacity of the available reactive power resources. Voltage stability is divided into small and large disturbances. Small disturbance voltage stability refers to the system's ability to maintain steady voltages when subjected to small perturbations such as incremental changes in load. This is primarily influenced by the load characteristics and the controls at a given point of time. The analysis of small disturbance voltage stability is normally carried out using power flow based tools (steady state analysis) where the power system is linearized around an operating point using Eigen values and eigenvectors [40]. Large disturbance voltage stability refers to the system's ability to maintain steady bus voltages following large disturbances such as a system faults, switching or loss of load or loss of generation. It requires computation of the non-linear response of the power system to include interaction between various devices like motors, transformer tap changers and generator field current limiters. Their study can be done using non- liner time domain simulations in the short-time frame and load-flow analysis in the long-term time frames (Steady state dynamic analysis) with a period of few tens of seconds to tens of minutes [40].

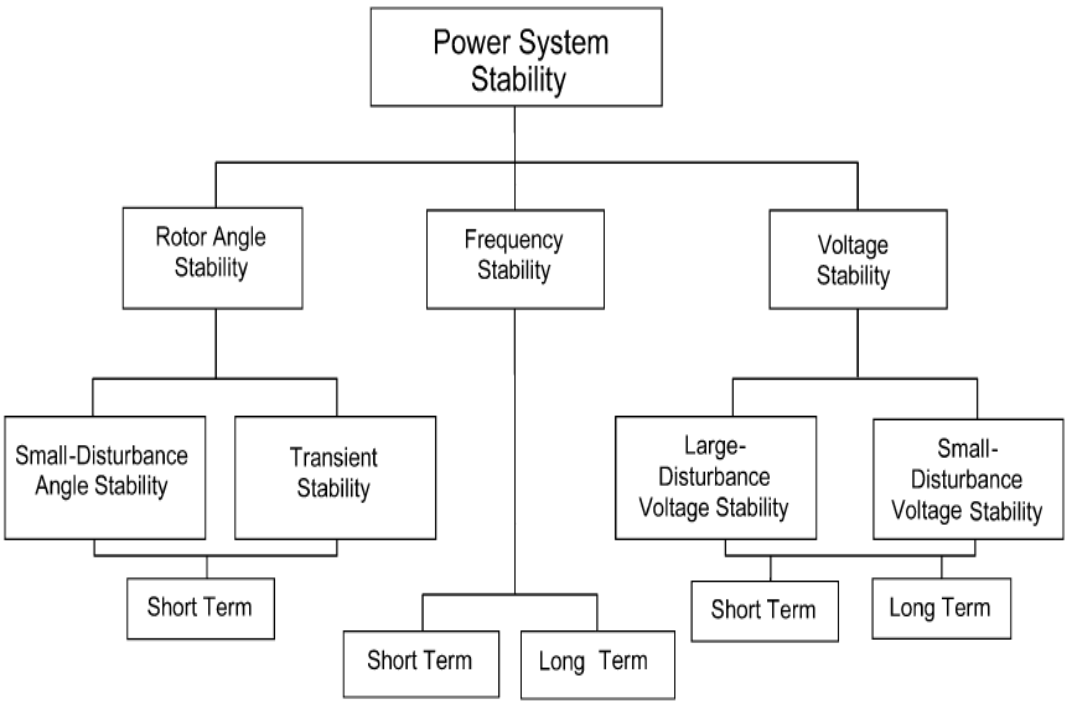

Figure 2.10: Classification of power system stability

Short term voltage stability involves dynamics of fast acting load components and a period of several seconds. Short term voltage instability is characterized by the presence of equipment such as induction machines, generators, AVRs and power electronics converters such as FACTS devices and HVDC links [44]. In AVRs, inappropriate tuning of the controllers may cause voltage instability while for induction motors, the contingency or rapid load increase may occur causing a decline in bus voltages to the extent that the induction motors stall. The main cause of short term voltage stability is the tendency of the dynamic loads to restore back in the system frame in a few seconds [40]. Long term voltage stability occurs if the system has survived short term voltage stability after a disturbance. As the system voltage decreases, controls to restore voltage near the pre-contingency levels are activated. These controls are automatic switched capacitors, under load tap changers, static VAr systems (SVS) and generator current limiters. Instability is due to loss of long-term equilibrium which extends from a few minutes to hours [40].

2.5.2 Causes of voltage instability

Voltage instability is the absence of voltage stability and results in progressive voltage collapse [32]. The main cause of voltage instability is the incapacity of system to provide required reactive power demand under heavily stressed conditions to keep the voltage at acceptable limits. When a system cannot be restored by the action of voltage control devices such as load tap changers, voltage dependence characteristics of the load and generator reactive power limits, it which can lead to system low voltage values in a large section of the system that eventually lead to partial total voltage collapse. Voltage stability is highly dependent of system loading and reactive power reserves [32].

2.5.3 Methods for preventing voltage instability

Preventive control refers to actions in the normal state to bring back system back from insecure to secure state. This involves operating system at higher cost. In the event that preventive controls do not restore to secure state, extreme measures will be taken like load shedding. Considering all possible disturbances, that it is almost impossible to find a secure power system [45]. For this reason, system security is checked with reference to a set of credible disturbances referred to as next contingencies. In long term voltage stability, the relevant contingencies are outages of transmission lines and generation facilities where N-1 criterion is used [32].

Methods of improving voltage stability include,

i. Load tap changers: Two types of tap changers can be used namely under load tap changers and off-load tap changers. Under load tap changers automatically changes main power transformers to enable utilization of different voltage levels across the system. Mostly the tap changing is done on the high voltage side due to its lower current and less insulation requirement. Similarly the HV side has more turns hence making regulation more precise. This type of regulation is applied when changes are required frequently due

to simultaneous changes in load such as daily variations. Off -load tap changers require the transformers to be inactive and it is normally applied when long-term variations are required such as seasonal changes. Tap changing allows voltage changes in the range of +-10% to +-15%.

ii. Compensation devices: These are used to control voltage by supplying or absorbing reactive power. These devices include static VAR compensators, synchronous condensers, shunt reactors and capacitors.

Static VAR compensators are shunt connected static reactive power generators or absorbers which are used to control individual phase voltages on the connected buses. They use thyristor controlled circuits where direct and quick voltage control/response is required. Series capacitors are connected in series hence line reactance is reduced allowing maximum power to be transferred with reduced reactive power requirements on that line.

Synchronous condensers are synchronous machines running without mechanical load. By controlling the field excitation it can either work to generate or absorb reactive power to automatically adjust reactive power output for voltage control using a voltage regulator. These condensers are often connected to tertiary windings of a transformer.

Shunt reactors are used to compensate for the effects of line capacitance. In case of over voltages on the system they are activated to absorb reactive power from the system on lightly loaded lines. On heavily loaded lines, they are not useful.

Shunt capacitors are used to compensate for reactive power in transmission lines to ensure voltage control during heavy power requirements. They are connected directly on a bus or at the tertiary winding of the main transformer. Use of these capacitors also minimizes losses and voltage drops and in effect allows maximum power transfers on the system. They are also used in

distribution systems for power factor correction at the point of use (near load point) as reactive power cannot be transferred over long distances.

iii. Load shedding: This is normally considered as a last resort as it involves disconnecting some customers. This can be done manually or automatically. Automatic load shedding is used during short term stability.

iv. Activation of generation units: These generation units ought to be fast starting machines that can start in a few seconds/minutes. Synchronous generators can generate (over-excited) or absorb (under-excited) reactive power. The capability of a generator to provide reactive support depends on the capability curve. Generators are limited by their current-carrying capability namely nominal rated voltage is limited by the a armature heating limit, production of reactive power by the field heating limit and absorption of reactive power by stator-end iron/Core-end heating limit as illustrated by Figure 2.11.Synchronous generators are normally equipped with AVRs which continuously adjust the excitation to control the armature voltage. Another way of preventing voltage instability using generation units is to ensure spinning reserves are available and synchronised to the power system with proper coordination.

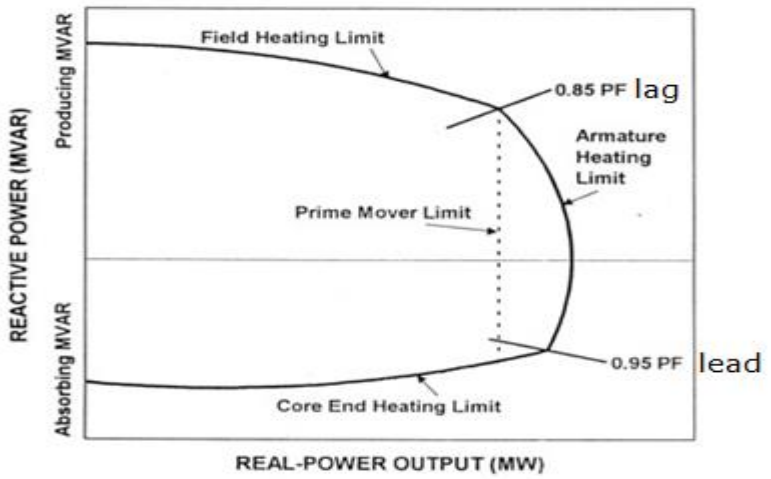

Figure 2.11: Reactive power capability for a synchronous generator

2.6 Power margin determination

In order to assess how close the system is to voltage collapse, PV and QV curves can be used to determine the power loading/maximum power transfer and reactive power requirements respectively. This is illustrated using a simplified two bus system shown in Figure [46].

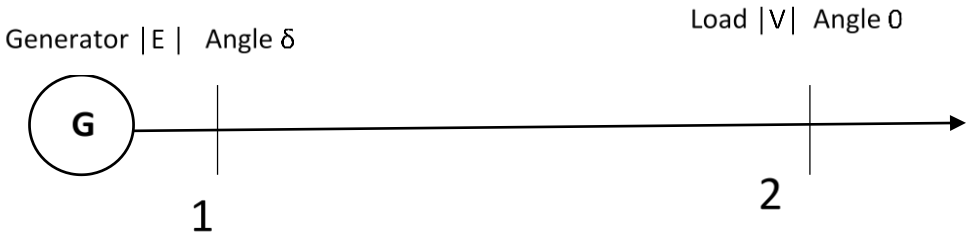

Figure 2.12: Two Bus System

The assumption made is that the system is lossless and that the power factor remains constant.

The power transferred is given by,

$$P = \left(\frac{EV}{X}\right) * sin(\delta) \tag{2.53}$$

The assumption made is that the system is lossless and that the power factor remains constant.

Reactive power transfer from bus 1 to 2 is given by:

$$Q = \left(-\frac{V^2}{X}\right) + \left(\frac{EV}{X}\right) * cos(\delta) \tag{2.54}$$

Where: E is voltage at bus 1 with angle δ, V is voltage at bus 2 with angle 0 , X is impedance of the line (neglecting resistance) and δ is power angle

2.6.1 PV curves:

A plot of PV curves as illustrated in Figure 2-13 corresponds to the graphical representation of power voltage function at the load bus [46]. The curve defines the specific power parameters that can be transferred at different voltage levels (high and low). Power systems are operated in the upper part of the PV-curve. This part of the PV-curve is statically and dynamically stable. The head of the curve is called the maximum loading point. The critical point where the solutions unite is the voltage collapse point. The maximum loading point is more interesting from the practical point of view than the true voltage collapse point, because the maximum of power system loading is achieved at this point. The maximum loading point is the voltage collapse point when constant power loads are considered, but in general they are different. The voltage dependence of loads affects the point of voltage collapse. The power system becomes voltage unstable at the voltage collapse point. Voltages decrease rapidly due to the requirement for an infinite amount of reactive power. The lower part of the PV-curve (to the left of the voltage collapse point) is statically stable, but dynamically unstable. The power system can only operate in stable equilibrium so that the system dynamics act to restore the state to equilibrium when it is perturbed. In order to maximize power transfer, the high voltage is desired and the vertex represent the maximum power that can be transmitted by the system. In order to define the voltage stability margins of a system, determination of the maximum amount of power that a system can supply to a load can be established by connecting and disconnecting certain loads using a PV curve [46]. An increase of P beyond the maximum power limits makes the system unstable.

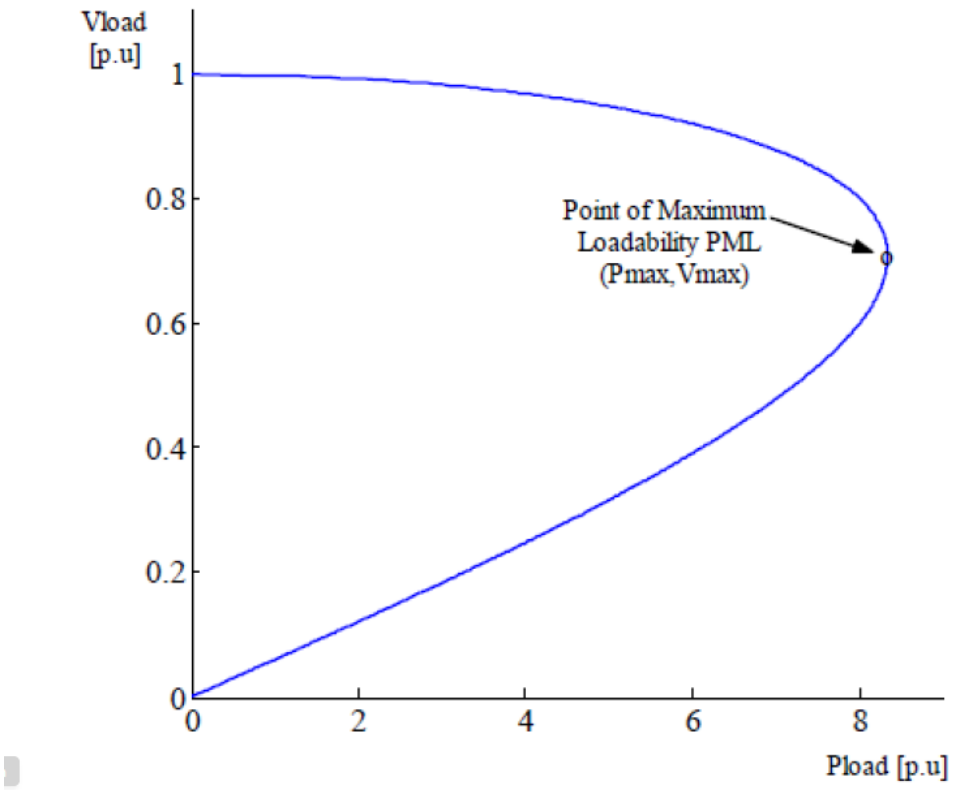

Figure 2.13: PV curve representation for the two bus system

2.6.2 V-Q curves:

V-Q curve method is one way of investigating voltage instability in power systems during post transient period [47]. Voltage at the critical bus or test bus is plotted against reactive power at that bus. Voltage security of a bus is closely related to the available reactive power reserve on that bus and can be found from the V-Q curve. Reactive power margin is the MVAR distance between the operating point and either the point where capacitor characteristics at the bus are tangent to the V-Q curve or the nose point of the V-Q curve. The greater the slope is the less stiff is the bus and hence more venerable to voltage collapse. Reactive power margin indicates how much further the Q- loading on that particular bus can be increased before its loading limit is exhausted leading to voltage collapse. This can be used as an index for

voltage instability. From the two bus system the value of power angle is computed for a specific value of power and used to obtain the value of reactive power. For a range of voltages and active power levels, normalized V-Q curves are as shown in Figure 2-14 [46]. The bottom of any given curve characterizes the voltage stability limit. On the right hand side of the limit, an increase in reactive power injection at the receiving end results in a receiving end voltage rise. The opposite is true on the left side because of the substantial increase in current at the lower voltage, which, in turn, increases reactive losses in the network substantially. The proximity to voltage instability or voltage stability margin is measured as the difference between the reactive power injection corresponding to the operating point and the bottom of the curve. As the active power transfer increases, the reactive power margin decreases, as does the receiving end voltage [40].

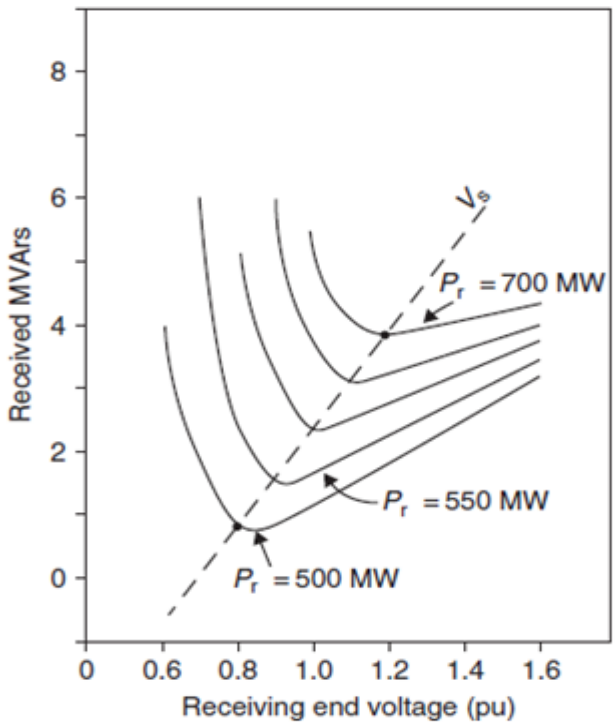

Figure 2.14: VQ curves representation for the two bus system

2.6.3 Voltage instability margin

The proximity to voltage instability or voltage stability margin as shown in Figure 2.15 is measured as the difference between the reactive power injection corresponding to the operating point and the bottom of the curve. As the active power transfer increases, the reactive power margin decreases, as does the receiving end voltage.

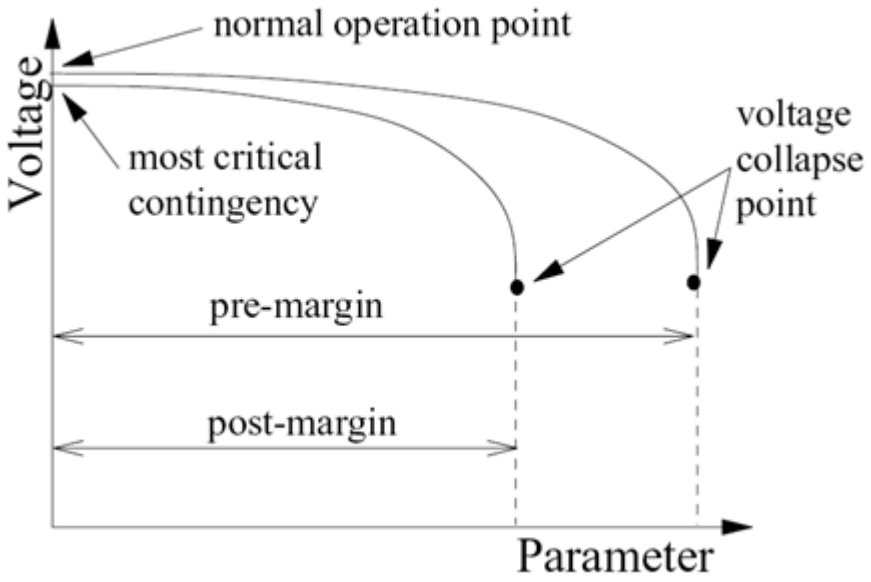

Figure 2.15: VQ curves representation for the two bus system

2.7 Static voltage stability indicators

In [48], analysis of voltage behaviour has been approached using static techniques, which have been widely used on voltage stability analysis. These techniques helps the operator to know how close the system is to voltage instability. The indexes are used to provide reliable information about proximity of voltage instability in a power system. Usually, their values change between 0 (no load) and 1 (voltage collapse).

FVSI was utilized as the measurement to indicate the voltage stability condition in the maximum loadability identification at several load buses, then Fuzzy logic based algorithm for contingencies ranking is presented [48]. Hence the Line Flow (L.F) Index and FVSI are used as a static voltage collapse proximity indicators.

2.7.1 Fast Voltage Stability Index (FVSI)

Voltage stability index proposed by [49] and [50] can be conducted on a system by evaluating the voltage stability referred to a line. The voltage stability index referred to a line is formulated from the 2-bus representation of a system. The voltage stability index developed is derived by first obtaining the current equation through a line in a 2-bus system. Representation of the system illustrated in Figure 2.16 [49].

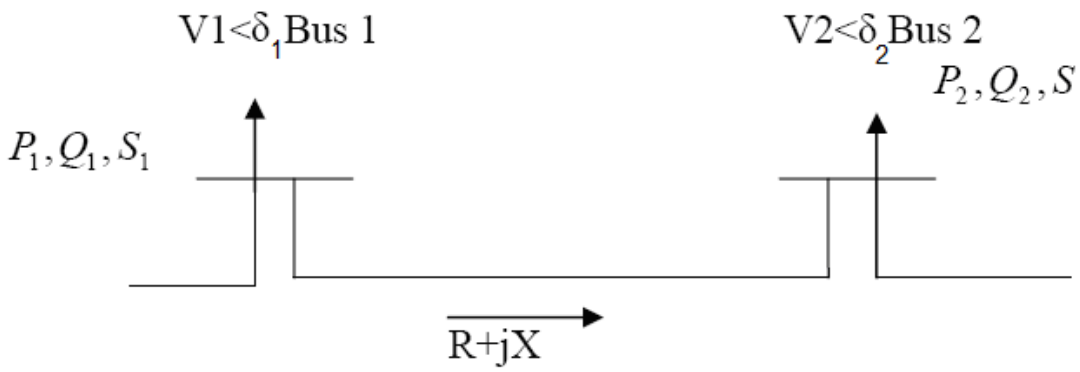

Figure 2.16: Bus System Model

$$FVSI_{ij} = \left(\frac{4 * Z^2 * Q_j}{V_i^{\,2} * X}\right) \tag{2.55}$$

Where: (Z) Line impedance, (X) Line reactance, (Q_j) Reactive power at receiving end and (V_i) Sending end voltage.

When FVSI of any line approaches unity (1) it means that the line is approaching its stability limits hence this index for any line must be lower than 1 at assure the stability of the power system.

2.7.2 Line Flow Index (L.F)

In [49] The Line Flow (L.F) index investigates the stability of each line of the system and they are based on the concept of maximum power transferred through a line as shown in Figure 2.17.

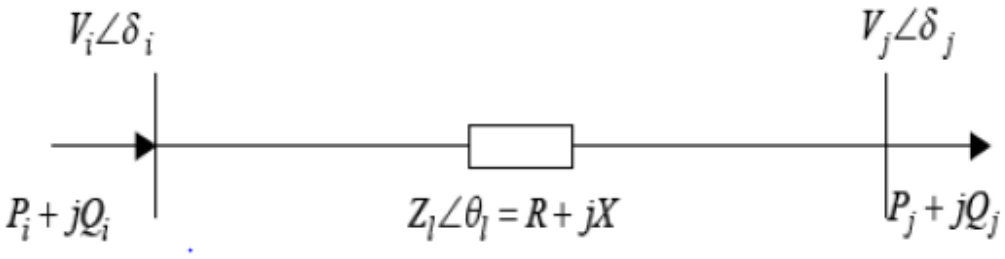

Figure 2.17: Transmission line of a power system network

$$LF_{index} = \frac{P_R}{P_{RMAX}} \tag{2.56}$$

Where:

P_R *is* obtained from conventional power flow calculations, and

P_{Rmax} is the maximum active power that can be transferred through a line

The Line Flow index varies from 0 (no load condition) to 1 (voltage collapse). In order to prevent the system from collapse point the index value should be less than 1.

$$P_{RMAX} = \left(\frac{V_i^{\,2}}{2Z_l}\right)\left(\frac{\cos\varphi}{1+\cos(\theta_l-\varphi)}\right) \tag{2.57}$$

Where: (V_i) is the voltage magnitude of sending bus of branch (i - j), (Z_l) is the magnitude of branch impedance and (θ_l) is the angle of branch impedance

2.8 Continuation Power Flow and Voltage Collapse Prediction

As presented in the previous section, PV curves can be used to predict the possibility of collapse in a power system. For a heavily loaded power system, the possibility of voltage collapse can be predicted by measuring the distance between the current operating point and the point of collapse. The point of collapse for a given bus is indicated by the bifurcation point (the 'nose') in the P-V curve at the bus, as shown in. This point corresponds to the maximum transmission capacity for active power.

Plotting of the P-V curve in the neighbourhood of the bifurcation point is not possible because of the singularity at the point. The continuation power flow [51] is a tool that can be used to plot the complete P-V curve including the singularity. The continuation power flow is a modification of the standard power flow and can be represented as:

$$p_h = p_G - p_L$$

$$q_h = q_G - q_L \tag{2.58}$$

Where: p_h is active power injected at bus h,$p_G$is active power generated at bus h,

p_L is load power consumed at bus h, q_h, q_G and q_L are reactive power injected, generated and consumed at bus h.

In the continuation power flow model, a loading factor, λ, is used to increment the load in fixed steps from a small value. In order to match power generation with the reduced load, all generator capacities are scaled by a participation factor k_g. The expressions for active power generated and load power (active and reactive) therefore become as:

$$p_G = (\lambda I_N + k_g I_N) p_{GO}$$

,

$$p_L = \lambda p_{LO} \tag{2.59}$$

$$q_L = \lambda q_{LO}$$

Where: I_N is the identity matrix of size N, N is the number of generators in the network and p_{GO}, p_{LO} and q_{LO} are base values for generated power, active load power and reactive load power respectively. A numerical solution of the continuation power flow is achieved through a series of prediction and correction steps as demonstrated in Figure 2-18. This eventually results in a plot of the complete P-V curve, including the bifurcation point and the lower and upper solutions.

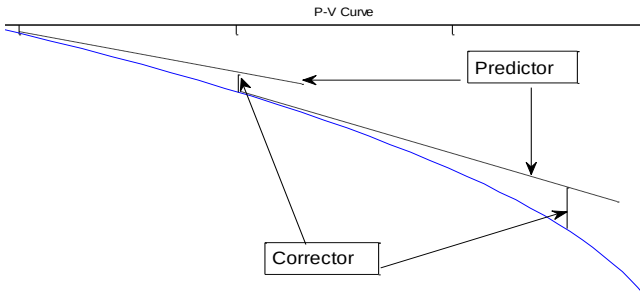

Figure 2.18: Predictor and corrector in continuation power flow

In [52], the method has been applied to a system with induction motor load. In [28], a method is proposed which incorporates the limits for reactive power generation in the continuation power flow solution. This is achieved by implementing reactive power generation limits in the implementation algorithm.

In continuation power flow, limits for reactive power generation and transmission line capacity are applied in the algorithm in order to ensure that solutions obtained are within the capacity of the network.

2.9 Summary of Research Gaps and Proposed Solutions

It has been noted in the literature that shore to ship power connection has been implemented in selected ports is USA and Europe. The challenges experienced in these developed countries are as listed in section 2.2.2 where the identified solutions have been implemented and the installations are successful. Research has also been done on determining the most suitable topology for connecting shore power [1], [2]. Other research done includes assessment of alternative maritime power (cold ironing) and its impact on port management in terms of project costs and environmental pollutants from the maritime sector [6]. In [16], transient analysis of a shore-to-ship power connection was analysed with fault current limitation. All the studies reviewed assumed that the on shore grid is perfect and is able to cope with the effects of ship to shore connection without any adverse effects such as voltage or frequency instability. There was therefore a need to carry out a study on the impact of connecting shore power on the stability of the on a power system. This is especially critical for power systems operating close to their maximum capacity and where the additional load will constitute a considerable increase on the total load on the system. Such systems are common in developing countries. Though a local phenomenon, voltage instability can cause total voltage collapse of the whole grid if left unchecked. This study modelled the case of Mombasa port in order to form the basis for formulation of mitigation factors that would work in Kenya and similar power systems to achieve shore power connections.

CHAPTER THREE

METHODOLOGY

3.1 Introduction

In this chapter, the procedure used to analyse the impact of connecting docking ships to the Kenyan coast power system is presented. This research was carried out in three phases. The activities in the three phases are:

i. Development of a composite load model for ships docked at the port of Mombasa. This has involved collection of data on ships and berthing facilities. Once the data was collected, motor loads and non-motor loads were separately aggregated in order to come up with a composite load model. A transient analysis of the composite load model was then used to validate the model by confirming that the model has the expected characteristics of a composite load. Results of load aggregation was then combined with data on availability of berthing facilities to develop a model of the total off-shore load at the port.
ii. Development of a model for the on-shore power network. This was achieved by collecting data from the electricity utility company, Kenya Power and the main electricity generating company KenGen. Additional data was obtained from reports from donors, Kenya government, and intergovernmental organisations like the East African Community.
iii. Simulating power flow study on the modelled grid in order to analyse the effect of the additional load on voltage stability. This included a baseline power-flow before the additional load is connected and a second load flow including the additional load.

The load aggregation was carried out and analysed using MATLAB/ SIMULINK. The network modelled and power flow study carried out using MATLAB/PSAT. The flow chart for the study is as shown in Figure 3.1

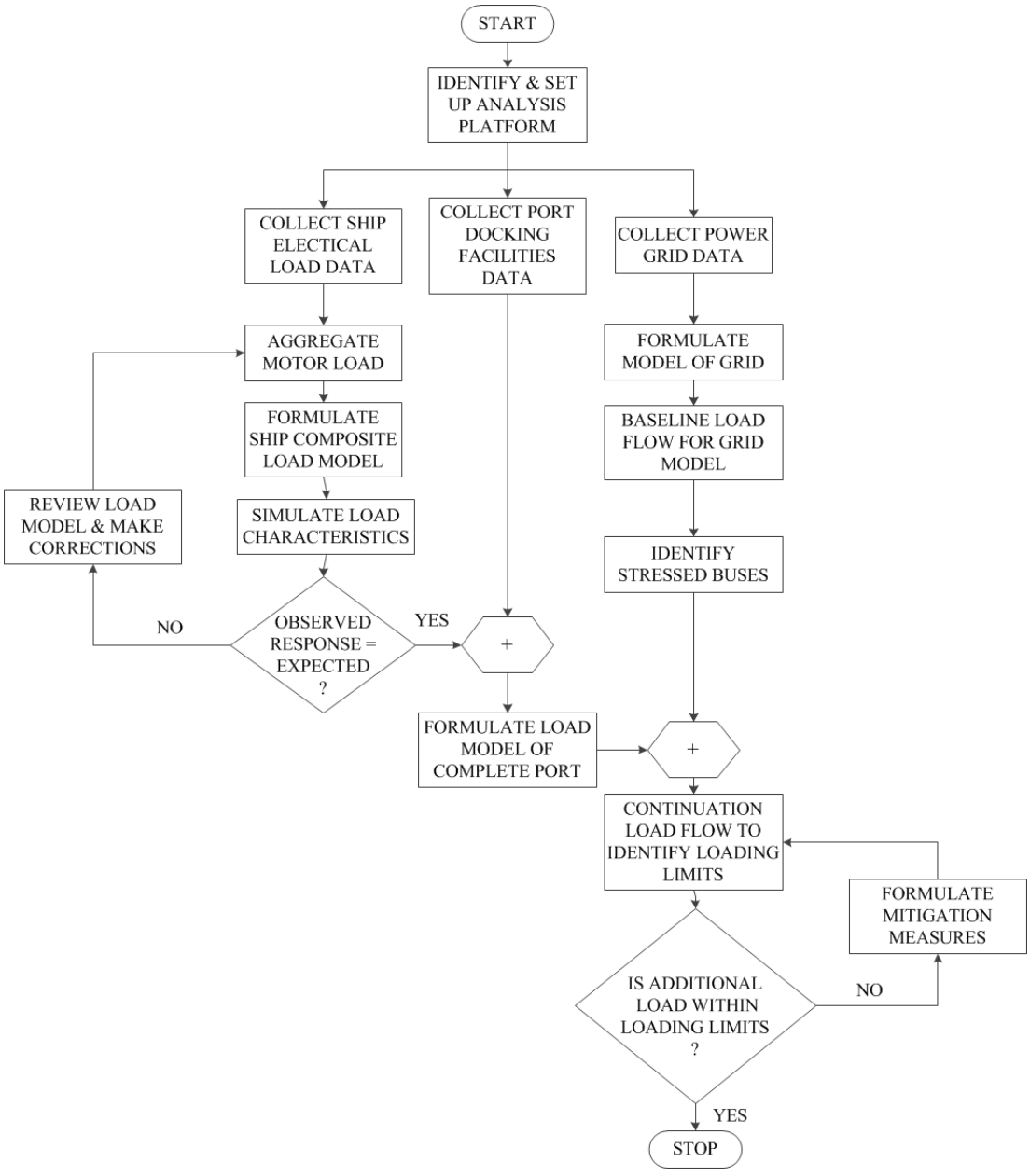

Figure 3.1: Flow chart describing methodology for shore power study

3.2 Data Collection

3.2.1 Load model data

Electrical ship loads data for each category of ship was collected from sampled docked ships. This was done by visiting the ship once it docks at Port of Mombasa. The ship captain in consultation with the chief engineer were able to give this information from the available manufacturers technical manuals. Each ship has on average 42 induction motors, lighting loads and cooking equipment. Considering that a maximum of 21 ships can be berthed at any one time, with a total of over 800 induction motors, aggregate induction motor model was developed to come up with 21 equivalent ship loads. At some instances less ships may dock depending on the season, number and type of ships within a period and rate of discharge. Induction motor aggregation was done using a single equivalent motor model which aims to simplify the computation for the dynamic behaviour simulation of ship loads. Based on the technical specifications obtained, a model of the power requirement of a docked ship was formulated. A sample of data collected from a ship is presented on Appendix A. The development of the load model is presented in sections 3.5 and 3.6.

3.2.2 Power network data

Data on peak loading and system configuration was obtained from Kenya Power personnel at Kipevu and Rabai stations and at the head office in Nairobi. The data supplied included system topology, generator ratings and loading, line parameters, transformer ratings, and system loads data. Additional information was obtained from reports on current status and development of the power network as in the references [53],[54],[55],[56]. A reduced transmission/distribution network single-line diagram model was developed using PSAT with 15 buses, 17 lines, 4 generators and 12 loads. The type of data collected from each system component are as in table 3.1. The data collected and the system modelled are represented in section 3.3.

Table 3.1: Elements and system parameters

Element	System Parameters					
Buses	Bus voltages (220 kV and 132 kV)	Type of bus- (load, generator, switching)				
Lines	Line length (km	Resistance of the line (per unit on 100 MVA base)	Reactance of the line (per unit on 100MVA base)	Susceptance of the line(per unit 100 MVA base)	Line Base voltage (kV)	Max. loading (MVA)
Generators	Min/Max. MW output	Min/Max. MVAr rating.	Rating (MVA, Voltage, power factor)			
Loads	Bus-loads Load (MW, MVAr)	System -loads peak load (MW,MVAR)				

3.3 Kenyan coast region 132kVpower transmission

The electricity distribution network for the coast region is shown in figure 3.2[55] and[54].The black line is a 132kV single circuit transmission lines from Juja Road Bulk Supply Station (BSP) in Nairobi to the Rabai BSP in Mazeras near Mombasa. The red line represents a 220kV single circuit transmission line from the Kiambere Power Station on the Tana River to the Rabai BSP. The green lines are 33kV distribution feeders. The system supplies power to the counties of Taita Taveta,

Kwale, Mombasa, Kilifi and Tana River. There are on-going plans to link the system to Lamu County, which is currently supplied by off-grid generation.

The coast network has four generating stations at Rabai, Kipevu I, Kipevu II (Tsavo Power) and Kipevu III. The capacity of the generating stations is summarised in Table 3.2 [54].

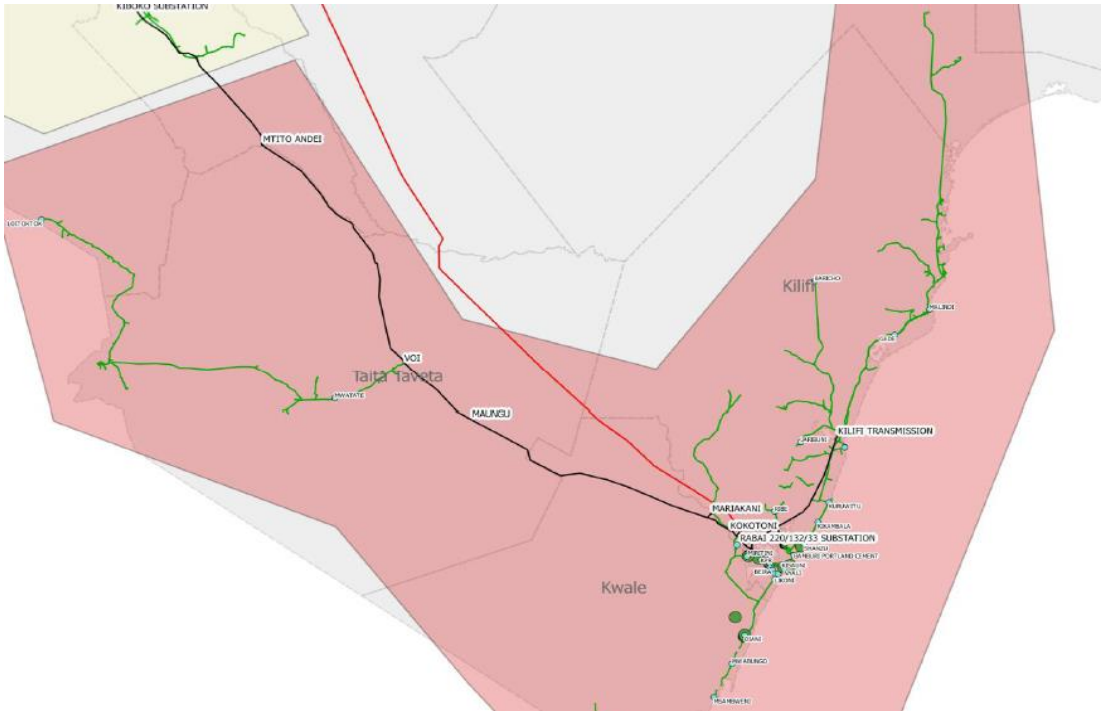

Figure 3.2: Coast power distribution network

Where,

Red line - represent 220kV line Kiambere to Rabai

Green Line - represents 33 kV distribution feeders to Taita Taveta, Kwale, Mombasa, Kilifi and Tana River

Black line - Represents 132kV line from Juja to Rabai

Table 3.2: Installed and effective generating capacity

Generating Station	Installed Capacity, MW	Effective Capacity, MW	Operator
Rabai	90	90	IPP (BWSC & Aldwych)
Kipevu I	75	51	KenGen
Kipevu III	120	115	KenGen
Kipevu II	74	74	IPP (Tsavo Power)

In addition, the Coast network is also connected to national the grid through a 132kV transmission line from Rabai to Juja Road BSP in Nairobi and a 220kV line from Rabai to the Kiambere power station. The connection to the national grid allows the Coast network to supply excess power to the national grid when local generation exceeds consumption. It also allows the network to draw power from the national grid when local consumption exceeds generation, hence the model used the connection to the national grid as a slack bus. All the generating stations supply power to the Rabai sub-station which acts as the bulk supply point for the coast network. Power is then distributed to the coast region through a 132kV network with interconnections as in [56], [57] and [53].

Table 3.3: Kenya power coast distribution network (132kV)

FROM	TO	DISTANCE, km	VOLTAGE. kV	CIRCUITS	CONDUCTOR
Rabai	Juja	476	132	Single	132_LYNX
Rabai	Kiambere	416	220	Single	220_CANARY
Rabai	Galu	60	132	Single	132_LYNX
Rabai	Kipevu I & III	17	132	Double	132_WOLF
Rabai	Kipevu I & III	17	132	Single	132_LYNX
Rabai	Kipevu II	17	132	Single	132_LYNX
Kipevu	KPA	1.5	132	Single	400mm^2 Cu U/G
Rabai	New Bamburi	22	132	Single	132_WOLF
New Bamburi	Vipingo	13	132	Single	132_WOLF
Vipingo	Mombasa Cement	12.5	132	Single	132_WOLF
Mombasa Cement	Kilifi	17.5	132	Single	132_WOLF

From Rabai, power is distributed to the using a 132kV network to bulk supply points at Galu near Diani on the South Coast, Kipevu just outside Mombasa Island and Bamburi, Vipingo and Kilifi on the North Coast. In addition to the bulk supply points, there are two 132kV stations feeding individual consumers. These are Mombasa Cement on the North Coast and KPA on Mombasa Island. There is also reactive power two (2) pieces of 15MVAr inductive compensation at the Rabai BSP. Each of the bulk supply stations in the coast region supply power through 132kV/33kV distribution transformers. The total load connected to each station is Table 3.4 [54].

Table 3.4: Bulk supply points load parameters

BSP	Galu	Kilifi	Kipevu	New Bamburi	Rabai	MSA Cement	KPA
Active Power, MW	14.25	13.38	99.86	26.47	7.63	10.98	6.30
Reactive Power, MVAr	6.90	6.48	48.37	12.82	3.70	5.32	3.05
Total MVA	15.83	14.87	110.95	29.40	8.47	12.20	7.00

In addition to the load distributed from Rabai BSP, the 132kV line from Juja Road BSP also supplies some small sub-stations along the route. The sub-stations, their distance from Juja Road and the load are presented in Table 3.5.

Table 3.5: Sub -Stations distances from Juja to Rabai

Sub-Station	Kokotoni	Mariakani	Maungu	Voi	Mtito Andei
Distance from Juja (km)	478	458	368	338	247
Distance from Rabai BSP (km)	5	18	108	138	229
Active Power, MW	6.75	11.07	3.35	3.48	4.22
Reactive Power, MVAr	3.27	5.36	1.62	1.69	2.05
Total MVA	10.83	46.81	3.64	3.79	4.77

3.4 Ship Load Model

A simulation of the electrical load on a ship is required in order to study the effect of interconnections of the ship to shore power grid. In this case, the loads are grouped for simulation as highlighted by the cell background colours in Appendix A. The grouping was based on:

i. Blue for motor loads with a load torque characteristic where torque is proportional to square of speed (fans and pumps).
ii. Green for motor loads with a load torque characteristic where torque is almost zero at starting speed and constant at higher speeds (compressors, hoists).
iii. Red for purely resistive or inductive loads without a substantial starting current.
iv. Yellow for loads that are not part of the ship and may not be always present (refrigeration containers).

3.4.1 Load Torque Model

Before the motors are grouped for aggregation, a model of load torque is required. The models used were:

1. Load torque is proportional to speed for fans and pumps. This is modelled as:

$$T_m = k\omega_r^2 \tag{3.1}$$

Where

T_m=Mechanical torque,

ω_r = rotor angular speed

$k = T_R/(\omega_R)^2$which is a constant

2. Constant torque (at higher speeds) for hoists and compressors. This is modelled as:

$$T_m = \begin{cases} k_1\left(\frac{\omega_R}{2}\right)^2 & \omega < {}^{\omega_R}/_{2} \\ T_R\omega \geq {}^{\omega_R}/_{2} \end{cases} \quad (3.2)$$

Where

T_R = full load torque and

ω_R = full load angular speed

T_m=mechanical torque

ω_r = rotor angular speed

Constant, $k_1 = T_R/(\omega_R/2)^2$.

3.4.2 Motor grouping for aggregation

In this study the aggregation method applied is the equivalent circuit of an induction motor as detailed in section 2.3.5 [24]. In this method the induction motors have been grouped together based on their speed- torque characteristic. The aggregation of motor loads with torque characteristics of fans and pumps are grouped together as in Table 3.6. The motors aggregated with torque characteristics of cranes and compressors are shown in Table 3.7. The aggregated motor parameters were determined from the motor manufacturer's data sheet.

Table 3.6: Fan and motor loads for Kota Hapas container ships

Description of load	Qty	KW	Total KW	Total HP	RsΩ	XsΩ	RrΩ	XrΩ	XmΩ	Jkgm2	Nr
Cooling sea w/pump	1	28.9	28.9	39	0.59	0.15	0.16	0.16	12.49	1.3	1470
C/fresh w/pump	1	12.4	12.4	17	1.38	0.29	0.18	0.18	23.57	0.57	1450
M/E lube oil	1	69.9	69.9	94	0.27	0.09	0.16	0.11	4.63	2.58	1484
Exhaust valve pump	1	4.4	4.4	6	4.02	1.46	2.05	2.05	69.73	0.19	1430
Fuel oil, boiler motor	2	2.8	5.6	8	3.45	1.2	1.63	1.63	59.77	0.26	1420
Fuel oil cir-c.pump	1	6.3	6.3	8	3.45	1.2	1.63	1.63	59.77	0.26	1435
Fuel oil tran-s.pump	1	8.5	8.5	11	2.61	0.82	1.01	1.01	44.82	0.36	1445
G/E sea w/pump	1	16.7	16.7	22	1.13	0.24	0.17	0.17	20.26	0.73	1465
G/E D.O sup-p.pump	1	3.8	3.8	5	4.3	1.59	2.26	2.26	74.72	0.16	1430
Ballast/pump	1	39.8	39.8	53	0.41	0.14	0.15	0.15	9.14	1.72	1480
Fire and GS	1	39.8	39.8	53	0.41	0.14	0.15	0.15	9.14	1.72	1480
Fire, ballast	1	86.4	86.4	116	0.23	0.07	0.14	0.09	3.66	3.24	1485
Engine R/vent	2	57.8	115.6	155	0.17	0.05	0.09	0.07	2.91	5.55	1483
A/C plant	1	28.9	28.9	39	0.59	0.15	0.16	0.16	12.49	1.3	1470
A/C fan	1	16.7	16.7	22	1.13	0.24	0.17	0.17	20.26	0.73	1465

Table 3.7: Crane and compressor motors

Description of load	Qty	KW	Total KW	Total HP	RsΩ	XsΩ	RrΩ	XrΩ	XmΩ	Jkgm2	Nr (RPM)
Air comp.	2	47.8	95.6	128	0.21	0.07	0.13	0.08	3.43	3.64	1483
Plant/comp.	1	4.4	4.4	6	4.02	1.46	2.05	2.05	69.73	0.19	1430
Cargo cranes	2	185	370	497	0.11	0.03	0.09	0.03	2.91	5.55	1487

3.4.3 Motor aggregation and ship load model

Using the MATLAB code in Appendix B and Appendix C, the grouped motors are aggregated into one fan motor and one pump motor. The non-motor loads were added together to form one R-L load. The aggregated motor parameters and impedance load values are presented in Appendix C. The composite load is as shown in MATLAB/SIMULINK model of ship loads Figure 3.3.

The model consists of the following components:

1. A 3 MVA, 415V 3 phase source to supply power for the test. The rating of the power supply because this power rating is one that is commercially available and has a capacity that can be accommodated within the existing installation at the Mombasa Port.
2. A damping resistor, which is required in Simulink when a power supply is connecting to an inductive load. It is 1 watt at 415 volts and 50Hz. This resistor decreases the quality factor (energy losses) and there by eliminates ringing.
3. Two asynchronous machine models to represent the aggregated motor loads. These have the following inputs and outputs:
    a. Motor parameters are input as settings for the asynchronous machines.
    b. A model for load torque. This was set as a function of speed.
    c. Operational measurements used were rotor speed and electromagnetic torque output.
4. An RL with load settings as given to represent non-motor loads.
5. Circuit breakers which are set to open or close as required for the simulation.
6. Current, voltage and power measurement blocks.
7. Oscilloscopes to display and save measured variables.

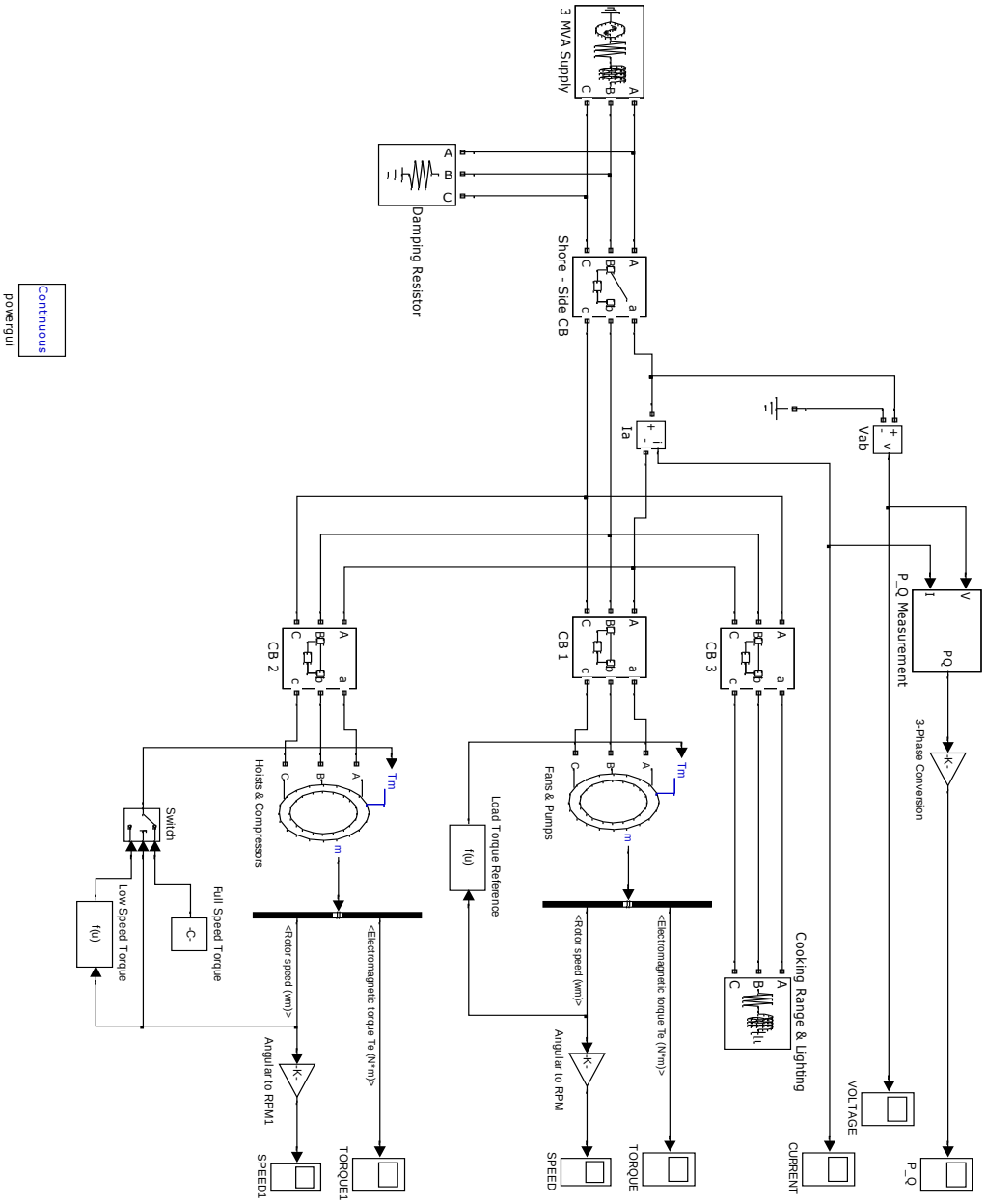

Figure 3.3: Simulink model of ship loads

The model has been tested in order to confirm that it meets the expected characteristics of the simulated load. The build-up of the load torque as motor gains speed after starting was observed. This was tested for connection to mains from rest and from full load / full speed. The aggregated ship load as modelled if figure 3.3 was simulated in MATLAB / SIMULINK. The motor was tested under the following conditions:

1. Motor starting from rest.
2. Motor runs to full speed, is disconnected from main for a short time and reconnected back to mains. This simulates the on-load transfer of on-ship generator to shore side power supply.
3. Running the motor for a long time to simulate steady state operations.

3.5 Network modelling

The power network described in section 3.1 is modelled on the PSAT/MATLAB platform. This involved defining network buses, identifying the interconnections between the buses and calculating the transmission line parameters for the interconnections. The network buses are identified in Table 3.8.

Table 3.8: Bus Loads

BUS NO.	BUS NAME	LOAD		STATIC VAR (MVAr)	BUS TYPE
		P (MW)	Q (MVAr)		
1	Grid	0	0	0	Slack
2	Rabai BSP	7.63	3.70	30	PQ
3	Galu	14.25	6.90	0	PQ
4	Kipevu BSP	99.86	48.37	0	PQ
5	KPA	6.30	3.05	0	PQ
6	New Bamburi	26.47	12.82	0	PQ
7	Vipingo	-	-	-	PQ
8	MSA Cement	10.98	5.32	0	PQ
9	Kilifi	13.38	6.48	0	PQ
10	Kipevu II	0	0	0	PV
11	Mtito	4.22	2.05	0	PQ
12	Voi	3.48	1.69	0	PQ
13	Maungu	3.35	1.62	0	PQ
14	Mariakani	11.07	5.36	0	PQ
15	Kokotoni	6.75	3.27	0	PQ

The load on each bus is also indicated in the Table 3.8. The connections to the national grid at Juja road and Kiambere are defined as one bus with the bus type being a slack bus. The generating stations were connected to the buses as shown in Table .

Table 3.9: Generation stations capacity

Generating Station	Bus	Power Generated (MW)
Rabai	Rabai BSP	90
Kipevu I	Kipevu BSP	51
Kipevu III	Kipevu BSP	115
Tsavo (Kipevu II)	Kipevu II	74

The network connections between the buses are defined in appendix E. The transmission lines are modelled as pi networks. The model parameters are defined in appendix F, where r is the total resistance of the line, x is the total inductive reactance of the line and b is the total capacitive susceptance of the line. The power and current ratings for the transmission lines were also included in the same table. These are used to set the limits for maximum load flows. The connection from Grid to Rabai BSP is through a 2- winding transformer 180MVA, 127kV with a 1.67 turns ration. Further, the Juja to Rabai BSP is through a 2- winding transformer 200MVA, 127kV with a 1.67 turns ration. The values in Tables 3.8, 3.9.Single phase values were applied, which is achieved by dividing power values by 3 and voltage values by √3. The base values used were:

Base Voltage	76.2kV
Base Power	100MVA
Base Current	1312.16A
Base Impedance	58.08 Ω

For the 220kV line, the per unit impedance values were first calculated using a base of 127kV then converted to a base of 76.2kV. The conversion was carried out as:

$$Z_{pu2} = Z_{pu1} \times \frac{Z_{base1}}{Z_{base2}} \tag{3.3}$$

Where Z_{pu1} is the impedance using the old voltage base, Z_{pu2} is the impedance using the new voltage base, Z_{base1} is the base impedance using the old voltage baseZ_{base2} is the base impedance using the new voltage base.

The MATLAB/PSAT single line model of the network is shown in Figure 3.4. The transmission lines are modelled as pi networks and the loads as PQ loads.

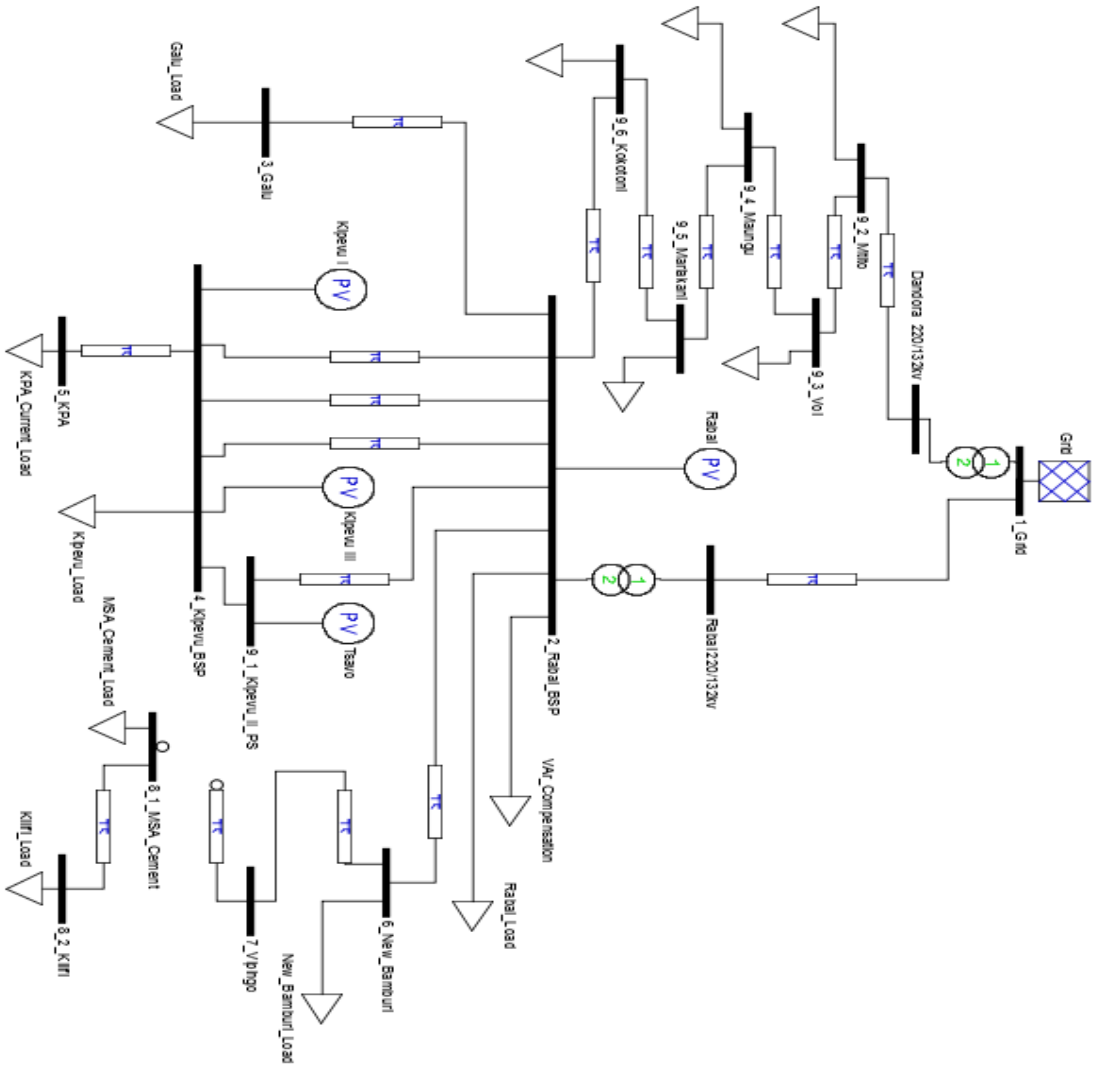

Figure 3.4: MATLAB/PSAT Model of Coast Network

Table 3.10: Generation

Generating Station	Bus	Power Generated, P (p.u.)
Rabai	Rabai BSP	0.3000
Kipevu I	Kipevu BSP	0.1700
Kipevu III	Kipevu BSP	0.3833
Tsavo (Kipevu II)	Kipevu II	0.2467

Table 3.11: Model parameters

FROM	TO	r (p.u.)	x (p.u.)	b (p.u.)
Rabai BSP	Galu	0.1962	0.4449	2.7789E-06
Rabai BSP	Kipevu BSP	0.0644	0.1274	7.7858E-07
Rabai BSP	Kipevu BSP	0.0644	0.1274	7.7858E-07
Rabai BSP	Kipevu BSP	0.0556	0.1261	7.8736E-07
Rabai BSP	Kipevu II	0.0556	0.1261	7.8736E-07
Kipevu BSP	KPA	0.0012	0.0058	4.1322E-09
Rabai BSP	N. Bamburi	0.0834	0.1649	1.0076E-06
N. Bamburi	Vipingo	0.0493	0.0974	5.9539E-07
Vipingo	M. Cement	0.0474	0.0937	5.7249E-07
M. Cement	Kilifi	0.0663	0.1312	8.0148E-07
Grid	Rabai BSP	0.5479	3.1515	1.8837E-05
Grid	Mtito	0.8078	1.8315	1.1440E-05
Mtito	Voi	0.2976	0.6748	4.2147E-06
Voi	Maungu	0.0981	0.2224	1.3895E-06
Maungu	Mariakani	0.2943	0.6673	4.1684E-06

Table 3.12: Bus data – Connected loads

BUS NO.	BUS NAME	LOAD		STATIC VAR (p.u)	BUS TYPE
		P (p.u.)	Q (p.u.)		
1	Grid	-	-	-	Slack
2	Rabai BSP	0.0254	0.0123	0.1000	PQ
3	Galu	0.0475	0.0230	-	PQ
4	Kipevu BSP	0.3329	0.1612	-	PQ
5	KPA	0.0210	0.0102	-	PQ
6	N. Bamburi	0.0882	0.0427	-	PQ
7	Vipingo	-	-	-	PQ
8	M. Cement	0.0366	0.0177	-	PQ
9	Kilifi	0.0446	0.0216	-	PQ
10	Kipevu II	0	0	0	PV
11	Mtito	0.0141	0.0068	-	PQ
12	Voi	0.0116	0.0056	-	PQ
13	Maungu	0.0112	0.0054	-	PQ
14	Mariakani	0.0369	0.0179	-	PQ
15	Kokotoni	0.0225	0.0109	-	PQ

The model has been used to run a power flow of the network. The power flow is performed using Newton Raphson method with trapezoidal rule integration method. The model parameters are included in Table 3.10 and Table 3.11.

3.6 Total expected off-shore load

The port of Mombasa has 22 deep water berths [58]. Of these, 9 are container berths,

9 are for general cargo, 2 are for oil tankers and 2 are for roll-on roll-off vehicle carriers. Port traffic is estimated as 38% container ship, 20% general cargo, 14% bulk carrier, 14% Ro-Ro and car carriers and 13% oil tankers. The power demand for each category of ship has been estimated by the following process:

1. Data on electrical loads on a ship was collected.
2. The load was modelled as a composite load comprising aggregated induction motor load and constant impedance loads.
3. The steady state PQ load for use in power flow was determined by an initialisation process.

From this analysis, an estimate of the total demand of ships in berth at the port of Mombasa is presented in Table 3.13. A shore to ship connection for the port of Mombasa will therefore be expected to carry a load of approximately 22MW.

Table 3.13: Estimated loads at port of Mombasa when berths at full capacity

Type of Berth	No.	Peak Load (kW)	In Port Demand	Berth Load (kW)
Container	9	4,000	20%	7,200
General Cargo	9	2,800	40%	10,080
Ro-Ro	2	1,800	30%	1,080
Oil Tanker	2	2,500	65%	3,250
Total	22			21,610

3.7 Analysis of coast power network with off-shore load

The MATLAB/ PSAT single line model of the network with off-shore load connected as shown in Figure 3.5. The transmission lines are modelled as pi networks and the loads as PQ loads.

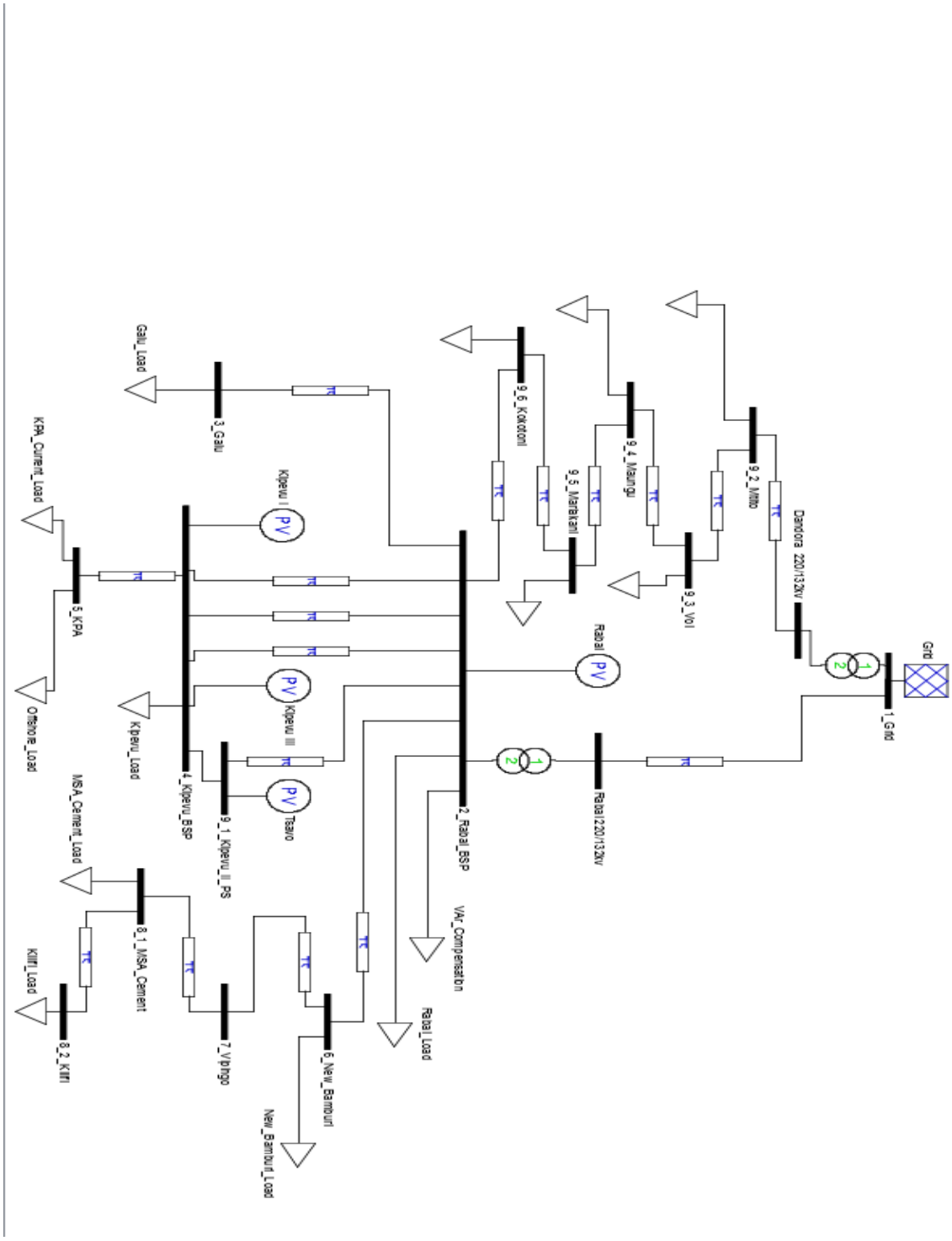

Figure 3.5: MATLAB/PSAT Model of Coast Network with Ship Load

CHAPTER FOUR

RESULTS AND DISCUSSION

4.1 Transient operation of aggregated ship load

During the simulations, measurements of phase to neutral voltage, phase current, active and reactive power, rotor speed and electromagnetic torque are taken. The results are presented in Figures 4.1 to Figure 4.9. The power disconnection event can be observed at 1.75 seconds. It is observed that the aggregated motors demonstrate the characteristics that are expected for an induction motor at start for speed, torque, voltage, current and power. It is also noted that the two motors have slightly different torque characteristics, as would be expected. The hoist motor has a more uniform torque, with maximum torque almost equal to full load torque. The 3MVA supply is able to start the motors from standstill to near the calculated full load speed. When the supply suffers a short disturbance as would be expected during change-over from one source to another, the model demonstrate an ability to quickly recover and settle at the same operating conditions as were existing before the disturbance.

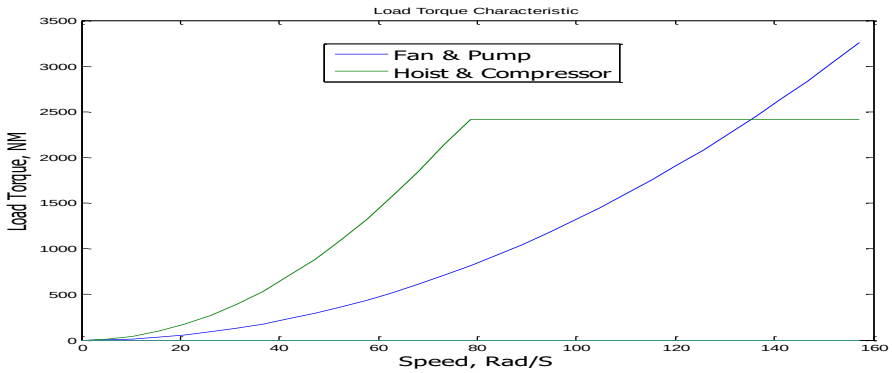

Figure 4.1: Load Torque Characteristics

The load torque characteristics shown on Figure 4-1 for the fans and hoist and compressor motors are very similar to the theoretical curves of similar motors.

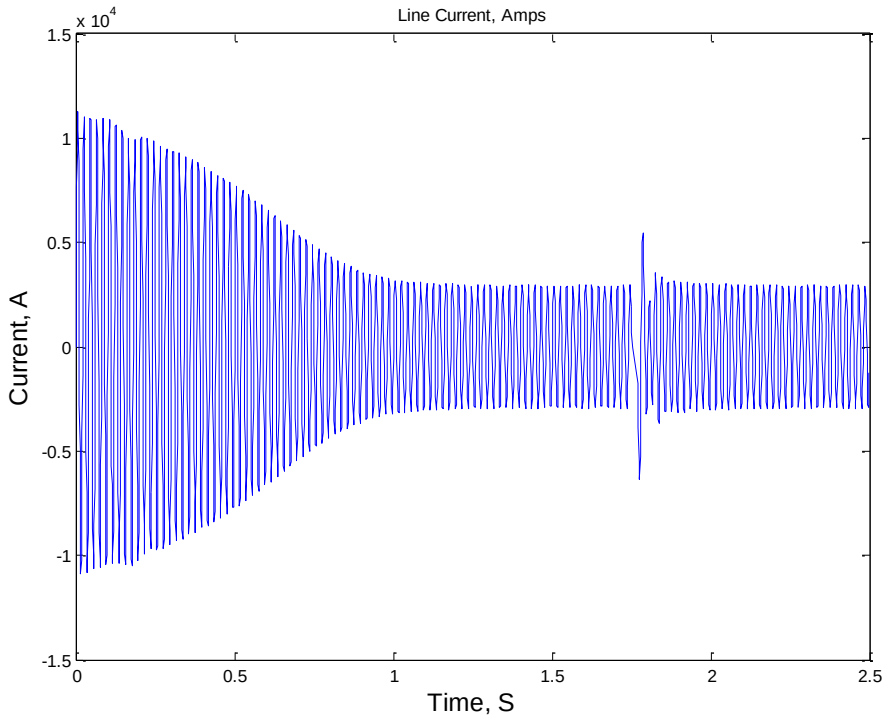

Figure 4.2: Total Line Current, (A) Phase

The line current curve is as shown on Figure 4-2. The current varies as expected during start and stop times.

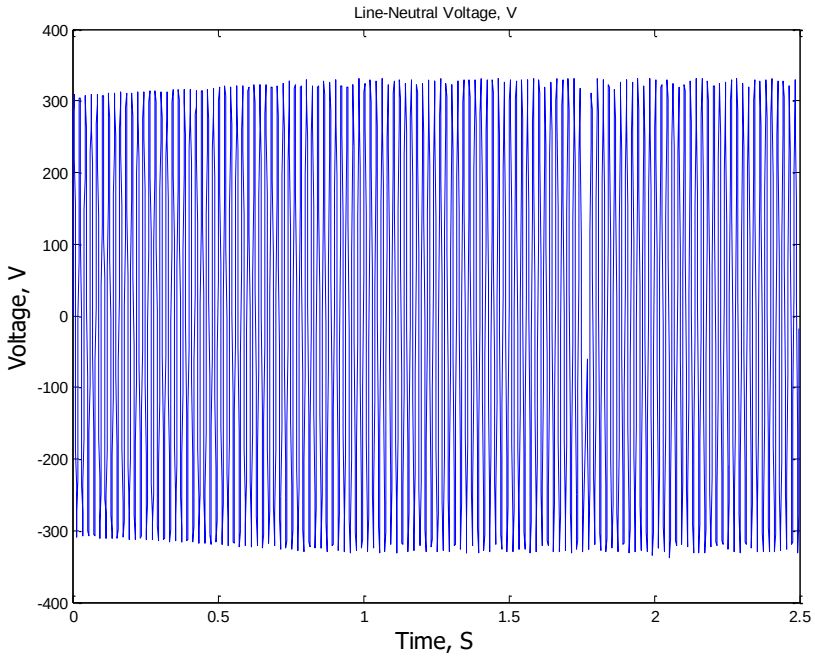

Figure 4.3: Line to Earth Voltage, Phase A

The line voltage curve is as shown on Figure 4.3. The voltage is within set limits.

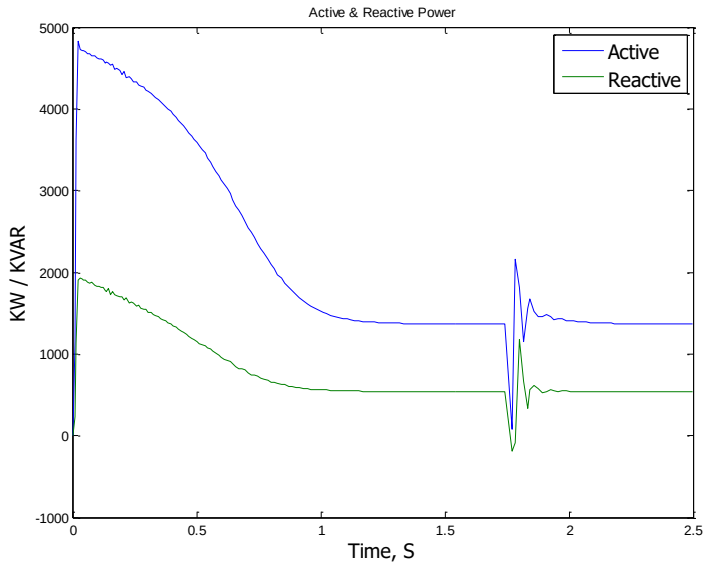

Figure 4.4: Total Ship Power (Active and Reactive)

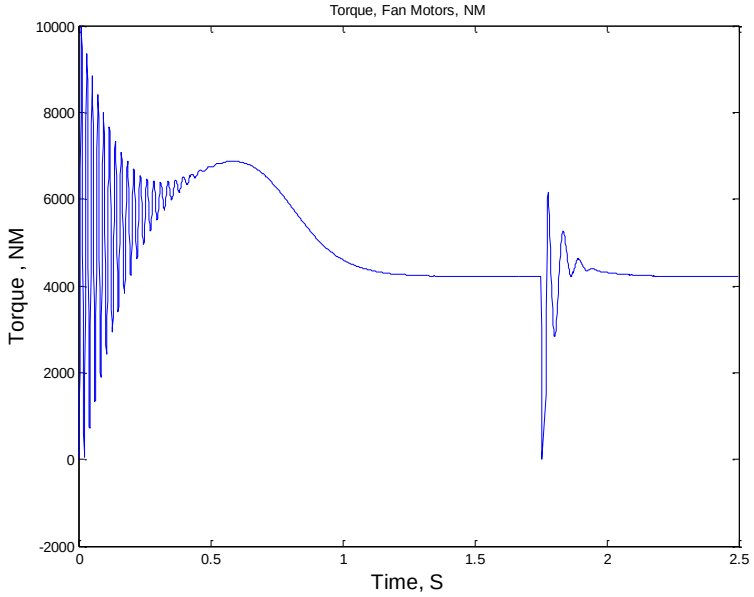

Figure 4.5: Electromagnetic Torque, Fan & Pump Motor

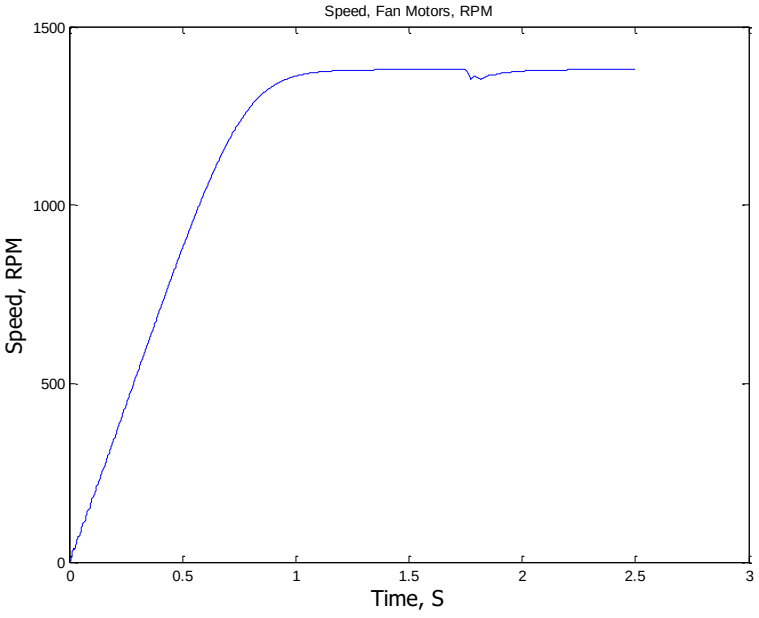

Figure 4.6: Rotor Speed, Aggregated Fan Motor

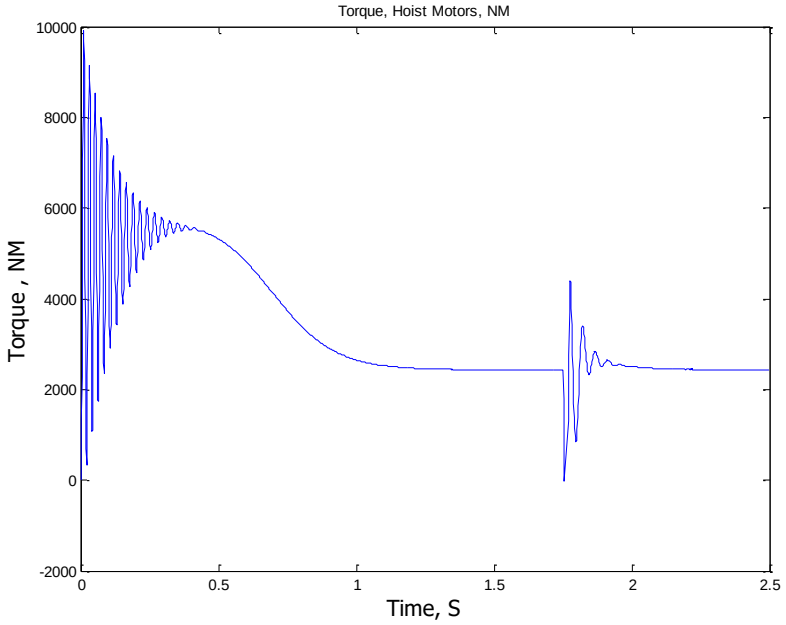

Figure 4.7: Electromagnetic Torque, Aggregated Hoist Motor

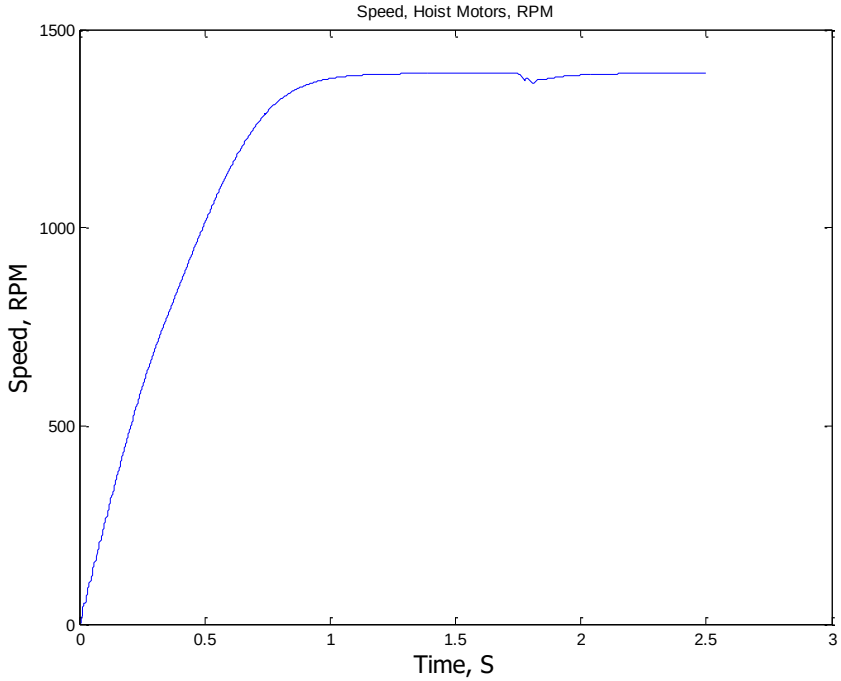

Figure 4.8: Rotor Speed, Aggregated Hoist

4.2 Steady state operation of aggregated ship load

The aggregated ship load is then simulated by running the motor for a long time to observe steady state operations. The results are in Table 4.1. The results shows a highly inductive load with the lighting capacitive.

Table 4.1: Steady state parameters for aggregated load

Description of load	Voltage		Current	
	Magnitude (V)	Angle (o)	Magnitude (A)	Angle (o)
Total Ship	239.6	0.0	2,051.3	-23.5
Fans	236.1	28.6	920.9	-26.4
Cranes	236.1	28.6	932.1	-19.7
Lighting etc.	236.1	-1.4	201.9	92.6

4.3 Base Line Power flow results – without off-shore load

The results of power flow on the model in Figure are presented in Tables 4.2 to 4.8 and Figures 4.9 to Figure 4.11.

Table 4.2: Bus voltages and power, per unit values

BUS	V (p.u.)	phase (rad)	P gen (p.u.)	Q gen (p.u)	P load (p.u.)	Q load (p.u.)
Grid	1.05	-	(0.31)	0.28	-	-
Rabai BSP	1.00	0.73	0.30	0.49	0.03	0.11
Galu	0.98	0.71	-	-	0.05	0.02
Kipevu BSP	1.00	0.74	0.55	0.08	0.33	0.16
KPA	1.00	0.74	-	-	0.02	0.01
New Bamburi	0.97	0.71	-	-	0.09	0.04
Vipingo	0.96	0.70	-	-	-	-
MSA Cement	0.95	0.69	-	-	0.04	0.02
Kilifi	0.95	0.69	-	-	0.04	0.02
Kipevu II	1.00	0.76	0.25	(0.10)	-	-
Mtito	0.93	0.34	-	-	0.01	0.01
Voi	0.93	0.49	-	-	0.01	0.01
Maungu	0.94	0.54	-	-	0.01	0.01
Mariakani	0.98	0.69	-	-	0.04	0.02
Kokotoni	0.99	0.72	-	-	0.02	0.01

The power flow converged in 5 iterations. No power mismatch was noted and all buses were within the allowed voltage limits of ±10%.

Table 4.3: Bus voltages and power, absolute values

BUS	V(kV)	Phase (deg)	P Gen (MW)	Q Gen (MVAr)	P Load (MW)	Q Load (MVAr)
Grid/Slack bus	138.6	0.0	(93.8)	85.1	0.0	0.0
Rabai BSP	132.0	41.7	90.0	147.6	7.6	33.7
Galu	129.3	40.7	0.0	0.0	14.3	6.9
Kipevu BSP	132.0	42.2	165.0	23.4	99.9	48.4
KPA	132.0	42.2	0.0	0.0	6.3	3.1
New Bamburi	128.2	40.4	0.0	0.0	26.5	12.8
Vipingo	127.1	40.0	0.0	0.0	0.0	0.0
MSA Cement	126.0	39.7	0.0	0.0	11.0	5.3
Kilifi	125.2	39.4	0.0	0.0	13.4	6.5
Kipevu II	132.0	43.8	75.0	(31.4)	0.0	0.0
Mtito	123.2	19.7	0.0	0.0	4.2	2.0
Voi	123.2	28.2	0.0	0.0	3.5	1.7
Maungu	124.1	31.1	0.0	0.0	3.4	1.6
Mariakani	129.8	39.8	0.0	0.0	11.1	5.4
Kokotoni	131.3	41.1	0.0	0.0	6.8	3.3

While all the buses have a voltage within the limits of ±10%, it is noted that the lowest voltages are obtained at Mtito and Voi buses. These buses are very far from any generating station. From Table , it can be observed that Mtito is 247km from Juja Rd (considered as the connection point to the grid) and 229km from Rabai BSP (which includes the Rabai generating station). Voi is closer to the distribution stations than Mtito, but is still 138 km from Rabai BSP and 338kM from the Juja Road. The two stations require local reactive power compensation to raise the bus voltage and reduce transmission losses

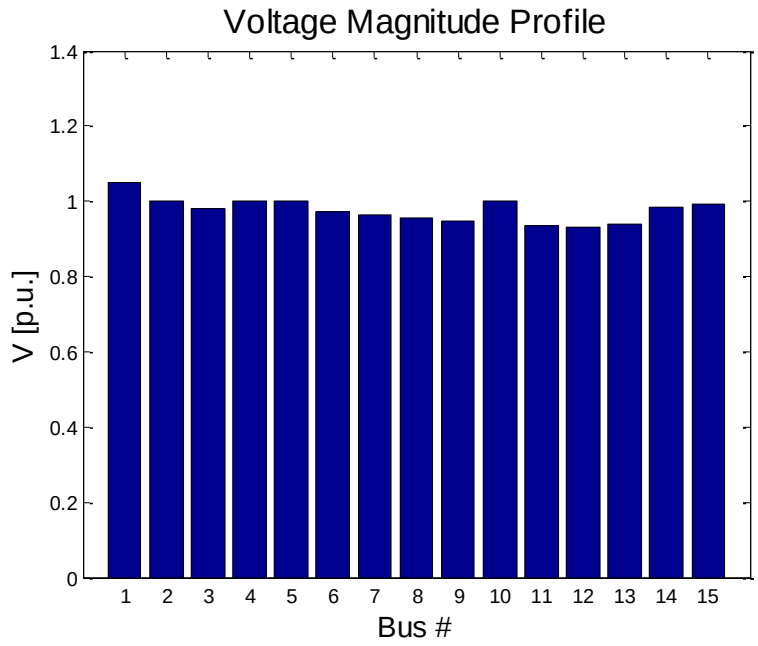

Figure 4.9: Bus Voltages Profile, p.u

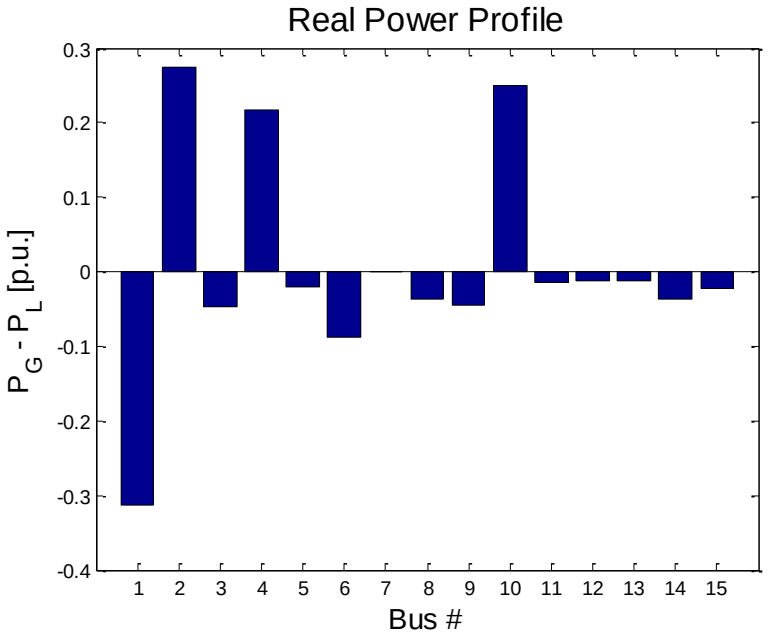

Figure 4.10: Real power profile for each bus, p.u

Figure 4.10 shows the real power profile on each of the buses displaying the amount of power load on each bus. This information can help in planning for consumers.

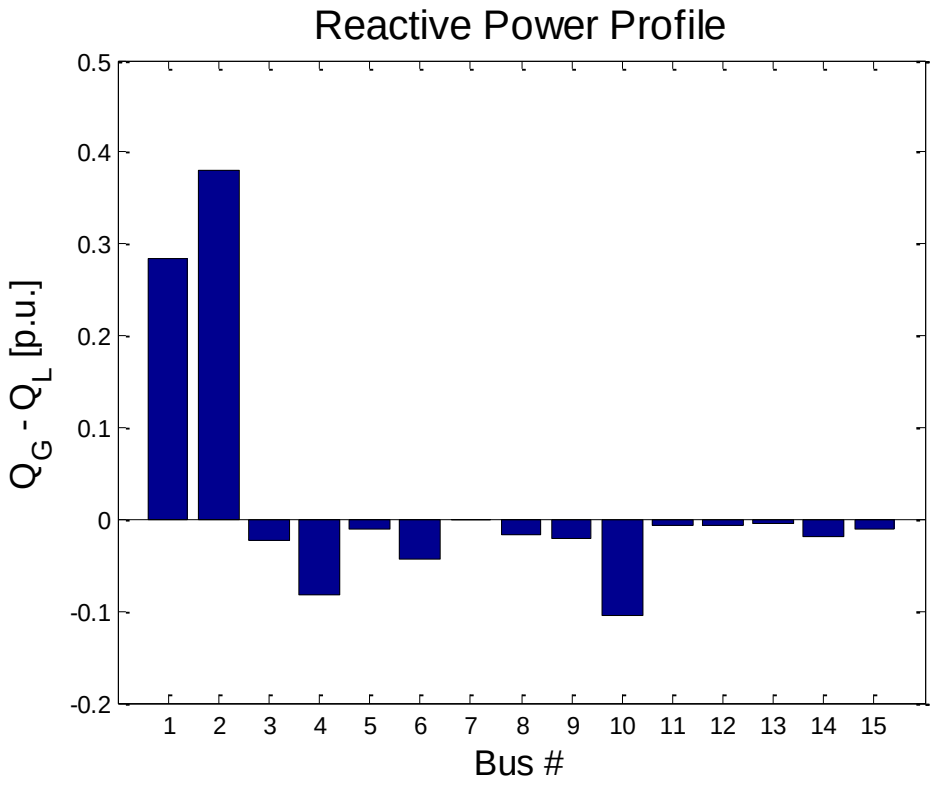

Figure 4.11: Reactive power profile for each bus, p.u

Figure 4.11 shows the reactive power profile on each of the buses displaying the amount of reactive load on each bus. This information can help in planning for consumers.

Table 4.4: Forward flows, per unit values

FROM	TO	LINE	P FLOW (P.U.)	Q FLOW (P.U.)	P LOSS (P.U.)	Q LOSS (P.U.)
Rabai BSP	Galu	1	0.0481	0.0243	0.0006	0.0013
Rabai BSP	Kipevu BSP	2	(0.0637)	0.0326	0.0003	0.0007
Grid Juja RD	Rabai BSP	3	(0.1979)	0.1353	0.0286	0.1643
Grid Juja RD	Mtito	4	(0.1146)	0.1482	0.0257	0.0584
Mtito	Voi	5	(0.1544)	0.0830	0.0105	0.0238
Voi	Maungu	6	(0.1765)	0.0536	0.0038	0.0087
Maungu	Mariakani	7	(0.1916)	0.0395	0.0127	0.0289
Mariakani	Kokotoni	8	(0.2412)	(0.0073)	0.0026	0.0058
Kokotoni	Rabai BSP	9	(0.2662)	(0.0240)	0.0012	0.0027
Rabai BSP	Kipevu BSP	10	(0.0637)	0.0326	0.0003	0.0007
Rabai BSP	Kipevu BSP	11	(0.0677)	0.0303	0.0003	0.0007
Rabai BSP	Kipevu II	12	(0.2459)	0.1140	0.0041	0.0093
Kipevu BSP	KPA	13	0.0210	0.0102	-	-
Rabai BSP	New Bamburi	14	0.1737	0.0904	0.0032	0.0063
New Bamburi	Vipingo	15	0.0823	0.0414	0.0004	0.0009
Vipingo	MSA Cement	16	0.0818	0.0405	0.0004	0.0008
MSA Cement	Kilifi	17	0.0448	0.0220	0.0002	0.0004

Table 4.5: Forward flows, absolute values

FROM	TO	LINE	P FLOW (MW)	Q FLOW (MW)	P LOSS (MW)	Q LOSS (MW)
Rabai BSP	Galu	1	14.42	7.29	0.17	0.39
Rabai BSP	Kipevu BSP	2	(19.12)	9.79	0.10	0.20
Grid	Rabai BSP	3	(59.38)	40.60	8.57	49.30
Grid	Mtito	4	(34.38)	44.47	7.72	17.53
Mtito	Voi	5	(46.33)	24.90	3.15	7.14
Voi	Maungu	6	(52.95)	16.09	1.15	2.61
Maungu	Mariakani	7	(57.47)	11.86	3.82	8.66
Mariakani	Kokotoni	8	(72.36)	(2.18)	0.77	1.74
Kokotoni	Rabai BSP	9	(79.87)	(7.19)	0.35	0.80
Rabai BSP	Kipevu BSP	10	(19.12)	9.79	0.10	0.20
Rabai BSP	Kipevu BSP	11	(20.31)	9.08	0.09	0.21
Rabai BSP	Kipevu II	12	(73.78)	34.19	1.22	2.78
Kipevu BSP	KPA	13	6.30	3.06	-	-
Rabai BSP	New Bamburi	14	52.10	27.12	0.96	1.90
New Bamburi	Vipingo	15	24.68	12.41	0.13	0.26
Vipingo	MSA Cement	16	24.54	12.15	0.13	0.25
MSA Cement	Kilifi	17	13.43	6.59	0.05	0.11

Table 4.6: Reverse flows, per unit values

FROM	TO	LINE	P FLOW (P.U.)	Q FLOW (P.U.)	P LOSS (P.U.)	Q LOSS (P.U.)
Galu	Rabai BSP	1	(0.0475)	(0.0230)	0.0006	0.0013
Kipevu BSP	Rabai BSP	2	0.0641	(0.0320)	0.0003	0.0007
Rabai BSP	Grid	3	0.2265	0.0290	0.0286	0.1643
Mtito	Grid	4	0.1403	(0.0898)	0.0257	0.0584
Voi	Mtito	5	0.1649	(0.0592)	0.0105	0.0238
Maungu	Voi	6	0.1804	(0.0449)	0.0038	0.0087
Mariakani	Maungu	7	0.2043	(0.0107)	0.0127	0.0289
Kokotoni	Mariakani	8	0.2437	0.0131	0.0026	0.0058
Rabai BSP	Kokotoni	9	0.2674	0.0266	0.0012	0.0027
Kipevu BSP	Rabai BSP	10	0.0641	(0.0320)	0.0003	0.0007
Kipevu BSP	Rabai BSP	11	0.0680	(0.0296)	0.0003	0.0007
Kipevu II	Rabai BSP	12	0.2500	(0.1047)	0.0041	0.0093
KPA	Kipevu BSP	13	(0.0210)	(0.0102)	-	-
New Bamburi	Rabai BSP	14	(0.1705)	(0.0841)	0.0032	0.0063
Vipingo	New Bamburi	15	(0.0818)	(0.0405)	0.0004	0.0009
MSA Cement	Vipingo	16	(0.0814)	(0.0397)	0.0004	0.0008
Kilifi	MSA Cement	17	(0.0446)	(0.0216)	0.0002	0.0004

Table 4.7: Reverse flows, absolute values

FROM	TO	LINE	P FLOW (MW)	Q FLOW (MW)	P LOSS (MW)	Q LOSS (MW)
Galu	Rabai BSP	1	(14.25)	(6.90)	0.17	0.39
Kipevu BSP	Rabai BSP	2	19.22	(9.59)	0.10	0.20
Rabai BSP	Grid	3	67.95	8.70	8.57	49.30
Mtito	Grid	4	42.10	(26.94)	7.72	17.53
Voi	Mtito	5	49.47	(17.77)	3.15	7.14
Maungu	Voi	6	54.11	(13.48)	1.15	2.61
Mariakani	Maungu	7	61.29	(3.20)	3.82	8.66
Kokotoni	Mariakani	8	73.12	3.92	0.77	1.74
Rabai BSP	Kokotoni	9	80.23	7.99	0.35	0.80
Kipevu BSP	Rabai BSP	10	19.22	(9.59)	0.10	0.20
Kipevu BSP	Rabai BSP	11	20.40	(8.87)	0.09	0.21
Kipevu II	Rabai BSP	12	75.00	(31.41)	1.22	2.78
KPA	Kipevu BSP	13	(6.30)	(3.06)	-	-
New Bamburi	Rabai BSP	14	(51.14)	(25.22)	0.96	1.90
Vipingo	New Bamburi	15	(24.54)	(12.15)	0.13	0.26
MSA Cement	Vipingo	16	(24.41)	(11.90)	0.13	0.25
Kilifi	MSA Cement	17	(13.38)	(6.48)	0.05	0.11

As in table 4.8, it is however noted that there is a lot of reactive power flow. This has resulted in a large power losses of 28.5MW. The network requires local reactive power compensation to reduce the reactive power flows and reduce line losses.

Table 4.8: Global summary of results

		p.u.	MW/MVAr
Total Generation	Real Power	0.78747	236
	Reactive Power	0.74882	225
Total Load	Real Power	0.6925	208
	Reactive Power	0.4353	131
Total Losses	Real Power	0.09497	28.5
	Reactive Power	0.31352	94.1

4.4 Base Line Power flow results – with off-shore load

The results of power flow on the model in Figure 4-12 are presented in Table 4.9.

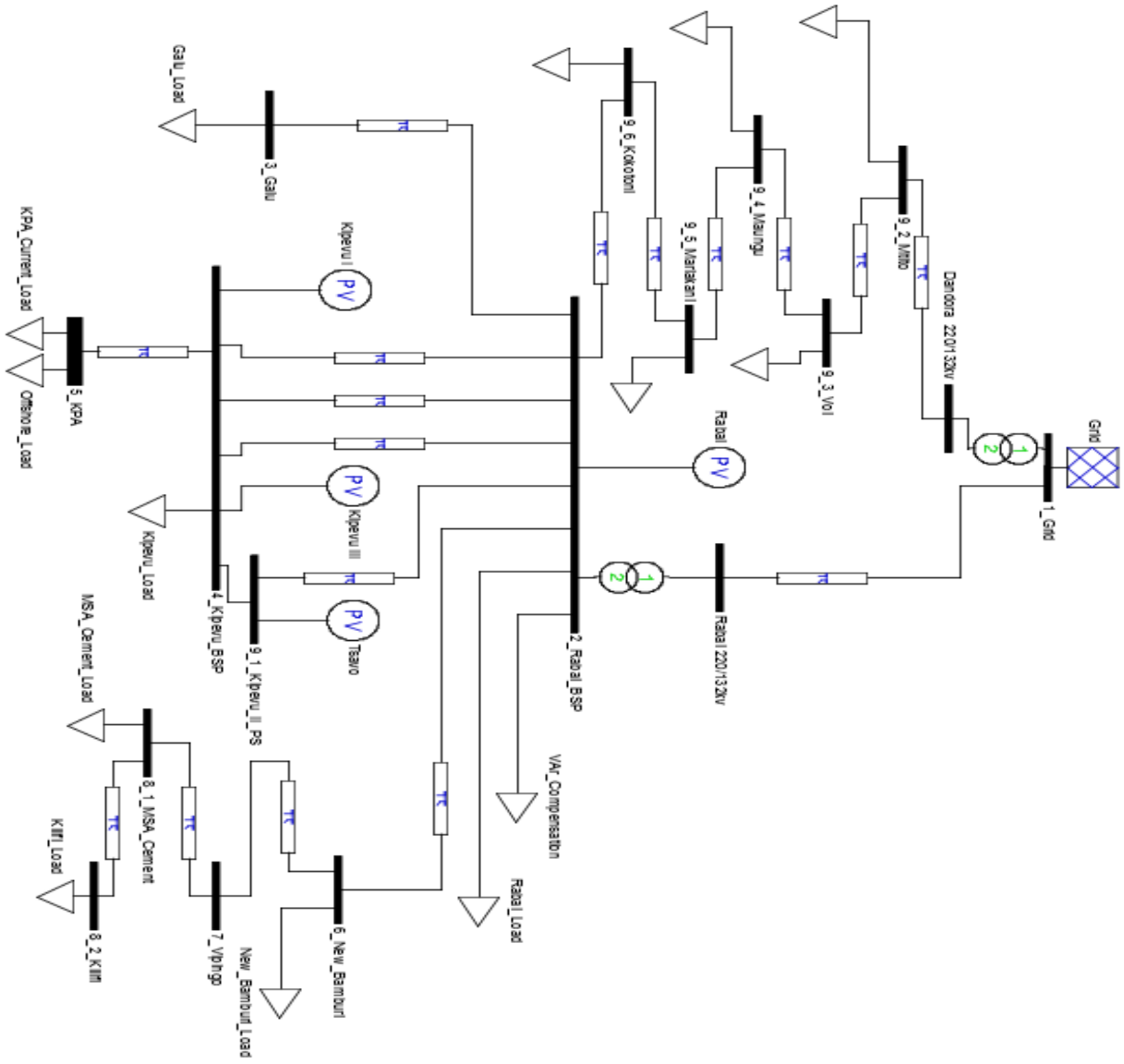

Figure 4.12: Model of Coast Power Network with Ship Load

Table 4.9: Base Case Power Flow Results – with Offshore Load

BUS	V (p.u.)	phase (rad)	P gen (p.u.)	Q gen (p.u)	P load (p.u.)	Q load (p.u.)
Grid	1.05	-	(0.16)	0.12	-	-
Rabai BSP	1.00	0.34	0.30	0.30	0.03	0.11
Galu	0.98	0.33	-	-	0.05	0.02
Kipevu BSP	1.00	0.34	0.55	0.37	0.33	0.16
KPA	1.00	0.34	-	-	0.24	0.18
New Bamburi	0.97	0.32	-	-	0.09	0.04
Vipingo	0.96	0.32	-	-	-	-
MSA Cement	0.95	0.31	-	-	0.04	0.02
Kilifi	0.95	0.30	-	-	0.04	0.02
Kipevu II	1.00	0.38	0.25	(0.10)	-	-
Mtito	0.98	0.15	-	-	0.01	0.01
Voi	0.98	0.22	-	-	0.01	0.01
Maungu	0.98	0.24	-	-	0.01	0.01
Mariakani	0.99	0.32	-	-	0.04	0.02
Kokotoni	1.00	0.34	-	-	0.02	0.01

4.5 Continuation Power Flow

A continuation power flow has been carried out with an additional 22MW load connected on bus 5 (KPA) to simulate the shore to ship connection. The resulting P-V curves are presented in figure 4.13. It is observed that the point of instability occurs at a loading of more than 5 per unit at KPA bus. This implies that even with the additional load, the network has a large margin of safety against voltage collapse. It is however noted that the voltage level falls below 0.9p.u when the load factor is

1.77p.u. This is the minimum voltage level set by the distribution company, Kenya Power to prevent effects such as motor stalling. This loading value provides a limit for the possible load on the network. The Kilifi bus, which is farthest from the generation point experiences the lower voltage.

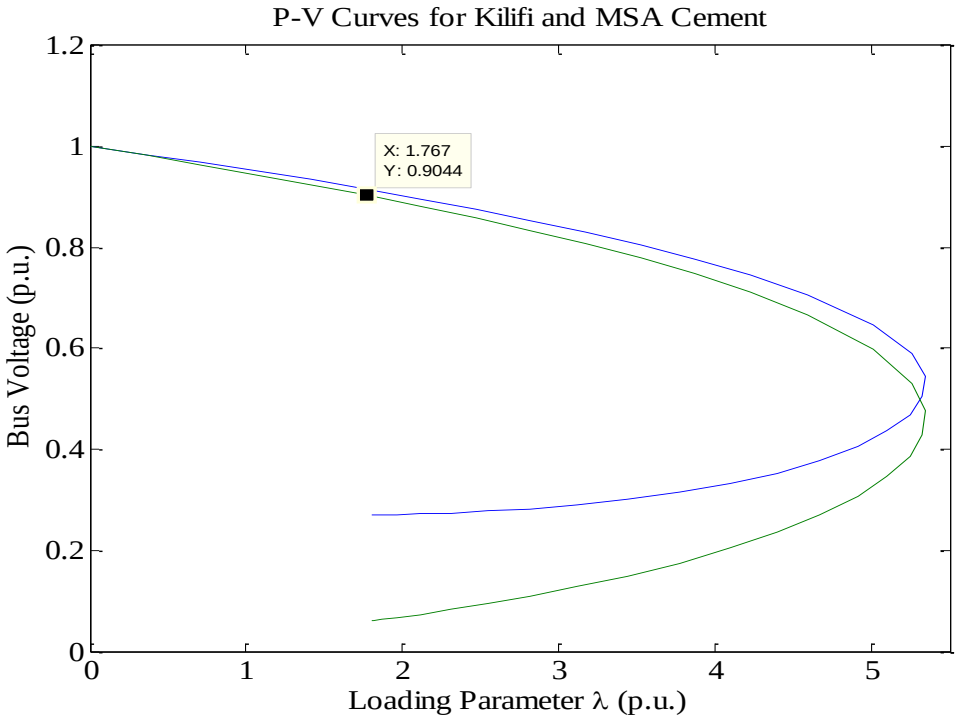

Figure 4.13: PV Curves for MSA Cement and Kilifi buses

A similar study for buses 3 (Galu) and 5 (KPA) is shown in Figure 4.14. It can be noted that the loading limit will not be reached even when the applied load is more than 5 times the modelled load. The Galu bus will however experience voltages below 0.9p.u. When the loading is above 4.7 times the actual modeled load. As earlier noted for Mtito and Voi uses, this can be mitigated by installation of appropriately sized static VAR compensation units.

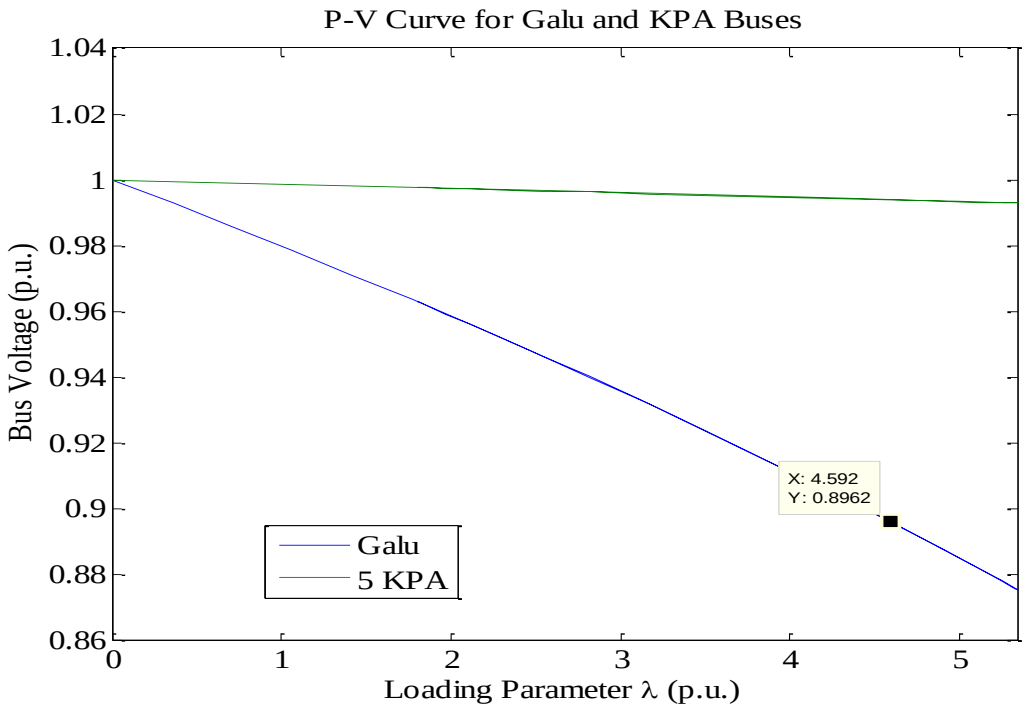

Figure 4.14: PV Curves for Galu and KPA buses

4.6 Effect of Line Outages

In order to investigate the effect of a line outage a load flow study was conducted with outages on selected lines. The lines were selected to either result in disconnection of a generating unit or major loss of load sharing between transmission lines. The selected outages were:

1. One of the Rabai – Kipevu transmission lines.
2. An outage on the Juja – Rabai transmission line (at Kokotoni).
3. An outage of the Kiambere – Rabai transmission line.

It was observed that in case (1), the power flow could be successfully concluded and the bus voltages were similar to those in section 4.4. In the case of (2) and (3), the power follow could not converge. Outage of any of the connections to the grid results in insufficient capacity for the system.

4.7 Mitigation Measures

It is observed from the load flow results that Voi and Mtito buses experienced the lowest voltages. This situation can be mitigated by connection of reactive power compensation (VAR) at the buses from Table 4.4, it can be observed that the reactive power flows from grid (Juja Road) to Mtito bus is 0.1482 per unit. The reactive power flow from Mtito to Voi is 0.083 per unit. The net reactive power consumption at Mtito bus is therefore 0.0652 per unit, which is equivalent to 6.52MVAr. The proposed mitigation measure is to generate this reactive power at the bus using static VAR device. Rounding the figures, the required amount of compensation is -7MVAr or -0.07 per unit. A load flow has been carried out with this additional load connected to Mtito bus. The results are shown Table 4.10 and Figure 4.15. The bus voltages before static VAR compensation are included in the table 4.10 for comparison.

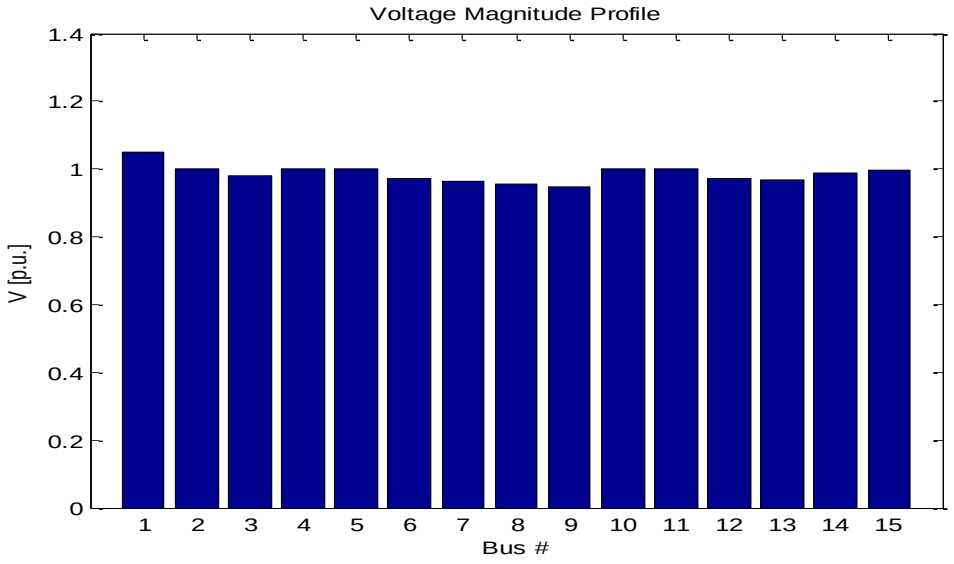

Figure 4.15: Voltage profile with static VAR compensation at Mtito (Bus No. 11)

Table 4.10: Voltage profiles, before and after static VAR compensation at Mtito

BUS	V (p.u.)	
	Without Compensation	With Compensation
Grid	1.05	1.05
Rabai BSP	1.00	1.00
Galu	0.98	0.98
Kipevu BSP	1.00	1.00
KPA	1.00	1.00
New Bamburi	0.97	0.97
Vipingo	0.96	0.96
MSA Cement	0.95	0.95
Kilifi	0.95	0.95
Kipevu II	1.00	1.00
Mtito	0.93	1.00
Voi	0.93	0.97
Maungu	0.94	0.97
Mariakani	0.98	0.99
Kokotoni	0.99	1.00

It can be observed that installation of appropriately sized static VAR compensation raises the voltage at Mtito bus from 0.93 p.u. to 1 p.u. The compensation also has an effect on the voltages at Voi, Maungu and Mariakani which also rise to achieve values closer to 1 p.u.

CHAPTER FIVE

CONCLUSION AND RECOMMENDATIONS

5.1 Aggregation of Ship Loads

A model for the electrical load on a ship has been developed and tested. The tests confirmed that model demonstrates the expected characteristics of an induction motor load. It was also noted that a 3MVA supply is able to take up the load of more than 1000KW which includes direct on line motor starting. Steady state operating conditions for the container ship model were also derived that were applied as initial conditions when performing a load flow study.

5.2 Continuation Power flow for the Coast 132kV power distribution network

A model of off-shore load at the port of Mombasa has been developed. The Coast Region power network has also been modelled. A power flow study has been applied to identify the buses with highest likelihood of voltage collapse. Continuation power flow has further been applied to identify the loading limit on the selected buses. This work has therefore demonstrated the application of power flow and continuation power flow in determining the impact of a shore to ship connection on a regional power network.

The study finds that there is sufficient capacity in the coast network to handle the additional load that would result from a shore to ship connection at the Mombasa port. Some of the buses in the power network would experience reduced voltage. The study has demonstrated that this can be mitigated by installation of appropriately sized static VAR compensation.

The study also finds that the system would collapse if there was an outage in any of the two transmission lines connecting the coast network to the national grid. Long

term stability of the system therefore requires reinforcement of the connection to the grid.

5.3 Recommendations

Ships are growing in length each day and will demand higher and higher power requirements. Given that it is difficult to regulate marine vessels air pollution globally by just lowering fuel sulphur limit from 4.5% to 0.1% alone, shore power supply can be recommended and preferred at Ports.

In this report, it has been shown that there is adequate capacity of power for shore to ship connections for vessels at Port of Mombasa and this method of air pollution reduction technology can be implemented. According to the current world wide trends where several Ports are investigating the possibilities of ship to shore power supply, this is going to happen. Further research is required on the most optimal size, type and module of frequency converters that can be used at Port of Mombasa.

REFERENCES

[1] Ericsson, P and Fazlagic, I. *Shore-side Power Supply: A feasibility study and technical solution for an on-shore electrical infrastructure to supply vessels with electric power while at port,* Goteborg,: Chalmers University of Technology / ABB, 2008.

[2] Radu, D., Jeannot, R., Megdiche, M. and Sorrel, J.P."Shore Connection Applications : Main challenges," Schneider Electric (White Paper), Cedex, France, 2013.

[3] . Bailey, D. and Solomon, G."Polution prevention at ports: clearing air," *Environmental Impact Assesment Review, 24,* 749 - 774, 2004.

[4] Fung, F., Zhu, Z., Becque, R. and Finamore, B."Prevention and Control of Shipping and Port Air Emissions in China," Natural Resources Defence Council (NRDC), 2014.

[5] "High Voltage Shore Connection (HVSC) Systems - General requirements," IEEE Standard Association , IEC/ISO /IEEE 80005 -1 Ed 1 Cold Ironing Part 1 .

[6] . Fiadomor, R. *Assessment of alternative maritime power (cold ironing) and its impact on port management and operations,* Malmo, Sweden: World Maritime University, 2009.

[7] Kenya Power, "Annual report and financial statement," Nairobi , Kenya, June 2016.

[8] Ali, H., Amjady, N. and Rabiee, A. "Reactive Power Pricing Problems & Proposals for a competitive Market," *IEEE Power & Energy Magazine, 7*(1), January/Feburuary 2009.

[9] Machowski, J., Bialek, J.W. and. Bumby, J. R. *Power Systems Dynamics: Stability and Control,* 2nd ed., Chichester, England: John Wiley and Sons, 2008.

[10] IEEE Task Force on Load Representation for dynamic Performance , “Load representation for Dynamic Performance analysis,” *IEEE Trans .power system, 8*(2), 472-482, 1993.

[11] IEEE/CIGRE Joint Task Force on Stability Terms and Definitions, “Definition and classification of power system stability,” *IEEE Transactions on Power Systems, 19*(2), 1387 - 1401, 2004.

[12] Hossain, J. and Pota, H.R. *Robust Control for Grid Voltage Stability: High Penetration of Renewable Energy*, Singapore: Springer Science, 2014.

[13] Seddiek, I.S.,. Mosleh, M.A. and Banawan, A.A “Fuel savings and emission cuts through shore-side power for high speed crafts in the Red Sea,” *Journal of Marine Science Application, Egypt,* 2005.

[14] T. Borkowski and D. Tarnapowicz, ““Shore to ship” system - An alternative electric power supply in port,” *Journal of KONES Powertrain and Transport, 19* (3), 49 - 58, 2012.

[15] Megdiche, M., Radu, D. and Jeanot, R.“Protection plan and safety issues in shore connection applications,” in *22nd International Conference on Electricity Distribution (CIRED 2013),* Stockholm, Swedeb, 2013.

[16] Ion, M., Megdiche, M., Bacha, S. and Radu, D. “Transient analyses of a shore-to-ship connection system,” in *International Conference on Power Systems Transients (IPST 2013),* Vancouver, Canada, 2013.

[17] Nord, T.“Voltage Stability in an Electric Propulsion System for Ships,” Electrical Engineering Electric Power Systems Royal Institute of Technology Stockholm , Sweden, 2006.

[18] IEEE Task force on load representation for dynamic performance, “Standard load models for power flow and dynamic performance simulation,” *IEEE Transactions on Power Systems,* 10(3), 1302 - 1313, 1995.

[19] Milanović, J.V., Yamashita, K., Villanueva, S., Djokić, S.Z. and Korunović, L.M. “International industry practice on power system load modeling,” *IEEE Transactions on Power Systems, 28*(3), 3038 - 3046, 2013.

[20] Liang, X., Xu, W.,. Chung, X.Y.. Freitas, W and Xiong, K.“Dynamic load models for industrial facilities,” *IEEE Transactions on Power Systems, 27*(1), 29 - 80, 2012.

[21] Wedeward, K., Adkins, C., Schaffer, M. Smith, M. and Patel, A.“Inventory of load models in electric power systems via parameter estimation,” *Electronic Letters, 23*(1), 20-28, 2015.

[22] Pillay, E. and Sabur, H.M “A model for induction motor aggregation for power system studies,” *Electric Power Systems Research, 42,* 225 - 228, 1997.

[23] Kataoka, T., Uchida, H., Nishikata, S., Kai, T and Funabashi, T., “A method for aggregation of a group of inductive motor loads,” in *POWERCON*, Perth, Australia, 2000.

[24] Karakas, A. Li, F and Adhikari, S. “Aggregation of multiple induction motors using MATLAB-based software package,” in *IEEE/PES Power Systems Conference and Exposition, 2009 (PSCE '09)*, Seattle, Washington, USA, 2009.

[25] Choi, Byoung-Kon; Chiang, Hsiao-Dong; Li, Yinhong; Li,Hua; Chen, Yung-Tien; Huang, Der-Hua; Lauby Mark G. , “Measurement-based dynamic load models: derivation, comparison, and validation,” *IEEE Transactions on Power Systems, 21*(3), 1276 - 1283, 2006.

[26] Mu, H. Jin, D. and Hill, D.“Composite Load Modelling Via Measurement Approach,” *IEEE Trans. Power System, 21*, 663-672, 2006.

[27] P. Aree, “Aggregating method of induction motor group using energy conservation law,” *ECTI Transactions On Electrical Engineering, Eelectronics and Communications, 12*(1), 1 - 6, 2014.

[28] Milano, F. *Power System Modelling and Scripting*, London: Springer-Verlag, 2010.

[29] World Ports Climate Initiative, “Ports using OPS,” 2015. Retrieved from http://www.ops.wpci.nl/opsinstalled/. 2015.

[30] *IEC/ISO/IEEE 80005-1 Ed.1: Utility Connections in PORT - Part 1: High Voltage Shore Connection (HVSC) Systems,* 2012.

[31] Karue, C.N., . Murage, D.K. and Muriithi, C.M."Shore to Ship Power for Mombasa Port: Possibilities and Challenges," in *Proceedings of the 2016 Annual Conference on Sustainable Research and Innovation*, Nairobi, 2016.

[32] Glover, J.D.. Sarma, K.S. and T. J. Overbye, Power System Analysis and Design, 5th ed., Toronto: Cengage Learning, 2012.

[33] J. Glover, M. Sarma and Overbye, T. *Power System Analysis and Design*, USA: West group, 2005.

[34] Kosterev, D. "Load Modelling in Power System Studies," *IEEE PES General Meeting - Conversion and Delivery of Electrical Energy inthe 21st Century*, pp. 1- 8, July 2008.

[35] Saffarian, A,. Moradzadeh, B,. Sanaye-Pasand, M., and Hosseinian, S.H., "On-line prediction of closest loadability margins using neural networks," in *Proceedings of IEEE Region 10 Conference (TENCON 2007)*, Taipei, 2007.

[36] Kosterev, D. and Meklin, A. "Load Modelling in WECC," in *IEEE PES Power Systems Conference and Exposition*, Atlanta, Georgia, USA, 2006.

[37] Kosterev, D. . Meklin, A.J.U,. Lesieutre, B,. Price, W., Chassin, D., Bravo, R. and Yang, S "Load modeling in power system studies: WECC progress update," in *IEEE Power and Energy Society General Meeting*, Pittsburg, PA, USA, 2008.

[38] WECC Modeling and Validation Work Group, "Composite Load Model for Dynamic Simulations," Western Electricity Coordinating Council, Salt Lake City, Utah, USA, 2012.

[39] Franklin, D , and , Moreleto, C.A., "Improving Dynamic Aggeregation of Induction Moptor Models," *IEEE/PES*, no. Winter Meet, Jan 30- Feb 3 1994.

[40] Kundur, P, *Power System Stability and Control*, New York USA: Mac Graw Hill, 1994.

[41] IEEE Power Engineering Society, "112: I*EEE Standard Test Procedure for Polyphase Induction Motors and Generators*," New York, NY,: IEEE, 2004.

[42] Aree, P. "Power Flow Computation Considering Nonlinear Characteristics of Composite Load Model," in *Proceedings of the International Electrical*

Engineering Congress 2014, 2014.

[43] Gordon, M."Impact of Load Behavior on Transient Stability and Power Transfer Limitations," *IEEE,* 2009.

[44] Hong, Y. and Gau, C. H, "Voltage Stability Indicator for indentification of the Weakest Bus Area in Power Systems," *IEEE Proceedings Generation Transmission Distribution , 144*(4), 1994.

[45] Refern, M., Uster, O. and Fielding, G. "Protection against loss of utility grid supply for a dispersed storage and generation unit," *IEEE transaction on power delivery, 8*(3), 948-954, 1993.

[46] Taylor, C.W. *Power Systems Stability and Control*, New York: Mcgraw Hill, 1993.

[47] Gupta, B.R. *Power Systems Analysis and Design,* New Delhi, India: S. Chand Company Ltd, 2010.

[48] Musirin, I. and Abdul Rahman, T.K. "Estimating Maximum Loadability of Weak Bus Indentifocation Using FVSI," *IEEE Power Engineering Review* , November 2002.

[49] Moghavvemi, M. and Faruque, O."Real-time contingency evaluation and ranking technique," *IEE Proceedings on Generation and Distribution, 145*(5), 517 - 524, 1998.

[50] Musirin, I and R. T. K. A. A., "Novel fast voltage stability index (FVSI) for voltage stability in power transmission systems," in *Student Conference on Research and Development,* Shah Alam, Malaysia, 2002.

[51] Ajjarapu, V., and Christy, C. "The continuation power flow: a tool for steady state voltage stability analysis," *IEEE Transactions on Power Systems, 7*(1), 416 - 423, 1992.

[52] Ngoo, L. M. Muriithi, C.M,. Nyakoe, G.N. and Njoroge, S.N. "A neuro fuzzy model of an induction motor for voltage stability analysis using continuation load flow," *Journal of Electrical and Electronics Engineering Research, 3*(4), 62-70, 2011.

[53] Kenya Ports Authority, “132kV - 11kV Power Supply Upgrade (Tender No. KPA/169/2010-11/EE),” KPA, Mombasa, 2010-2011.

[54] Kenya Power, “Power Sector Medium Term Plan 2015 - 2020,” Nairobi, 2015.

[55] Kenya Power & Lighting Company Ltd, “Kenya Distribution Master Plan,” Vol. 1, Nairobi, 2013.

[56] East African Community, “Regional Power System Master plan and Grid Code Study,” Vol.11 EAC, 2011.

[57] KETRACO, “Power Engineering International Online Magazine,” KETRACO, Nairobi, Jan.1. 1999.

[58] JICA, *Mombasa Port Master Plan including Dongo Kundu,* Japan International Cooperation Agency, 2015.

[59] Liang, X. W, Chung, Y., Freitas, C.K. Xio, K. and Liang, X “Dynamic load models for industrial facilities,” *IEEE Transactions on Power Systems, 1*(27), 29 - 80, 2012.

APPENDICES

Appendix A: Electrical load for various ships

I. Electrical data for container ship Kota Hapas 29

Description of load	Qty	KW	Total KW	Total HP	RsΩ	XsΩ	RrΩ	XrΩ	XmΩ	Jkgm2	Nr (RPM)
Cooling sea w/pump	1	28.9	28.9	39	0.59	0.15	0.16	0.16	12.49	1.3	1470
C/fresh w/pump	1	12.4	12.4	17	1.38	0.29	0.18	0.18	23.57	0.57	1450
M/E lube oil	1	69.9	69.9	94	0.27	0.09	0.16	0.11	4.63	2.58	1484
Exhaust valve pump	1	4.4	4.4	6	4.02	1.46	2.05	2.05	69.73	0.19	1430
Fuel oil, boiler motor	2	2.8	5.6	8	3.45	1.2	1.63	1.63	59.77	0.26	1420
Fuel oil cir-c.pump	1	6.3	6.3	8	3.45	1.2	1.63	1.63	59.77	0.26	1435
Fuel oil tran-s.pump	1	8.5	8.5	11	2.61	0.82	1.01	1.01	44.82	0.36	1445
G/E sea w/pump	1	16.7	16.7	22	1.13	0.24	0.17	0.17	20.26	0.73	1465
G/E D.O sup-p.pump	1	3.8	3.8	5	4.3	1.59	2.26	2.26	74.72	0.16	1430
Ballast/pump	1	39.8	39.8	53	0.41	0.14	0.15	0.15	9.14	1.72	1480
Fire and GS	1	39.8	39.8	53	0.41	0.14	0.15	0.15	9.14	1.72	1480
Fire, ballast	1	86.4	86.4	116	0.23	0.07	0.14	0.09	3.66	3.24	1485
Air comp.	2	47.8	95.6	128	0.21	0.07	0.13	0.08	3.43	3.64	1483
Engine R/vent	2	57.8	115.6	155	0.17	0.05	0.09	0.07	2.91	5.55	1483
A/C plant	1	28.9	28.9	39	0.59	0.15	0.16	0.16	12.49	1.3	1470
A/C fan	1	16.7	16.7	22	1.13	0.24	0.17	0.17	20.26	0.73	1465
Cooking range	4	25	100	134	0.2	0.06	0.12	0.08	3.31	3.84	
Plant/comp.	1	4.4	4.4	6	4.02	1.46	2.05	2.05	69.73	0.19	1430
Cargo cranes	2	185	370	497	0.11	0.03	0.09	0.03	2.91	5.55	1487
Lightings(all)	1	22.86	22.86	31	0.71	0.16	0.16	0.16	14.69	1.03	
Refer containers	150	34.8	5220	7005	0.32	0.14	0.15	0.15	9.14	1.72	
TOTAL	177		6296.56	8449							

II. CARGO SHIP - M/V SIOUX MAIDEN- FROM PHILLIPINES- MANILA

All loads at 440 Volts , 0.8 PF, 60 HZ and 3 phase

Description of item	**Capacity (KW)**
NO. 1 Generator	512.5KVA
No. 2 Generator	512.5 KVA
No. 3 Generator	512.5 KVA
Emergency generator	80 KVA
No. 1 deck crane main pump Motor	140
Oil cooler fan motor	3.7
Servo pump motor	1.5
Booster pump motor	1.5
No. 2 Deck Crane main pump Motor	140
Oil cooler fan motor	3.7
Servo pump motor	1.5
Booster pump motor	1.5
No. 3 Deck crane main pump motor	140
Oil cooler fan motor	3.7
Servo pump motor	1.5
Booster pump motor	1.5
No. 4 Deck crane main pump motor	140
Oil cooler fan motor	3.7
Servo pump motor	1.5
Booster pump motor	1.5
No. 1 windlass Hydraulic pump motor	70
No. 2 windlass Hydraulic pump motor	70
No. 1 Hatch cover hydraulic motor	15

No. 2 Hatch cover hydraulic motor	15
No. 1 mooring winch hydraulic motor	50
No. 2 mooring winch hydraulic motor	50
No. 1 Steering gear motor	7.5
No. 2 Steering gear motor	7.5
Emergency fire pump motor	26
No.1 Reefer compressor motor	3.7
No.2 Reefer compressor motor	3.7
Fish room fan motor	0.1
Meat room fan motor	0.1
Vegetable room fan motor	22
Accomodation Air -con motor	3
Accomodation Air -con fan motor	3
Galley supply fan motor	4
Galley exhaust fan motor	4
Deck air compressor motor	100
No.1 Engine room vent fan motor	11
No.2 Engine room vent fan motor	11
No.1 G/E L.O primimg pump	0.2
No.2 G/E L.O Primimg pump	0.2
No.3 G/E L.O Primimg pump	1.5
Sewage discharge pump motor	0.75
Sewage blower fan motor	2.2
Lathe machine motor	2
Engine room overhead crane	15
Electric grider motor	1
Engine room welding machine	2.2
Deck welding machine	1.5
Incinerator fan motor	1.5
Incinerator burner motor	0.4

Boiler D/F fan motor	3.7
Engine control room air con.compressor	120
Engine control room air con. Fan motor	30
No. 1 Main air compressor motor	37
No. 2 main air compressor motor	37
No. 1 Feed water pump motor	5.5
No. 2 Feed water pump motor	5.5
No. 1 M/E auxilliary blower	18.5
No. 2 M/E auxilliary blower	18.5
No.1 F.O booster pump	3.7
No. 2 F.O Booster pump	3.7
No.1 H.F.O purifier	5.5
No.2 H.F.O purifier	5.5
L.O purifier motor	5.5
No. 1 Crosshead L.O pump	18.5
No. 2 Crosshead L.O pump	18.5
No. 1 Jackect C F W pump	15
No. 2 Jackect C F W Pump	15
Air -con hot water circulating pump	1.5
Hot water circulating pump	1.5
Fresh water circulating pump	5.5
Distillate pump motor	0.75
Domestic fresh water pump	3.7
Drinking water pump	3.7
Sludge pump motor	1.5
Bilge pump motor	0.75
Fire & G.S pump motor	30
Fire bilge &ba;;ast pump motor	90
Ballast & ST/ By C.S W pump motor	33
Main cooling sea water pump motor	30

Auxillirary S.W Cool pump motor	11
Auxillirary F.O transfer pump motor	1.5
H.F.O transfer pump motor	7.5
Air-con /Ref C.S.W pump motor	7.5
Provision ref C.S W pump motor	2.2
L.O transfer pump motor	1.5
L.O purifier feed pump motor	0.75
No. 1 G/E F O circulating pump motor	1.5
No. 2 G/E F.O Circulating pump motor	1.5
No.1 Main Engine L.O. Pump motor	45
No. 2 Main Engine L.O pump Motor	45
M/E turnig gear motor	1.5
Provision crane hoisting motor	11
Provision crane luffing motor	1.5
Provision crane slewing motor	1.5
Lifeboat winch motoe starboard	3.7
Life boat winch motor port side	3.7
Window wiper motor	0.75
Electric cooking range	12
Crane no. 1 CRD winch motor	3
Crane no. 1 rope drum motor	2.2
Grab no. 1 pump motor	28
Crane no. 2 CRD winch motor	3
Crane no. 2 rope drum motor	2.2
Grab no. 2 pump motor	28
Crane no. 3 CRD winch motor	3
Crane no. 3 rope drum motor	2.2
Grab no. 3 pump motor	28
Crane no. 4 CRD winch motor	3
Crane no. 4 rope drum motor	2.2

Grab no. 4 pump motor	28

III. FUEL SHIP / TANKER - CANAL STREET

60 HZ, 440 V and at 0.8 PF

	PURPOSE	KW	QTY
1	M/E Auxilliary blower	40.2	2
2	M/E turning gear	1.9	1
3	Central cooling fresh water pump	70.7	2
4	Main cooling sea water pump	59.8	2
5	Jackect cooling fresh water pump	12.4	2
6	Lubricating oil pump	59.8	2
7	Stern tube L.O Pump	0.5	2
8	F.O booster pump	1.9	2
9	F.O Circulating pump	4.4	2
10	Alpha Lubrication pump	2.7	2
11	Air cooler cleaning pump	1.9	1
12	G/E F.O booster pump	1	2
13	G/E F.O Circulating pump	1.9	2
14	G/E L.O priming pump	1.1	3
15	Aux. Boiler pilot burner pump	0.5	1
16	Aux. Boiler F.O burning pump	4.4	2
17	Aux. Boiler F.D fan	80.6	1
18	Aux. boiler primary air fan	12.4	1
19	Main feed water pump	59.8	2
20	Auxilliary feed water pump	16.7	2
21	Boiler water circulating pump	6.3	2

22	Aux. condenser circulating pump	24.2	1
23	Condensate pump	6.3	2
24	Inert gas scrubber cool , water pump	20.3	1
25	Inert gas fan	40.2	2
26	C.O.P.T. L.O . Priming pump	1.2	4
27	Sample feed pump (ballast Monitor)	3	1
28	Valve control hyd. Oil pump	1.9	2
29	Auto unload system vacuum pump	0.3	2
30	IG deck seal water pump	1.9	2
31	Bilge seperator service pump	2.7	1
32	Ballast pump	95.7	2
33	Fir, Bilge & GS pump	80.6	1
34	Fire , bilge & ballast pump	80.8	1
35	Bilge pump	1	1
36	Sludge pump	4.4	1
37	Fresh water pump	4.4	2
38	Drinking water pump	2.7	1
39	Hot water circulating pump	0.5	1
40	Heavy F.O transfer pump	8.5	1
41	D.O transfer pump	2.7	1
42	F.O purifier	6.3	2
43	L.O purifier	6.3	2
44	L.O transfer & L .O purifier supp pump	1.9	2
45	Main air compressor	32.6	2
46	Engine room exhauster Fan	16.7	4
47	Purifier room exhauster Fan	1.9	1
48	Pump room exhauster pump	16.7	1
49	Dist. Plant (Ejector pump)	16.7	1
50	Dist. Plant (Dist. pump)	1	1
51	Sewege treatment (blower)	1.9	1

52	Waste oil incinerator (Burner)	1	1
53	Waste oil Incinerator (Exhaust fan)	8.5	1
54	Control room unit cooler (Comp.)	4.4	1
55	Control room unit cooler (Fan)	0.5	1
56	Control room unit cooler (heater)	7.5	1
57	Overhead crane (Hoist)	2.7	2
58	Overhead crane (travel)	1	1
59	Lathe	4	1
60	Drill	0.5	1
61	Grinder	1	1
62	Electric welder (300A)		2
63	MGPS	0.1	1
64	I.C.C.P	12	1
65	Steering gear	27.5	2
66	Windlass & deck crane hyd oil pump	68.5	2
67	Mooring winch hyd. Oil pump	59.8	2
68	Rescue boat winch	9.3	1
69	Boat winch	7.5	1
70	Provision crane (Hoisting)	2.7	1
71	Provision crane (Hoisting)	4.7	1
72	Provision crane (Luffing)	1.9	1
73	Provision crane (Slewing)	1.9	1
74	Galley unit cooler (Comp.)	3.6	1
75	Galley unit cooler (Fan)	0.5	1
76	Galley Unit cooler (Heater)	6	1
77	Prov. Ref compressor	5.3	2
78	Air cond. Compressor	52.4	1
79	Air Cond. Fan	16.7	1
80	Galley exhaust fan	0.5	1
81	Steering hear room exhaust fan	1	1

82	Fore bos'n store supply fan	1	1
83	Water mist low press pump	14.2	1
84	Emergency fire pump	59.8	1
85	High expansion form liquid pump	2.7	1
86	Emergeny generator room exhaust fan	2.7	1
87	Electric cooking range	30	1
88	Electric fryer	5	1
89	Disposer	1.2	1
90	Lavatory exhaust fan	0.3	1
91	Nautical equipment	5	1
92	Battery charger	1	1
93	AC220V circuit(lighting)	100	1

IV. RO-RO SHIP - JOLLY CRISTALLO GENOVA - DIAMANTE LINEA MESSINA

All loads at 440 Volts , 0.8 PF, 60 HZ and 3 phase

Description of item	QTY	Capacity (KW)	RPM	Total KW
Feed water pump for EGB	2	15		30
Dumping condenser	1	2		2
Fresh water generator	1	1.5		1.5
Incinerator	1	2		2
Bilge water seperator	1	2		2
lathe	1	5		5
Air intake trunks	5	3.5		17.5

shaft power meter	1	1		1
E/R bilge pump	1	4		4
Bilge water seperator pump	1	6		6
Water based local fire fighting system	1	8.6		8.6
Emmision monitoring system	1	1.5		1.5
Control air compressors	2	16.7	3550	33.4
G/E emergency air reservior	1	3		3
Main air reservoirs	2	34		68
Service air compressor	1	30	3550	30
MDO purifier	1	3.7	3480	3.7
Service air compressor	1	210		210
Control air compressors	1	130		130
Air reservoir & control panel for QCV	1	23		23
Control air drier (1EA) service air dryer(1EA)	2	20		40
Boiler scrubber	1	2		2
Aux. Engine scrubber	1	6.2		6.2
Wash water supply pumps	3	99		297
Wash water return pumps	3	43		129
Reaction water pumps	2	51		102
Boiler ID fan	1	6.7		6.7
Aux. Engine ID fans	4	18		72
Boiler sealing air fan	1	1.3		1.3
Aux engine sealing air fans	4	1.3		5.2
Deaeration tank ventilation fan	1	1.3		1.3
Water treatment plants	2	8.9		17.8
Deplume heater for boiler scrubber	1	4		4
Deplume heater for AUX.engine scrubber	4	3		12
Feed water pumps for aux. boiler	2	11		22
L O Transfer pump	1	3.5		3.5

M/E L O Purifiers	2	8.6	3460	17.2
G/E L O Purifiers heaters	2	8.6	3460	17.2
M/E L O Purifiers feed pumps	2	1.3		2.6
M/E L O purifier heaters	2	7.2		14.4
Stern tube LO pumps	2	0.9		1.8
Hand pump	1	7.5		7.5
Main LO pumps	2	110		220
Stern tube LO cooler	2	23		46
Main Lo cooler	1	20		20
G/E F O flow meter	1	1		1
Main cooling SW pumps	3	55		165
Central FW coolers	2	13		26
M/E Jackect cooling F W pumps	2	30		60
M/E Jackect cooling F W coolers	2	30		60
Welding area exhaust fan	1	25		25
M/E Jacket cooling FW preheater	1	25		25
MGPS	1	2		2
Main air compressors	2	30		60
G/E L O purifier feed pumps	2	1.3		2.6
Cylinder oil transfer pump	1	0.45		0.45
MDO transfer pump	1	12.5		12.5
FWF HFO transfer pumps	2	13		26
HFO purifiers	2	26.5	3520	53
HFO purifier feed pumps	2	4.6		9.2
HFO purifier heaters	2	63		126
MDO purifier feed pump	1	0.9		0.9
Sludge pump	1	2.55		2.55
M/E cooling transfer pump	1	2.2		2.2
M/E FO viscosity controller	1	4.6		4.6
M/E FO circulating pumps	2	4.6		9.2

G.E FO Viscosity controller	1	2.7		2.7
M/E F O supply pumps	2	2.5		5
M/E F O Auto filter	1	2		2
M/E F O heaters	2	34		68
M/EF O flow meter	1	1		1
M/E F O indicator filter	1	3		3
Aux. Boiler	1	35		35
Aux. Boiler burner	1	46		46
Aux boiler F O heater	1	32		32
Aux. boiler supply pumps	2	0.66		1.32
Aux. boiler FO ignition pumps	2	0.22		0.44
Cooling F W boost pumps for accom.	2	30		60
Salinity indicator	1	2		2
Exhaust gas boiler	1	34		34
GE Lo Priming pumps	4	2.2		8.8
G/E MDO pump	1	0.9		0.9
G.E F O supply pumps	2	1.3		2.6
G/E F O Circulating pumps	2	3.5		7
G/E Emergency MDO pump	1	3.5		3.5
G/E FO heaters	2	20		40
G/E FO auto filter	1	20		20
G/E FO indicating filter	1	3		3
M/E L O manual simplex filters	2	7		14
HFO transfer pump	1	12.7		12.7
Distilled water Hyd. Tank	1	3		3
Hot water circulating pumps	2	3.7		7.4
Low temp cooling FW pumps	3	45		135
Dist. Water hyd. Pump	1	7.5		7.5
Hot water calorifier	1	30		30
M/E air cooler clean W circulating pump	1	2.2		2.2

FW re hardening filter	1	4		4
FW hydrophore tank	1	4		4
Domestic FW sterilizer	1	54		54
Sewage discharge pump	1	5.5		5.5
Main engine	1	22.89	108	22.89
Controllable pitch propeller	1	5		5
Propeller shaft	1	32		32
Intermediate shaft	1	20		20
Rotor shaft	1	32		32
Of- box shaft	1	3		3
Sleeve coupling	1	4		4
Inter shaft bearing	2	2		4
Forward stern tube bearings	1	2		2
After stern tube seal	1	4		4
Shaft coupling bolts and nuts	26	1.5		39
Shaft earthing device	1	1.2		1.2
Total power requirement	-	-	-	**3150.75**

V. ELECTRICAL LOADS ON A MILLITARY SHIP

Equipment Description	Type	Qty.	Power	R.P.M.	Voltage
Motor of Laundry's tank pump	M2VA80A-2	1	0,9kW	3420	3A
Motor of sludge pump	M3AA090S-4	1	1,3kW	1700	440V, 2,66A

Motor of Lube oil transfer pump	M3AA090S-4	1	1,3kW	1700	440V; 2,66A
Motor of fuel oil transfer pump 1	M3AA100LA-4	1	2,5kW	1720	440V; 60Hz; 4,9A
Motor 1 of Fresh Water Transfer and RAS P.	M3AA1325B-2	1	8,6KW	3415	440V; 14,7A
Motor 2 of Fresh Water Transfer and RAS P.	M2AA90L-2	1	2,5KW	3470	440V; 4,6A
Motor 1 of FI-FI Emergency Hydrophore Pump	M3AA160MA-2	1	14KW	3505	440V; 23A
Motor 2 of FI-FI Emergency Hydrophore Pump	M2AA90L-2	1	2,5KW	3470	440V; 4,6A
Motor 1 of Ballast and Bilge Pump	M3AA160MA-2	1	14KW	3505	440V; 23A
Motor 2 of Ballast and Bilge Pump	M2AA90L-2	1	2,5KW	3470	440V; 4,6A
Motor 1 of Ballast and	M3AA160MA-2	1	14KW	3505	440V; 23A

Bilge Pump 2					
Motor 2 of Ballast and Bilge Pump 2	M2AA90L-2	1	2,5KW	3470	440V; 4,6A
Motor 1 of General Service Pump	M3AA160MA-2	1	14KW	3505	440V; 23A
Motor 2 of General Service Pump	M2AA90L-2	1	2,5KW	3470	440V; 4,6A
Motor 1 of General Service Pump 2	M3AA160MA-2	1	14KW	3505	440V; 23A
Motor 2 of General Service Pump 2	M2AA90L-2	1	2,5KW	3470	440V; 4,6A
Motor of Fuel oil transfer pump 2	M3AA100LA-4	1	2,5kW	1720	440V; 4,9A
Motor of Sanitary F.W. Hydrophore	M3AA100LA-4	1	2,5kW	1720	440V; 4,5A
Motor of Hydrophore Reservation	M3AA100LA-4	1	2,5kW	1720	
Motor for Lube Oil Transfer	M2VA7-1B4	1	0,45kW	1700	440V;

Electro Pump					
Motor for Lube Oil Transfer Electro Pump	M2VA7-1B4	1	0,45kW	1700	440V;
Motor of Stabilizer power pack pump	M2VA80B-2	1	1,3KW	3420	440V; 4,2A
Motor of Self Primming Pump	L-48	1	3,1 kW	1500	
Motor for Food Service Lift	AM80ZAA4	1	0,63KW	1700	440V; 2,9A
Motor for Etaprime Self Primming Pump	D910 L03	1	42,6KW	3000	
Waste-Disposal Unit	T-1 Luxe	1	0,5CV		110V,5,25A
Deck Crane Palfinger	PK 23080M S25	1	22.3		
Motor of Electro Hydraulic Unit	M2AA 180 L4	1	25,5KW	1760	440V; 43A
Motor 1 of Steering Gear	1LA7113-4AA11	1	4,6KW	1740	440;7,9 A;
Motor 2 of Steering Gear	1LA7113-4AA11	1	4,6KW	1740	4407,9 A;

Motor for Hydraulic Plant	LS200LT-T	1	30KW	1762	440V; 49,7A
Motor for Hydraulic Plant	LS200LT-T	1	30KW	1762	440V; 49,7A
Motor for Stabilizer Power Pack Pump	M2VA80B-2	1	1,3kW	3420	440V; 4,2A
Motor for Antenna Pedestal Mechanism	AM90L/A4	1	0,37KW	1740	440V;0,95A
Transducer	50B-12	1	2KW		50Khz
Intercom System	A4279	1			500V; 8A
Searchlight with morseshutter	463 HGS		1000W		125V; 60Hz
Searchlight with morseshutter	463 HGS		1000W		125V; 60Hz
Navigation Lights Control Panel	TEF-4730	1	500W		2 x 24V
Motor of Windlass	DM1 112 M4	1	4KW	1440	400V; 50Hz;8,04A
Motor of Capstan	DM1 180 L8	1	11KW	720	400; 50Hz;13,7A

Lathe	SP/165	1	2,2KW	1700	440V; 60HZ
Drilling Machine	KS	1	0,8KW	3600	440V; 60HZ
Standard Electric Grinding	EE-2	1	0,6CV	3420	440V; 60Hz
Motor 1	RRT 4.61866-2	1	7 KW	1435/1730	50/60Hz; 400/440V
Motor 2	RRT 4.61866-2	1	7 KW	1435/1730	50/60Hz; 400/440V
Motor for Rescue Boat 1	90PTO	1	67,1 KW	5500	
Motor for Rescue Boat 2	90ELPTO	1	66,2 KW	5500	
Rigid Rescue Boat 3	RIBO 600	1	88,4W;		
Outboard for Rigid Rescue Boat 3	90PTO	1	67,1 KW	5500	
Rigid Rescue Boat 4	RIBO 600	1	88,4W		
Outboard for Rigid Rescue Boat 4	90PTO	1	67,1 KW	5500	
UPS Computer	DHS	1			115V/230V; 50/60Hz; 2,0/1,0A
Computer Monitor	E153FPf	1			100/240V; 50/60Hz; 1A
UPS Computer	DHS	1			115V/230V; 50/60Hz; 2,0/1,0A
Computer Monitor	E153FPf	1			100/240V; 50/60Hz; 1A
UPS Computer	DHS	1			115V/230V; 50/60Hz; 2,0/1,0A
Computer	E153FPf	1			100/240V; 50/60Hz;

Monitor					1A
Television	21TXS Real Flat	1	55W		240V; 50HZ
Television	21TXS Real Flat	1	55W		240V; 50HZ
Compressor Motor for Cold Storage Plant	M2AA100LB-4	1	3,2 KW	1720	440V; 60Hz; 6,6A
Compressor Motor for Cold Storage Plant	M2AA100LB-4	1	3,2 KW	1720	440V; 60Hz; 6,6A
Electropump Motor for Cold Storage Plant	AM71ZBA2	1	0,63KW	1750	440V; 60Hz; 2,9A
Electric Cooker	CPB-167	1	28000W		440V; 60HZ
Deep Fat Fryer	FE-770	1	18600W		440V; 60HZ
Refrigeration Cabinet	300-R	1	394W		110V; 60HZ
Refrigeration Cabinet	300-R	1	394W		110V; 60HZ
Refrigeration Cabinet	300-R	1	394W		110V; 60HZ
Water Boiler (Tea)	RT-14	1	1500W		110V; 60HZ
Electric Toaster	TPS/1	1	1800W		110V; 60HZ
Refrigerator	EA-3210	1	115W		110V; 60HZ
Refrigerator	EA-3210	1	115W		110V; 60HZ
Refrigerator	EA-3210	1	115W		110V; 60HZ
Rice and Pasta Cooker	CP/47	1	6900W		440V; 60HZ
Refrigerator	300-R	1	394W		110V; 60HZ
Water Cooler	RA-10Gi	1	320W		110V; 60HZ
Water Cooler	RA-10Gi	1	320W		110V; 60HZ
Water Cooler	RA-10Gi	1	320W		110V; 60HZ
Drying Tumbler	T-5205C	1	2860W		230V; 50HZ
Drying Tumbler	T-5205C	1	2860W		230V; 50HZ

Washer Extractor	WS-5425	1	5050W		440V; 60HZ
Washer Extractor	WS-5425	1	5050W,		440V; 60HZ
Rotary Ironer	HM-16-83	1	2500W		230V; 60HZ
Drying Tumbler	T-5205C	1	2850W		230V; 60Hz
Washer Extractor	WS-5425	1	5050W		440V; 60Hz
Motor for Food Service Lift	AM80ZAA4	1	0,63 KW	1700	440V; 60HZ; 2,9A
Motor of Fan Wood	D-132	1	7,5KW	1734	440V; 60Hz
Motor for Air Conditioned Unit 2	M2AA180M2	1	22KW	2925	380V; 50HZ
Circulating Pump Electrical Motor 1	K21R112M4 FDS	1	4,8KW	1720-1740	400-500V; 60Hz; 8,7/9 A
Circulating Pump Electrical Motor 2	K21R112M4 FDS	1	4,8KW	1720-1740	400-500V; 60Hz; 8,7/9 A
Motor for Aerofoil Axial-Flow Fan	D160-M	1	15,6K W		440V; 60Hz; 27,2A
Motor for Aerofoil Axial-Flow Fan	D160-M	1	15,6K W		440V; 60Hz; 27,2A
Motor for Aerofoil Axial-Flow Fan	D132	1	7,5KW		440V; 60Hz; 14,9A
Motor for Aerofoil Axial-Flow Fan	D132	1	7,5KW		440V; 60Hz; 14,9A

Diesel Oil Separation System	MMB 305	1	3KW	3600	60Hz
Motor for Diesel Oil Separator	M2AA100L2 / 3GAA10100	1	3,70KW	3480	254/440V; 11,3/6,5A
Motor for electro pump	M2AA80L-4	1	1,75KW	1710	440V; 60Hz; 3,5A
Lube Oil Separation System	MMB 305	1	3KW	3600	
Motor for Lube Oil Separator	M2AA100L2 / 3GAA10100	1	3,70KW	3480	254/440V; 11,3/6,5A;
Heatpacpor Lube Oil Separator	EHM / EHS	1	24KW		440V
Motor for Electro pump	M2VA80A-4	1	0,65KW	1680	440V; 60Hz; 2,4A
Motor for Air Compressor 1	PLS180L-T	1	34KW	1740	440V; 60Hz; 58,6A
Motor for Air Compressor 2	PLS180L-T	1	34KW	1740	
Motor for Air Compressor 3	PLS180L-T	1	34KW	1740	
Motor for Electrical Pump 1	AM100LBA4	1	3,5KW	1720	440V; 60Hz; 11,5A
Motor for Electrical Pump 2	AM100LBA4	1	3,5KW	1720	440V; 60Hz; 11,5A

Motor for Electrical Pump 3	AM100LBA4	1	3,5KW	1720	440V; 60Hz; 11,5A
Motor for Electrical Pump 4	AM71ZBA2	1	0,63KW	1720	440V; 60Hz; 2,9A
Air Compressor 1	HL2/90	1	10,8kw	1750	
Motor for Air Compressor 1	M3AA132MB	1	11KW	1750	440V; 60Hz; 19 A
Air Compressor 1	HL2/90	1	10,8kw	1750	
Motor for Air Compressor 1	M3AA132MB	1	11KW	1750	440V; 60Hz; 19 A

Appendix B: MATLAB aggregation programme code for crane motors

```
% This script carries out aggregation of multiple induction motor
loads.

% The motor data is saved in an excel sheet named
'Motors_Crane.xlsx'. This

% should be saved in the same folder as this script (or in a
directory that

% is included in the Matlab path).

% The data should be arranged in columns A to L of the excel sheet.
The

% number of rows to be used depends on the total number of motors to
be

% aggregated. Data for equivalent motors does not have to be
repeated and

% can be included in the same row.

% Row 1: Contains the heads describing the motor data. The cells
should not

% contain characters that could be identified as a number.

% Column A: Contains the name of the motor load category.

% Column B: Contains the number of motors included in the category

% Column C: Contains the power rating, in KW of each motor in the
category.

% Column D: Contains the total power of the particular category in
KW.
```

```
% Column E: Contains the total power of the particular category in
HP.

% Column F: Stator resistance in ohms (for one motor).

% Column G: Stator inductive reactance in ohms (for one motor).

% Column H: Rotor resistance in ohms, Referred to the stator (for
one motor).

% Column I: Rotor inductive reactance in ohms, Referred to the
stator (for one motor).

% Column J: Magnetizing reactance in ohms (for one motor).

% Column K: Motor + Load Moment of inertia in KGm2 (for one motor).

% Column L: Motor speed at full load, in RPM

% NOTE: Information in columns C and D is not used. The columns may
be left

% blank, but must be included. The script does not use the column
titles

% and instead depends on the column numbers to identify nature of
input

% data.



% Other inputs to be amended before running are:

%           Rated motor voltage (RMS), in volts;

%           Rated motor frequency in Hz.

%           Number of pole pairs for the motor;
```

```
%           Name of file containing the motor may be changed.


% The script outputs the parameters required to model the aggregated
motor

% in SIMULINK. The parameters are written to an excel sheet named

% 'Aggregated_Motor_Parameters_Fan.xlsx' in the MATLAB working
directly.

% The parameters are saved in two options. The first option has
inductances

% in ohms and speed in RPM. The second option has inductances in
Henrys and

% speed in radians per second.

% The parameters are saved in a separate sheet from the data titles.

% Also included in the output are the starting variables required to
test

% the transient response when starting point is rated speed.

% REVISION STATUS: Modified March 28: Reverted to original Pn but
retained modified IAgg.

V=400;
% Enter motor rated voltage

poles=2;
% Enter motor pole pairs

f=50;
% Enter rated frequency
```

```
A=xlsread('Motors_Crane.xlsx');                                % Read
in data for motors to be aggregated.



% Separate the rows in the input data that have more than one motor

M=uint16(sum(A(:,1)));

[P,N]=size(A);

B=zeros(M,N);

m=0;

for p=1:P;

    Q=A(p,1);

for q=1:Q;

B(m+1,:)=A(p,:);

B(m+1,1)=1;

        m=m+1;

end;

end;



ZNL=complex(B(:,5),B(:,6)+B(:,9));                        % Evaluate
No load impedance for each motor

ZLR=complex(B(:,5)+B(:,7),B(:,6)+B(:,8));            % Evaluate
Locked rotor impedance for each motor
```

```
ZNLEq=1/(sum(1./(ZNL)));                                    %
Evaluate equivalent No Load impedance for aggregated motor

ZLREq=1/(sum(1./(ZLR)));                                    %
Evaluate equivalent No Locked rotor impedance for aggregated motor



RRAgg=real(ZLREq)-real(ZNLEq);                          % Evaluate
Rotor Resistance for aggregated motor

RSAgg=real(ZNLEq);                                          %
Evaluate Stator Resistance for aggregated motor



% Assume Design D motor. Xs/Xr=1

XSAgg=0.5*imag(ZLREq);                                  % Evaluate
Stator Reactance for aggregated motor

XRAgg=0.5*imag(ZLREq);                                  % Evaluate
Rotor Reactance for aggregated motor

XMAgg=imag(ZNLEq)-0.5*imag(ZLREq);                  % Evaluate
Magnetising Reactance for aggregated motor



% Motor slip Evaluation

Ns=60*f/poles;                                              %
Synchronous speed

Nr=B(:,11);
% Rated speed from input data

s=(Ns-Nr)./Ns;                                              %
Slip
```

```
Zs=complex(B(:,5),B(:,6));                                          %
Motor stator impedance from input data

Zm=complex(0,B(:,9));                                               %
Motor magnetising impedance from input data

Zr=complex((B(:,7)./s),B(:,8));                                     % Motor
rotor impedance (at rated speed) from input data

Z=Zs+((Zm.*Zr)./(Zm+Zr));                                           % Motor
total impedance (at rated speed) from input data

ZEq=1/(sum(1./(Z)));                                                %
Total impedance (at rated speed) for aggregated motor



% Evaluation of aggregated slip

alpha=((XMAgg+XRAgg)^2)*(real(ZEq)-RSAgg);

beta=-1*RRAgg*XMAgg^2;

gamma=(real(ZEq)-RSAgg)*RRAgg^2;

sAgg=(-1*beta-(beta^2-4*alpha*gama)^0.5)/(2*alpha);



Power=B(:,2)*1000;
% Reading pated power from input data

PAgg=sum(Power);                                                    %
Evaluation of aggregated motor power
```

```
J=B(:,10);
% Reading inertia from input data

w=(2*pi/60).*Nr;                                                    %
Converting rated speed from RPM to Radians per Sec

ws=(2*pi/60)*Ns;                                                    %
Synchronous speed in Radians per Sec.

NAgg=Ns*(1-sAgg);                                                    %
Evaluating aggergated motor speed (in RPM)

wrAgg=NAgg*2*pi/60;                                                 %
Evaluating aggregated motor speed (in Rad. per Sec)

JAgg=sum(J.*((w./wrAgg).^2));                                % Evaluating
aggregated motor inertia

Torque=(0.8*PAgg)/wrAgg;                                             %
Evaluating aggregated motor torque

k=Torque/(wrAgg^2);                                                 %
Evaluating constant in speed - torque relation (T=kw^2)

k1=Torque/((wrAgg/2)^2);                                           %
Evaluating constant in speed - torque relation (T=k1(w/2)^2) for
constant torque

Ff=0.005*0.8*PAgg/(wrAgg^2);                                 % Evaluating
Friction Factor (Based on friction loss = 0.5% of PAgg)



% Evaluate parameters for supply change-over at rated speed.

ZSAgg=complex(RSAgg,XSAgg);                                % Stator
impedance for aggregated motor

ZRAgg=complex(RRAgg/sAgg,XRAgg);                     % Rotor impedance
for aggregated motor at aggregated slip
```

```
ZMAgg=complex(0,XMAgg);                                          %
Magnetising impedance for aggregated motor

ZAgg=ZSAgg+((ZMAgg.*ZRAgg)./(ZMAgg+ZRAgg)); % Motor total impedance
(at aggregated slip) for aggregated motor

IAgg=V/(ZAgg*3^0.5);                                              %
Current for aggregated motor at rated speed

IaMag=abs(IAgg);                                                    %
Magnitude of current at rated speed.

% Phase of

if angle(IAgg) < 0

IaPh=360+angle(IAgg)*180/pi;

elseIaPh=angle(IAgg)*180/pi;

end;



if (IaPh+120)<360

IbPh=IaPh+120;

elseIbPh=(IaPh+120)-360;

end;



if (IbPh+120)<360

IcPh=IbPh+120;

elseIcPh=(IbPh+120)-360;
```

```
end;


%Arranging parameters in one array and exporting to excel

Param_Ohm_RPM=[PAgg,V,f,RSAgg,XSAgg,RRAgg,XRAgg,XMAgg,JAgg,Ff,poles,
k,k1,sAgg,IaMag,IaPh,IbPh,IcPh,Torque,NAgg,NAgg/2];

Param_Hen_RadPS=[PAgg,V,f,RSAgg,XSAgg/(2*pi*f),RRAgg,XRAgg/(2*pi*f),
XMAgg/(2*pi*f),JAgg,Ff,poles,k,k1,sAgg,IaMag,IaPh,IbPh,IcPh,Torque,w
rAgg,wrAgg/2];

S1={'Pn(VA)''Vn(V)''Fn(Hz)''Rs(Ohms)''Ls(Ohms)''Rr(Ohms)''Lr(Ohms)''
Lm(Ohms)''J(Kg.m2)''Friction_f(N.m.s)''Pole_pairs''k''k1''slip''FlCu
rr,A''PH Angle, Ia''PH Angle, Ib''PH Angle,
Ic''Torque''Speed(RPM)''Half Speed'};

S2={'Pn(VA)''Vn(V)''Fn(Hz)''Rs(Ohms)''Ls(Henry)''Rr(Ohms)''Lr(Henry)
''Lm(Henry)''J(Kg.m2)''Friction_f(N.m.s)''Pole_pairs''k''k1''slip''F
lCurr,A''PH Angle, Ia''PH Angle, Ib''PH Angle,
Ic''Torque''Speed(Rad/s)''Half Speed'};

xlswrite('Aggregated_Motor_Parameters_Crane.xlsx',Param_Ohm_RPM','Oh
m_Data');

xlswrite('Aggregated_Motor_Parameters_Crane.xlsx',S1','Ohm_Title');

xlswrite('Aggregated_Motor_Parameters_Crane.xlsx',Param_Hen_RadPS','
Henry_Data');

xlswrite('Aggregated_Motor_Parameters_Crane.xlsx',S2','Henry_Title')
;
```

Appendix C: MATLAB aggregation programme code for fan motors

```
% This script carries out aggregation of multiple induction motor
loads.

% The motor data is saved in an excel sheet named 'Motors_Fan.xlsx'.
This

% should be saved in the same folder as this script (or in a
directory that

% is included in the current Matlab path).

% The data should be arranged in columns A to L of the excel sheet.
The

% number of rows to be used depends on the total number of motors to
be

% aggregated. Data for equivalent motors does not have to be
repeated and

% can be included in the same row.

% Row 1: Contains the heads describing the motor data. The cells
should not

% contain characters that could be identified as a number.

% Column A: Contains the name of the motor load category.

% Column B: Contains the number of motors included in the category

% Column C: Contains the power rating, in KW of each motor in the
category.

% Column D: Contains the total power of the particular category in
KW.
```

```
% Column E: Contains the total power of the particular category in
HP.

% Column F: Stator resistance in ohms (for one motor).

% Column G: Stator inductive reactance in ohms (for one motor).

% Column H: Rotor resistance in ohms, Referred to the stator (for
one motor).

% Column I: Rotor inductive reactance in ohms, Referred to the
stator (for one motor).

% Column J: Magnetizing reactance in ohms (for one motor).

% Column K: Motor + Load Moment of inertia in KGm2 (for one motor).

% Column L: Motor speed at full load, in RPM

% NOTE: Information in columns C and D is not used. The columns may
be left

% blank, but must be included. The script does not use the column
titles

% and instead depends on the column numbers to identify nature of
input

% data.



% Other inputs to be amended before running are:

%           Rated motor voltage (RMS), in volts;

%           Rated motor frequency in Hz.

%           Number of pole pairs for the motor;
```

```
%           Name of file containing the motor may be changed.


% The script outputs the parameters required to model the aggregated
motor

% in SIMULINK. The parameters are written to an excel sheet named

% 'Aggregated_Motor_Parameters_Fan.xlsx' in the MATLAB working
directly.

% The parameters are saved in two options. The first option has
inductances

% in ohms and speed in RPM. The second option has inductances in
Henrys and

% speed in radians per second.

% The parameters are saved in a separate sheet from the data titles.

% Also included in the output are the starting variables required to
test

% the transient response when starting point is rated speed.


% REVISION STATUS: Modified March 28: Reverted to original Pn but
retained modified IAgg.


V=400;
% Enter motor rated voltage

poles=2;
% Enter motor pole pairs
```

```
f=50;
% Enter rated frequency


A=xlsread('Motors_Fan.xlsx');                                    % Read in
data for motors to be aggregated.


% Separate the rows in theinput data that have more than one motor
M=uint16(sum(A(:,1)));
[P,N]=size(A);
B=zeros(M,N);
m=0;
for p=1:P;
    Q=A(p,1);
for q=1:Q;
B(m+1,:)=A(p,:);
B(m+1,1)=1;
        m=m+1;
end;
end;


ZNL=complex(B(:,5),B(:,6)+B(:,9));                          % Evaluate
No load impedance for each motor
```

```
ZLR=complex(B(:,5)+B(:,7),B(:,6)+B(:,8));            % Evaluate
Locked rotor impedance for each motor



ZNLEq=1/(sum(1./(ZNL)));                                    %
Evaluate equivalent No Load impedance for aggregated motor

ZLREq=1/(sum(1./(ZLR)));                                    %
Evaluate equivalent No Locked rotor impedance for aggregated motor



RRAgg=real(ZLREq)-real(ZNLEq);                          % Evaluate
Rotor Resistance for aggregated motor

RSAgg=real(ZNLEq);                                          %
Evaluate Stator Resistance for aggregated motor



% Assume Design B motor. Xs/Xr=2/3

XSAgg=0.4*imag(ZLREq);                                  % Evaluate
Stator Reactance for aggregated motor

XRAgg=0.6*imag(ZLREq);                                  % Evaluate
Rotor Reactance for aggregated motor

XMAgg=imag(ZNLEq)-0.4*imag(ZLREq);                % Evaluate
Magnetising Reactance for aggregated motor



% Motor slip Evaluation

Ns=60*f/poles;                                                  %
Synchronous speed
```

```
Nr=B(:,11);
% Rated speed from input data

s=(Ns-Nr)./Ns;                                                    %
Slip



Zs=complex(B(:,5),B(:,6));                                        %
Motor stator impedance from input data

Zm=complex(0,B(:,9));                                             %
Motor magnetising impedance from input data

Zr=complex((B(:,7)./s),B(:,8));                                   % Motor
rotor impedance (at rated speed) from input data

Z=Zs+((Zm.*Zr)./(Zm+Zr));                                         % Motor
total impedance (at rated speed) from input data

ZEq=1/(sum(1./(Z)));                                              %
Total impedance (at rated speed) for aggregated motor



% Evaluation of aggregated slip

alpha=((XMAgg+XRAgg)^2)*(real(ZEq)-RSAgg);

beta=-1*RRAgg*XMAgg^2;

gama=(real(ZEq)-RSAgg)*RRAgg^2;

sAgg=(-1*beta-(beta^2-4*alpha*gama)^0.5)/(2*alpha);
```

```
Power=B(:,2)*1000;
% Reading pated power from input data

PAgg=sum(Power);                                                    %
Evaluation of aggregated motor power



J=B(:,10);
% Reading inertia from input data

w=(2*pi/60).*Nr;                                                        %
Converting rated speed from RPM to Radians per Sec

ws=(2*pi/60)*Ns;                                                        %
Synchronous speed in Radians per Sec.

NAgg=Ns*(1-sAgg);                                                       %
Evaluating aggergated motor speed (in RPM)

wrAgg=NAgg*2*pi/60;                                                     %
Evaluating aggregated motor speed (in Rad. per Sec)

JAgg=sum(J.*((w./wrAgg).^2));                                % Evaluating
aggregated motor inertia

Torque=(0.8*PAgg)/wrAgg;                                                %
Evaluating aggregated motor torque

k=Torque/(wrAgg^2);                                                     %
Evaluating constant in speed - torque relation (T=kw^2)

k1=Torque/((wrAgg/2)^2);                                                %
Evaluating constant in speed - torque relation (T=k1(w/2)^2) for
constant torque

Ff=0.005*0.8*PAgg/(wrAgg^2);                                 % Evaluating
Friction Factor (Based on friction loss = 0.5% of PAgg)

% Evaluate parameters for supply change-over at rated speed.
```

```
ZSAgg=complex(RSAgg,XSAgg);                                % Stator
impedance for aggregated motor

ZRAgg=complex(RRAgg/sAgg,XRAgg);                    % Rotor impedance
for aggregated motor at aggregated slip

ZMAgg=complex(0,XMAgg);                                    %
Magnetising impedance for aggregated motor

ZAgg=ZSAgg+((ZMAgg.*ZRAgg)./(ZMAgg+ZRAgg)); % Motor total impedance
(at aggregated slip) for aggregated motor

IAgg=V/(ZAgg*3^0.5);                                              %
Current for aggregated motor at rated speed

IaMag=abs(IAgg);                                                    %
Magnitude of current at rated speed.

% Phase of

if angle(IAgg) < 0

IaPh=360+angle(IAgg)*180/pi;

elseIaPh=angle(IAgg)*180/pi;

end;



if (IaPh+120)<360

IbPh=IaPh+120;

elseIbPh=(IaPh+120)-360;

end;
```

```
if (IbPh+120)<360

IcPh=IbPh+120;

elseIcPh=(IbPh+120)-360;

end;



%Arranging parameters in one array and exporting to excel

Param_Ohm_RPM=[PAgg,V,f,RSAgg,XSAgg,RRAgg,XRAgg,XMAgg,JAgg,Ff,poles,
k,k1,sAgg,IaMag,IaPh,IbPh,IcPh,Torque,NAgg,NAgg/2];

Param_Hen_RadPS=[PAgg,V,f,RSAgg,XSAgg/(2*pi*f),RRAgg,XRAgg/(2*pi*f),
XMAgg/(2*pi*f),JAgg,Ff,poles,k,k1,sAgg,IaMag,IaPh,IbPh,IcPh,Torque,w
rAgg,wrAgg/2];

S1={'Pn(VA)''Vn(V)''Fn(Hz)''Rs(Ohms)''Ls(Ohms)''Rr(Ohms)''Lr(Ohms)''
Lm(Ohms)''J(Kg.m2)''Friction_f(N.m.s)''Pole_pairs''k''k1''slip''FlCu
rr,A''PH Angle, Ia''PH Angle, Ib''PH Angle,
Ic''Torque''Speed(RPM)''Half Speed'};

S2={'Pn(VA)''Vn(V)''Fn(Hz)''Rs(Ohms)''Ls(Henry)''Rr(Ohms)''Lr(Henry)
''Lm(Henry)''J(Kg.m2)''Friction_f(N.m.s)''Pole_pairs''k''k1''slip''F
lCurr,A''PH Angle, Ia''PH Angle, Ib''PH Angle,
Ic''Torque''Speed(Rad/s)''Half Speed'};

xlswrite('Aggregated_Motor_Parameters_Fan.xlsx',Param_Ohm_RPM','Ohm_
Data');

xlswrite('Aggregated_Motor_Parameters_Fan.xlsx',S1','Ohm_Title');

xlswrite('Aggregated_Motor_Parameters_Fan.xlsx',Param_Hen_RadPS','He
nry_Data');

xlswrite('Aggregated_Motor_Parameters_Fan.xlsx',S2','Henry_Title');
```

Appendix D: Composite Parameters for Ship Kota Hapas 29

Aggregate Motor Parameters

Parameter	Fans Aggregate	Cranes Aggregate
Rated Power, Pn(VA)	4.8370E+05	4.7000E+05
Rated Voltage (RMS) Vn(V)	4.0000E+02	4.0000E+02
Rated Frequency Fn(Hz)	5.0000E+01	5.0000E+01
Stator Resistance Rs(Ohms)	3.1297E-02	3.7777E-02
Stator Inductance Ls(Henry)	2.5700E-05	3.4995E-05
Rotor Resistance Rr'(Ohms)	1.3635E-02	2.4814E-02
Rotor Inductance Lr'(Henry)	3.8550E-05	3.4995E-05
Magnetizing Inductance Lm(Henry)	1.7756E-03	2.4801E-03
J(Kg.m2)	2.6610E+01	1.8551E+01
Friction Factor Ff(N.m.s)	1.0158E-01	9.7095E-02
Number of Pole pairs	2.0000E+00	2.0000E+00

Appendix E: Initial conditions

Parameter	Start from Rest	Starting from Rated Speed	
	All	Fans Aggregate	Cranes Aggregate
Rotor Slip	1	1.7669E-02	9.5866E-03
Rotor Electrical Angle	0	0	0
Current at Aggregated Slip, Ia (A)	0	8.4389E+02	5.2129E+02
Current at Aggregated Slip, Ib (A)	0	8.4389E+02	5.2129E+02
Current at Aggregated Slip, Ic (A)	0	8.4389E+02	5.2129E+02
Stator Current Phase Angle, Ia	0	3.0806E+02	2.8920E+02
Stator Current Phase Angle, Ib	0	6.8061E+01	4.9198E+01
Stator Current Phase Angle, Ic	0	1.8806E+02	1.6920E+02

Static Load- *Non – Motor loads*

Description of load	Qty	KW	Total KW	PF	Total KVA	Total KVAR
Cooking range	4.00	25.00	100.00	0.90	111.11	48.43
Lightings(all)	1.00	22.86	22.86	0.90	25.40	11.07
TOTAL			122.86			59.50

Appendix F: Buses Interconnections Line Parameters

FROM	TO	r (Ω)	x (Ω)	b (S)	CURRENT (A)	POWER (MVA)
Rabai BSP	Galu	11.40	25.84	1.61E-04	425	97
Rabai BSP	Kipevu BSP	3.74	7.40	4.52E-05	389	89
Rabai BSP	Kipevu BSP	3.74	7.40	4.52E-05	389	89
Rabai BSP	Kipevu BSP	3.23	7.32	4.57E-05	425	97
Rabai BSP	Kipevu II	3.23	7.32	4.57E-05	425	97
Kipevu BSP	KPA	0.07	0.34	2.40E-07	550	126
Rabai BSP	New Bamburi	4.84	9.58	5.85E-05	389	89
New Bamburi	Vipingo	2.86	5.66	3.46E-05	389	89
Vipingo	MSA Cement	2.75	5.44	3.33E-05	389	89
MSA Cement	Kilifi	3.85	7.62	4.66E-05	389	89
Grid	Rabai BSP	31.82	183.04	1.09E-03	720	274
Grid	Mtito	46.92	106.37	6.64E-04	425	97
Mtito	Voi	17.28	39.19	2.45E-04	425	97
Voi	Maungu	5.70	12.92	8.07E-05	425	97
Maungu	Mariakani	17.09	38.76	2.42E-04	425	97
Mariakani	Kokotoni	2.47	5.60	3.50E-05	425	97
Kokotoni	Rabai BSP	0.95	2.15	1.35E-05	425	97

Appendix G : Bus Loadings in per unit

BUS NO.	BUS NAME	LOAD		STATIC VAR (p.u)	BUS TYPE
		P (p.u.)	Q (p.u.)		
1	Grid	-	-	-	Slack
2	Rabai BSP	0.0254	0.0123	0.1000	PQ
3	Galu	0.0475	0.0230	-	PQ
4	Kipevu BSP	0.3329	0.1612	-	PQ
5	KPA	0.0210	0.0102	-	PQ
6	New Bamburi	0.0882	0.0427	-	PQ
7	Vipingo	-	-	-	PQ
8	MSA Cement	0.0366	0.0177	-	PQ
9	Kilifi	0.0446	0.0216	-	PQ
10	Kipevu II	0	0	0	PV
11	Mtito	0.0141	0.0068	-	PQ
12	Voi	0.0116	0.0056	-	PQ
13	Maungu	0.0112	0.0054	-	PQ
14	Mariakani	0.0369	0.0179	-	PQ
15	Kokotoni	0.0225	0.0109	-	PQ

Appendix H: Generation stations capacity in per unit

Generating Station	Bus	Power Generated, P (p.u.)
Rabai	Rabai BSP	0.3000
Kipevu I	Kipevu BSP	0.1700
Kipevu III	Kipevu BSP	0.3833
Tsavo (Kipevu II)	Kipevu II	0.2467

Appendix I: Line Parameters in per unit values for between Sub- Stations

FROM	**TO**	**r (p.u.)**	**x (p.u.)**	**b (p.u.)**	**CURRENT (p.u.)**	**POWER (p.u.)**
Rabai BSP	Galu	0.1962	0.4449	2.7789E-06	3.2389E-01	0.3233
Rabai BSP	Kipevu BSP	0.0644	0.1274	7.7858E-07	2.9646E-01	0.2967
Rabai BSP	Kipevu BSP	0.0644	0.1274	7.7858E-07	2.9646E-01	0.2967
Rabai BSP	Kipevu BSP	0.0556	0.1261	7.8736E-07	3.2389E-01	0.3233
Rabai BSP	Kipevu II	0.0556	0.1261	7.8736E-07	3.2389E-01	0.3233
Kipevu BSP	KPA	0.0012	0.0058	4.1322E-09	4.1916E-01	0.4200
Rabai BSP	New Bamburi	0.0834	0.1649	1.0076E-06	2.9646E-01	0.2967
New Bamburi	Vipingo	0.0493	0.0974	5.9539E-07	2.9646E-01	0.2967
Vipingo	MSA Cement	0.0474	0.0937	5.7249E-07	2.9646E-01	0.2967
MSA Cement	Kilifi	0.0663	0.1312	8.0148E-07	2.9646E-01	0.2967
Grid	Rabai BSP	0.5479	3.1515	1.8837E-05	9.1452E-01	0.9133
Grid	Mtito	0.8078	1.8315	1.1440E-05	3.2389E-01	0.3233
Mtito	Voi	0.2976	0.6748	4.2147E-06	3.2389E-01	0.3233
Voi	Maungu	0.0981	0.2224	1.3895E-06	3.2389E-01	0.3233
Maungu	Mariakani	0.2943	0.6673	4.1684E-06	3.2389E-01	0.3233
Mariakani	Kokotoni	0.0425	0.0964	6.0210E-07	3.2389E-01	0.3233
Kokotoni	Rabai BSP	0.0164	0.0371	2.3158E-07	3.2389E-01	0.3233